

University of Southern Queensland
Faculty of Health, Engineering and Sciences

**Using Engineering Cementitious Composites as an
adhesive for near-surface mounted FRP bars
strengthening concrete/masonry structures**

A dissertation submitted by

Mr. Jared Hawkins

Student Number

in fulfilment of the requirements of

ENG4111/ENG 4112 Research Project

towards the degree of

Bachelor of Engineering (Honours) (Civil)

Submitted October, 2016

ABSTRACT

Internationally, the cost of maintenance and rehabilitation of infrastructure is growing, and has reached roughly 50% of total construction expenditure in many countries. The near-surface mounted (NSM) FRP method has attracted increasing attention worldwide as one of the most promising techniques for structural strengthening and as an effective alternative to the externally bonded FRP method. In the NSM FRP method, grooves are cut into the concrete cover of a concrete member for the embedding of FRP bars using an adhesive. Compared to the externally bonded FRP method, the NSM FRP method has a number of advantages including a reduced risk of de-bonding failure and better protection of the FRP reinforcement. However, the brittle nature of cement paste as the groove filling material leads to a preference to use epoxy adhesives as they have better tensile and ductile properties. The proposed project aims to use engineered cementitious composites (ECC) as groove filling material as it has higher tensile strength and excellent ductility. A series of laboratory testing will be conducted to study the bond-slip behaviour for NSM FRP bars using ECC and the testing results can also be used for the calibration of the theoretical model which will be developed as part of the project.

University of Southern Queensland
Faculty of Health, Engineering and Sciences
ENG4111/ENG4112 Research Project

Limitations of Use

The Council of the University of Southern Queensland, its Faculty of Health, Engineering & Sciences, and the staff of the University of Southern Queensland, do not accept any responsibility for the truth, accuracy or completeness of material contained within or associated with this dissertation.

Persons using all or any part of this material do so at their own risk, and not at the risk of the Council of the University of Southern Queensland, its Faculty of Health, Engineering & Sciences or the staff of the University of Southern Queensland.

This dissertation reports an educational exercise and has no purpose or validity beyond this exercise. The sole purpose of the course pair entitled “Research Project” is to contribute to the overall education within the student’s chosen degree program. This document, the associated hardware, software, drawings, and other material set out in the associated appendices should not be used for any other purpose: if they are so used, it is entirely at the risk of the user.

University of Southern Queensland
Faculty of Health, Engineering and Sciences
ENG4111/ENG4112 Research Project

Certification of Dissertation

I certify that the ideas, designs and experimental work, results, analyses and conclusions set out in this dissertation are entirely my own effort, except where otherwise indicated and acknowledged.

I further certify that the work is original and has not been previously submitted for assessment in any other course or institution, except where specifically stated.

J. Hawkins

001016936



Signature

13th October 2016

Date

ACKNOWLEDGEMENTS

I would like to thank my supervisor, Associate Professor Dr. Yan Zhuge for her support and guidance during the completion of this project.

In addition I would like to thank Darren Lutze from Inconmat Pty Ltd for donating the VROD fibre reinforced plastic reinforcing rod and Wayne Crowell from the Centre for Excellence in Engineered Fibre Composites for his assistance during the testing phase of this project.

Finally I thank my family for their support throughout the duration of this project

Jared Hawkins

13th October 2016

CONTENTS

Abstract.....	ii
List of figure	x
List of Tables	x
Nonmenclature.....	xiii
1 Project Introduction	1
1.1 Limits of Current Studies	2
1.2 Project Aim	2
1.3 Research Objectives	3
1.4 Beyond Scope.....	3
1.5 Expected Outcomes and Benefits.....	4
2 Literature Review	5
2.1 Infrastructure Maintenance Requirement.....	5
2.2 Retrofitted Strengthening Systems.....	6
2.2.1 Surface mounted/Externally Bonded Systems.....	6
2.3 Other Retro fit systems.....	9
2.4 Near Surface Mounted Systems	9
How a near surface mounted system works.....	11
Applications	11
2.4.1 Flexural Strength.....	12
2.4.2 General Failure Modes of NSM systems	13
2.5 Engineered Cementitious Composites	18
2.6 Finite Element Analysis	21
2.6.1 ECC Models.....	21
2.6.2 Interfacial Bonds.....	22
2.7 Literature Review Summary	23
3 Methodology	24

3.1	Experimental Analysis	24
3.1.1	Method of test	24
3.2	Direct Shear Test Design – Sample	25
3.2.1	FRP Rod.....	25
3.2.2	Concrete Prism.....	25
3.2.3	Final dimensions for prism.	28
3.2.4	Construction of Base Prism	28
3.2.5	Engineered Cementitious Composite.....	30
3.2.6	ECC Materials.....	32
3.2.7	Building the samples.....	33
3.2.8	Tensile Testing.....	34
3.2.9	Design of Testing Base	35
3.3	Dye penetration	37
3.3.1	Method.....	37
3.4	Post processing of raw data.....	38
3.4.1	Correction for initial settlement.....	38
3.4.2	Example of Correction method Using Sample ECC3-1	38
3.4.3	Correction for Elongation in the FRP.....	39
3.4.4	Calculation of Bond Stress	40
4	Results.....	41
4.1	Sample Set C1 Summary Results.....	41
4.1.1	Discussion.....	41
4.2	Sample Set C1 Detailed Results.....	43
4.3	Sample Set C1 Graphical Results.	43
4.4	Sample Set ECC1 Summary Results.....	46
4.4.1	Discussion.....	46
4.5	Sample Set ECC1 Detailed Results.....	49

4.5.1	Sample Set ECC1 Force/Slip and Bond Stress/Strain Relationships.....	50
4.6	Sample Set ECC2 Summary Results.....	53
4.6.1	Discussion.....	53
4.7	Sample Set ECC2 Detailed Results.....	56
4.7.1	Sample Set ECC2 Force/Slip and Bond Stress/Strain Relationships.....	57
4.8	Sample Set ECC3 Summary Results.....	60
4.8.1	Discussion.....	60
4.9	Sample Set ECC3 Detailed Results.....	62
4.9.1	Sample Set ECC3 Load/Slip and Bond Stress/Strain Relationships.....	62
4.10	Sample Set ECC4 Summary Results.....	63
4.10.1	Discussion.....	63
4.11	Sample Set ECC4 Detailed Results.....	65
4.11.1	Sample Set ECC4 Load/Slip and Bond Stress/Strain Relationships.....	66
4.12	Additional Data on ECC4-1.....	67
4.12.1	Discussion.....	67
4.12.2	ECC4-1B Load/Slip and Bond Stress/Strain Relationships.....	68
4.13	Summary of results.....	68
5	Discussion of results.....	70
5.1	Bond Strength Results.....	70
5.1.1	Comparison to previous studies.....	70
5.1.2	Impact of fly ash on cohesive bond.....	71
5.1.3	Impact of rheology on fibre distribution.....	73
5.2	Workability of wet adhesives.....	74
5.3	Bond Strength Prediction.....	75
5.3.1	NSM Potential Bond Strength – Zhang Model.....	75
6	Conclusion.....	79

6.1	Key findings	79
6.1.1	De-bonding at the ECC/FRP reinforcement interface.	79
6.1.2	De-bonding between the sand coating and the ECC1 adhesive.....	79
6.1.3	Workability	80
6.2	Future research	80
6.3	Closing Remark.....	81
7	References.....	82
	Appendix 1 – Project Specification	86
	Appendix B – Project Plan.....	88
	Appendix C – Mix Design Calculations	93
	Appendix 4 – Concrete Prism Test Results	97
	Appendix 5 – Material Data Sheet – V.Rod	99
	Appendix 6 – PVA Fibre Data Sheet.....	101
	Appendix 7 – Matlab codes	103

LIST

Figure 2-1 Surface Mounted CFRP Reinforcing, Caswell Drive, Canberra	7
Figure 2-2 Surface Mounted Reinforcing Typical Arrangement.....	7
Figure 2-3 De-bonding failure of FCRM, note the reinforcing strip protruding from the base of the beam (Ombres 2012)	8
Figure 2-4 Near Surface Mounted Reinforcing Typical Arrangement.....	10
Figure 2-5 Typical Near Surface Mounted Placements	11
Figure 2-6 Load deflection curves from Sharaky study, CB = Control Beam remainder are NSM reinforced with alternate combinations of epoxy and CFRP reinforcement. (Sharaky et al. 2014)	12
Figure 2-7 De-bonding Origins in NSM Systems (Coelho et al. 2015)	14
Figure 2-8 NSM De bonding classifications (De Lorenzis & Teng 2007).....	15
Figure 2-9 Bond Stress - Slip Relationship (Hong & Park 2012)	16
Figure 2-10 Shear Stress/Strain Test results showing Steel fibre ECC(DRECC) with excellent shear strength and PE Fibre ECC with excellent ductility (SPECC). (Li et al. 1994)	20
Figure 2-11 Comparison of Numerical Model and Experimental results for Tensile testing of ECC. (Kunieda et al. 2011).....	21
Figure 3-1 Base Prism.....	28
Figure 3-2 Prism Molds - Ready for Casting.....	28
Figure 3-3 Concrete Testing On Prisms	29
Figure 3-4 Base Prisms Cast.....	29
Figure 3-5 Prisms Stripped ready for final notch detailing.	30
Figure 3-6 Prism and reinforcing rod setup ready for ECC adhesive. The Prisms were washed thoroughly prior to remove any dust that may affect the bond strength.	33
Figure 3-7 All materials ready for mixing. Note: syringe was used to measure out super plasticiser.....	34
Figure 3-8 Completed Specimen shortly after ECC pour.....	34
Figure 3-9 Tensile Test Machine MTS Insite 100 (MTS 2011).....	35
Figure 3-10 Test Base, Isometric View.	36
Figure 3-11 Testing Base.....	37
Figure 3-12 Correction of data for initial slip.....	38

Figure 4-1 Cover splitting in Sample C1-1	42
Figure 4-2 Load/Slip & Stress/Strain Relationship, Sample C1-4	45
Figure 4-3 Sample Set ECC1 Typical Failure Mode - Brittle	48
Figure 4-4 ECC1 FRP bar showing sand coating de-bonding.....	48
Figure 4-5 Cross Section of ECC1 sample showing dense adhesive and no apparent air voids.....	49
Figure 4-6 Load/Slip & Stress/Strain Relationship, Sample ECC1-1	50
Figure 4-7 Load/Slip & Stress/Strain Relationship, Sample ECC1-2	50
Figure 4-8 Load/Slip & Stress/Strain Relationship, Sample ECC1-3	51
Figure 4-9 Load/Slip & Stress/Strain Relationship, Sample ECC1-4	51
Figure 4-10 Load/Slip & Stress/Strain Relationship, Sample ECC1-5	52
Figure 4-11 Dye Penetration - ECC2-4 (Left) ECC2-2 (Right)	55
Figure 4-12 ECC4 samples showing good of ECC on external facing side and poor bond on internal facing side.....	55
Figure 4-13 ECC2-2 Section View	56
Figure 4-14 Load/Slip & Stress/Strain Relationship, Sample ECC2-1	57
Figure 4-15 Load/Slip & Stress/Strain Relationship, Sample ECC2-2	57
Figure 4-16 Load/Slip & Stress/Strain Relationship, Sample ECC2-3	58
Figure 4-17 Load/Slip & Stress/Strain Relationship, Sample ECC2-4	58
Figure 4-18 Load/Slip & Stress/Strain Relationship, Sample ECC2-5	59
Figure 4-19 Sample 3-1 Dye Penetration	61
Figure 4-20 Sample ECC3-1 Section View	61
Figure 4-21 Load/Slip & Stress/Strain Relationship, Sample ECC3-1	62
Figure 4-22 Load/Slip & Stress/Strain Relationship, Sample ECC3-1	63
Figure 4-23 ECC4 Thixotropic Consistency	64
Figure 4-24 Sample ECC4-2 Dye Penetration.....	65
Figure 4-25 Sample ECC4-1 FRP rod after extraction from ECC4 adhesive.	65
Figure 4-26 Load/Slip & Stress/Strain Relationship, Sample ECC4-1A	66
Figure 4-27 Load/Slip & Stress/Strain Relationship, Sample ECC4-2	66
Figure 4-28 Load/Slip & Stress/Strain Relationship, Sample ECC4-1B.....	68
Figure 4-29 ECC1 Regression Analysis	69
Figure 4-30 ECC2 Regression Analysis	69
Figure 5-1 a) Tensile Strain/VMA content relationship. b) Tensile strength/VMA content relationship. (Li & Li 2012).....	74
Figure 5-2 Base Concrete Failure Plane (De Lorenzis & Teng 2007).....	76

LIST OF TABLES

Table 3-1 Adhesive mix designs.....	31
Table 3-2 ECC Characteristics – Previous Studies.....	32
Table 3-3 Samples Summary	32
Table 4-1 Sample Set C1 Quantitative Result Summary.....	41
Table 4-2 Sample Set C1 Qualitative Observations	41
Table 4-3 Sample Set C1 Detailed Results	43
Table 4-4 Sample Set ECC1 Quantitative Results Summary	46
Table 4-5 Sample Set ECC1 Qualitative Observations	46
Table 4-6 Sample Set ECC1 Detailed Results.....	49
Table 4-7 Sample Set ECC2 Quantitative Results.....	53
Table 4-8 Sample Set ECC2 Qualitative Observations	53
Table 4-9 Sample Set ECC2 Detailed Results.....	56
Table 4-10 Sample Set ECC3 Quantitative Results Summary	60
Table 4-11 Sample Set ECC3 Qualitative Observations	60
Table 4-12 Sample Set ECC3 Detailed Results.....	62
Table 4-13 Sample Set ECC4 Quantitative Results Summary	63
Table 4-14 Sample Set ECC4 Qualitative Observations	63
Table 4-15 Sample Set ECC4 Detailed Results.....	65
Table 4-16 ECC4-1B Detailed Result	67
Table 5-1 Comparison of results with similar studies	71

NONMENCLATURE

a'_e	edge distance, measured from the centre of the reinforcing bar to the edge of concrete substrate
A	Area
A_{frp}	Cross Sectional Area of FRP Reinforcement (excluding sand coating)
$C_{failure}$	Cross-sectional contour of the failure surface, i.e. the perimeter of the groove
CFRP	Carbon Fibre Reinforced Plastic
d	nominal diameter of reinforcing bar (i.e. pultruded GFRP excluding the sand coating)
d_r	outside diameter of the reinforcing bar
E	Modulus of Elasticity
E_{frp}	Tensile modulus of FRP reinforcement
F.O.S.	Factor of Safety
f'_c	Characteristics strenght of concrete in compression
FRP	Fibre Reinforced Plastic
FRCM	fibre reinforced cementitious mortar
G_f	Interfacial fracture energy
GFRP	Glass Fibre Reinforced Plastic
G.P.	General Purpose Fillet Weld
l	length
L_b	bonded length

L_{eg}	effective length for groove
NSM	Near Surface Mount
P	Applied Load/Force
P_u	Predicted Bond Strength
R^2	Coefficient of determination
s	slip
VMA	Viscosity Modifying Agent
β_L	Bonded length reduction factor
γ	groove depth to width ratio
σ	stress
Δl	change in length
ε	strain
η	fracture mechanics parameter
τ_{cmax}	max stress at failure plane in concrete substrate
τ_{ult}	ultimate bond stress, measured at the adhesive/reinforcement interface

1 PROJECT INTRODUCTION

While the first instance of near surface mounted (NSM) strengthening was documented in 1949, it is only since the early 2000's that NSM has experienced a resurgence in research attention. This may be due to the availability of fibre reinforced plastic (FRP) reinforcement which makes retrofitting existing structures much easier due to its low weight and high strength properties. It may also be due to the ever increasing volume of structures which require strengthening. It is most likely a combination of both factors.

Engineered Cementitious composites (ECC) are coming to a point in their research lifecycle where development where their physical characteristics and potential benefits of ECC are well known and backed up by significant experimental data. It is now necessary for research to be conducted to identify real world applications and prove ECC a valid competitor to current industry norms. It is essential that ECC demonstrates comparable strength and durability as well as offering at least a material cost benefit. ECC is a generic term for cementitious matrix reinforced with any fibre, however in this study PVA fibres will be used. This will allow the study to leverage multiple works by Li and Hesse in an attempt to reduce the volume of testing required.

This study aims to address the need for research into suitable application of ECC by studying its performance as an adhesive/groove filler in an NSM strengthening system. Currently there are only a few commercially available NSM systems which typically use an epoxy groove filler and carbon fibre reinforced plastic (CFRP), one example is Sika® CarboDur® NSM. It is possible to use traditional cementitious mortar as an adhesive however due to its poor tensile strength it is prone to brittle failure mode with little to no residual load capacity. It is anticipated that the greater tensile strength and ductility of

ECC compared to traditional cementitious mortar will demonstrate characteristics similar to epoxy groove filler, avoiding brittle failure.

Victor C. Li, one of the leading researchers into ECC, has suggested in his paper “Engineered Cementitious Composites for Structural Applications” (Li & Kanda 1998) that ECC could be a suitable replacement for high strength concrete where reinforcement and concrete come into contact as it is less likely to fracture. As this is the typical use of the adhesive in an NSM system it seems likely that ECC would be a suitable material for this application.

More detailed information will be presented in the literature regarding the demand for strengthening systems, the types of strengthening systems as well as ECC and its desirable material characteristics.

1.1 Limits of Current Studies

After the completion of a comprehensive literature review, there has been no significant studies found which cover the use of ECC as an adhesive in a NSM system to strengthen existing concrete or masonry structures. As such there is an opportunity to complete some unique research which may lead to the identification of suitable application for ECC. One similar study by Afefy et al (Afefy & Mahmoud 2014) was found which was similar. In Afefy’s precast ECC strips were cast into the tension cover zone of a reinforced concrete girder during fabrication of the girder, this is dissimilar to a typical NSM system in that it is not a retrofitted system. However the arrangement of the system is similar in that it replaces concrete with a material which would perform better than concrete when loaded in tension. Afefy’s research was able to demonstrate that the ECC strips lead to improved performance of the affected girders in regard to both serviceability and strength.

1.2 Project Aim

As ECC has greater tensile strength and ductility compared to traditional cementitious mortar, this research project will aim prove that ECC will allow for greater tensile capacity as well as a more desirable failure mode when used as the adhesive in a near surface mounted strengthening system.

In summary the aims of this project will be to;

- Demonstrate that ECC is an effective adhesive for a near surface mounted system by;
 - demonstrating ductile failure mode
 - providing better bond compared to cementitious paste to the reinforcement due to the increased tensile strength in the ECC
- Demonstrate it is a cost effective alternative to epoxy adhesive typically used in a near surface mounted system.

1.3 Research Objectives

The primary objectives for this research project are as follows:

- Develop an understanding of various retrofitted strengthening systems
- Develop an understanding of ECC and how its micromechanical behaviour affects ductility and tensile strength
- Identify suitable test methods
- Develop a suitable test strategy with a number of alternative mix designs
- Source material characteristics from previous studies relating to the compressive and tensile of comparable ECC materials
- Produce technical performance data for ECC binder in bond slip tests
- Produce comparison data using cement binder
- Assess the performance of ECC as an adhesive in a near surface mounted reinforcing system

1.4 Beyond Scope

This project will not include a study into changes in flexural capacity for a beam section fitted with near surface mounted ECC/FRP reinforcement. The increases in flexural capacity of beam sections with near surface mounted FRP reinforcement has been proven in many studies. It should be possible, with further study, to extrapolate the data from the bond slip analysis to produce a model for increased flexural capacity, however this should be proven with further experimental study.

1.5 Expected Outcomes and Benefits

It is expected that the experimental program will demonstrate that ECC adhesive outperforms cement paste adhesive. The primary benefit will be the demonstration of a ductile failure mode, this is desirable in structural design as it provides warning of failure of a structure that is overloaded. Secondary to this, it is expected that the increase in tensile strength should lead to greater strength over typical cement paste. While the PVA fibres will not add to the cohesive bond between the ECC and the FRP bar it is expected that the fibres will entangle with the mechanical bond features, be it rough surface treatment or bar deformations, and . The stress/strain relationships generated through the testing should also demonstrate strain hardening behaviour rather than brittle fracture as is typical of cement paste. It may be the additional tensile capacity and the improved ductility should result in a more even stress distribution through the system and result in greater capacity. The strain hardening behaviour of the ECC should also be evident in the test results.

2 LITERATURE REVIEW

In order to effectively complete this research project a comprehensive literature review was conducted to develop a solid understanding of the materials, systems and theories surrounding near surface mounted strengthening system. Much of the information was sourced from journal articles, research papers as well as commercial catalogues and prior studies completed at University of Southern Queensland.

Upon completion of the literature review it will be possible to provide a thoughtful and educated assessment of the experimental program and confirm if the project objectives have been achieved.

2.1 Infrastructure Maintenance Requirement.

The case for developing a cost effective maintenance/strengthening system for concrete infrastructure is clear. According to the Department of Infrastructure and Regional Development (2014), heavy vehicle traffic is expected to increase by approximately 50% by 2030.

Maintenance expenditure, as a proportion of total investment in infrastructure decreased significantly as the mining boom drove up the investment in new infrastructure and overshadowed the existing underspend in asset maintenance (GHD 2015). Total investment in Infrastructure is expected to decline as the resources boom recedes, but maintenance requirements are expected to remain constant.

However it is still likely that the amount invested in maintenance will remain insufficient. This underspend will be most notable in regional areas which experience a high proportion of heavy vehicle traffic compared to total traffic volume. The spatial

distribution of industry leads to the need for heavy vehicle transport to transport commodities between production zones to market. Due to the low traffic numbers, the political will to commit limited funding to maintenance programs is lacking.

Some also argue that there is an imbalance in the funding tiers, when local governments are charged with maintaining local infrastructure and state or national governments imposing limits on revenue raising. With these issues in mind it is clear the need to develop a cost competitive solution for strengthening and maintaining infrastructure is critical. Particularly in regional areas with an increase in industry but decrease in population.

A brief investigation into the cost of current surface mounted systems that utilise epoxy binder was conducted. The two main commercial suppliers in Australia are currently Sika with Carbodur and BASF with MasterBrace. Both systems rely upon epoxy binders with high tensile capacity and also high cost, Figure 2-1 shows a Master Brace installation on the soffit of a bridge girder in Canberra.

The cost of epoxy can range from \$150 - \$300 for 5kg. In comparison 20kg of high performance mortar with similar PVA fibre content is available for \$60 for 20kg, a 60-80% saving (based on current commercial rates in Canberra). This demonstrates a significant commercial benefit, particularly when considering large scale projects such as bridges or dams. At present the PVA Fibres used in experimental studies are quite expensive. This is a result of limited demand and production. If an NSM system that utilises a PVA based ECC becomes widely accepted and readily commercially available the cost of the PVA fibre should decrease. This is evident by the low cost and availability of PE and PVA fibres used in decorative concrete.

2.2 Retrofitted Strengthening Systems

The use of retrofitted strengthening systems is not a new concept. Near surface mounted systems have been implemented as early as 1949. The characteristics of Fibre Reinforced Polymers lead to easier installation and greater benefits due to their high strength and low weight, improving the efficacy of retrofitted systems.

2.2.1 Surface mounted/Externally Bonded Systems

Surface mounted reinforcement systems have been exhaustively researched and this has resulted in a number of design guides and off the shelf commercial systems becoming available. Surface mounted systems rely on reinforcing strips adhered to the surface of

the structural member, typically with an epoxy adhesive. Once installed the structural members benefit from flexural capacity.



Figure 2-1 Surface Mounted CFRP Reinforcing, Caswell Drive, Canberra

Surface mounted systems have the benefit of being able to be applied to any substrate, as long as it is sound. Improvements in strength have been demonstrated in steel, timber and concrete structures using a variety of reinforcing materials, typically CFRP or GFRP. Other reinforcing materials have been used including steel and fibre reinforced cementitious mortar.

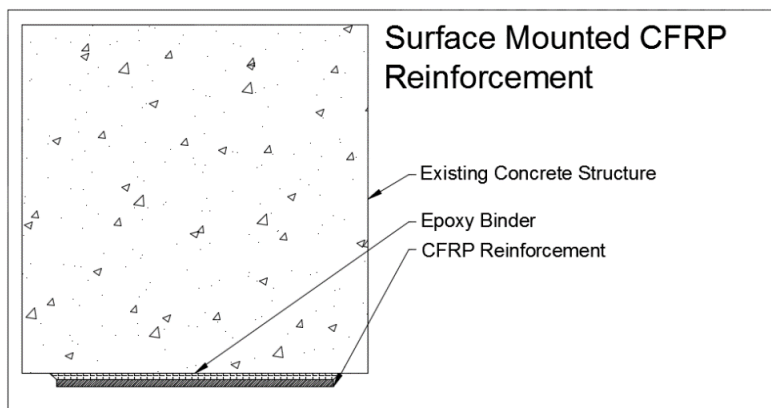


Figure 2-2 Surface Mounted Reinforcing Typical Arrangement

One study of particular interest is Ombres (2012) who conducted de-bonding analysis of reinforced concrete beams strengthened with fibre reinforced cementitious mortar (FRCM). Ombres' method was to apply a woven fibre matrix, held together and bound to the RC beam in the surface mounted style with a cementitious mortar. This study found that the surface mounted reinforcing did in fact increase flexural capacity, with de-bonding as the predominant failure mode. Figure 2-3 illustrates that the de-bonding failure is sudden and complete, occurring at the interface between the existing concrete

and the reinforcing system. This is the expected result for a typical cementitious mortar which has low ductility.



Figure 2-3 De-bonding failure of FCRM, note the reinforcing strip protruding from the base of the beam (Ombres 2012)

Issues and concerns with Surface mounted systems.

While effective, many studies have shown significant inefficiencies in surface mounted systems. As noted by Serecino et al (2007), placement of a surface mounted system in negative moment regions exposes the surface mounted system to damage by traffic. Use in these zones will also generate an uneven surface unless the entire base is levelled with additional material after the surface mounted system is installed, increasing the volume of work and potentially necessitating the removal of flooring or wearing surfaces.

The surface mounted systems are also exposed and prone to fire, vandalism and ultra violet radiation, the latter being a significant concern for CFRP and GFRP systems.

Surface mounted systems also need to be installed on relatively smooth surfaces, any uneven surfaces will need to be treated prior to installation. NSM on the other hand caters for the uneven surfaces with the depth of the groove.

2.3 Other Retro fit systems

There are other means of strengthening existing structures such as;

- External post tensioning however this comes with its own issues including:
 - Steel post tensioning requires maintenance to prevent corrosion
 - Significant size & weight add to structure's dead load
 - Costly installation
- Member thickening/bolstering
 - Typically involves increase in member size
 - Complex formwork requirements for upgrades to concrete structures
 - Potential damage and instability of structure during reinforcement work

These options are not part of this study.

2.4 Near Surface Mounted Systems

Near surface mounted reinforcement has been identified as a potential improvement to the already accepted practice of surface mounted reinforcement. De Lorenzis and Teng (2007) observe the following benefits of near surface mounted systems compared to surface mounted systems:

- Reduced installation time
 - The current required preparation for surface mounted systems on concrete structures is abrasive preparation of the concrete to remove all laitance and spalling concrete. This is often achieved using grit blasting, which in turn requires full encapsulation to control environmental impacts.
- Less prone to de-bonding from the concrete
 - The bonds benefit from the containment of the adhesive within the groove, improving the bond while under load. The containment pressures help to resist de-bonding.
- Near surface mounted bars can be more easily anchored to adjacent members
 - For example on a fixed support bridge, the reinforcing could be continued into the abutment to provide better reinforcement and help prevent pull-out of the FRP reinforcing.
- Better suited to negative moment installation as the reinforcing is protected by the adhesive.
- NSM bars can be more easily pre-stressed.

- NSM systems are less prone to accidental damage, impact or vandalism.
- NSM systems using cementitious groove filler also have better fire resistance.
- Less visual impact, this makes it particularly good for structures of cultural importance.

A typical near surface mounted system is constructed by cutting a groove into the substrate, then installing a reinforcing member, be it a rod or strip, and using an adhesive/groove filler to hold the reinforcement in place. The earliest documented example of this method of reinforcing was by Asplund in 1949 (Asplund 1949). In this example steel reinforcing bars were installed into the soffit of a bridge girder using cementitious grout in Sweden.

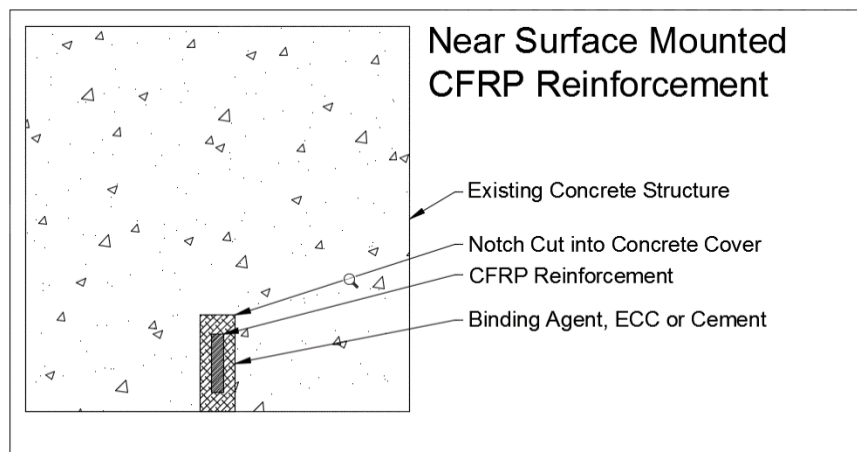


Figure 2-4 Near Surface Mounted Reinforcing Typical Arrangement

Near surface mounted systems are typically used in concrete structures but there has been research into the use of near surface mounted systems on timber structures. Research by Lu et al (2015) demonstrated flexural strength gains ranging from 34-52%. An interesting result in this study was the glulam beams reinforced with the NSM system demonstrated pseudo ductile when the NSM system was installed. This behaviour is a favourable outcome for structural safety. Examples of near surface mounted systems on steel structures were unable to be located.

In summary there has been considerable research into near surface mounted system performance. In a number of full scale tests significant improvements to flexural strength have been demonstrated.

How a near surface mounted system works.

In a simple near surface mounted system, the increase in strength is attributed to the provision of reinforcing in the cover zone of the concrete that produces additional tensile capacity in the tensile zone during bending.

The reinforcing is placed further out from the centroid of the girder and hence the strain is greater on the new reinforcing.

In order for the reinforcing to be fully utilised the bond between the concrete and the reinforcing has to provide sufficient bond length so the tensile capacity of the FRP can be fully utilised. This is the same principle as development length for steel reinforcing used in traditional reinforced concrete structures.

The key issue to overcome is bond slip as the reinforcement is placed closer to the surface and there is less containment material to resist the shear forces presented when the member is loaded, hence the current preference to use epoxy adhesives due to their better tensile and adherent characteristics.

Applications

The application of near surface mounted strengthening systems is broad. It is typically used to improve:

- Flexural capacity both negative and positive bending moments;
- Shear Capacity;
- Axial Compression capacity in columns as well as flexural capacity for columns subject to eccentric axial loads.

Figure 5 below details the placement of typical NSM configuration.

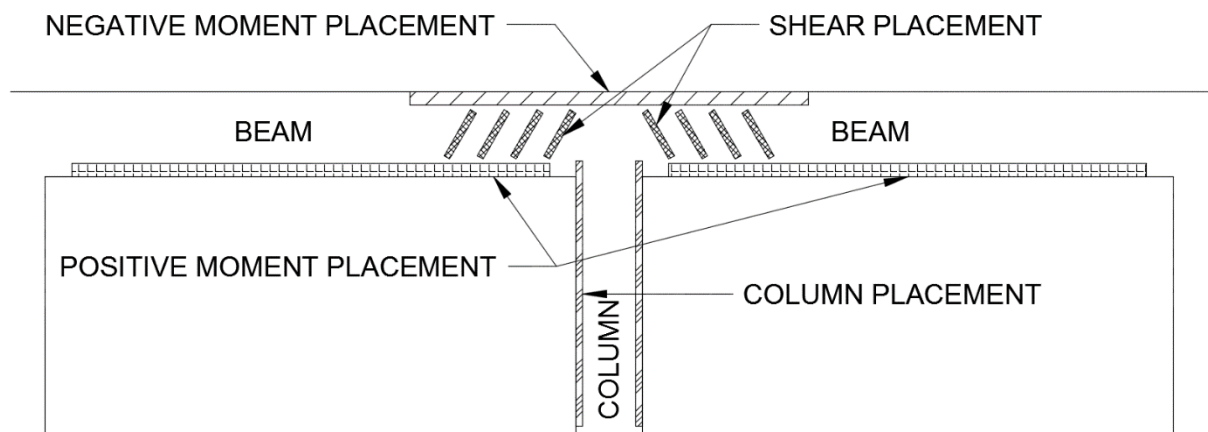


Figure 2-5 Typical Near Surface Mounted Placements

2.4.1 Flexural Strength

Typically NSM systems are used to improve flexural capacity of structural members. Improvements can be made to both positive and negative bending capacity in structures. As suggested in section 2.4, NSM systems are much better suited to negative moment applications than surface mounted systems as they are protected from wear.

Sharaky et al (2014) demonstrated that a reinforced concrete beam will see a 66% increase in flexural strength under 4 point bending tests when fitted with near surface mounted CFRP reinforcement. As is evident from Figure 6 below, the peak load in all NSM strengthened systems is significantly higher than the strengthened system.

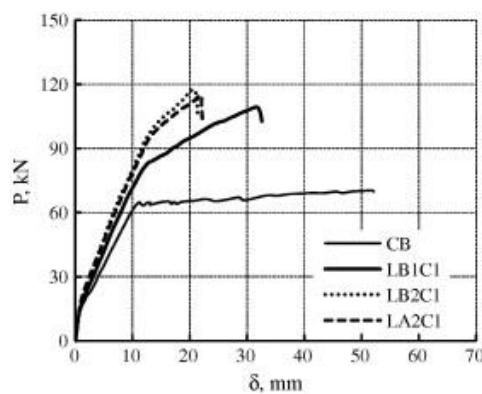


Figure 2-6 Load deflection curves from Sharaky study, CB = Control Beam remainder are NSM reinforced with alternate combinations of epoxy and CFRP reinforcement. (Sharaky et al. 2014)

In addition to flexural strength improvements there has been research into the use of NSM systems to improve shear capacity. Jalali et al (2012) conducted an experimental study on the effect of installing NSM CFRP on reinforced concrete girders. In this study Jalali et al were able to demonstrate significant shear capacity increases. Jalali et al also made a comparison to a study by Chen and Teng (2003) who predicted the strength gains of comparable surface mounted FRP using sheets with equivalent fibre content. Jalali et al were able to demonstrate better shear capacity increases compared to Chen & Teng's predictions. It is suggested that this is a tribute to the better bond behaviour in the NSM system.

In another investigation by Haddad and Almasaied (2016) NSM was utilised to repair fire damaged reinforced concrete beams. In the study Haddah and Almasaied installed NSM strips on the vertical faces of rectangular reinforced concrete beams which had been previously exposed to various temperatures (300 – 600 degrees Celsius). These beams

were then subjected to 3 point loading. The results demonstrated that the beams were able to regain full or partial strength dependant on the level of fire damage and temperature exposure. The critical issue identified by this study was the de-bonding failure between the existing reinforcing steel and concrete caused by the heat exposure. This highlights the importance of the bond behaviour between the concrete and reinforcement.

2.4.2 General Failure Modes of NSM systems

In the instance where a girder has been strengthened by a near surface mounted system there are three general failure modes:

1. Concrete Crushing in the compression zone due to the increased tensile capacity in the tensile zone.
 - a. Concrete crushing in the compression zone demonstrates that the member does not have sufficient compressive capacity compared to tensile capacity. In this case the reinforcement has not been designed appropriately and the addition of the NSM system has overloaded the compression zone of the beam.
2. Fracture of the reinforcing in tensile zone;
 - a. Fracturing of the reinforcement suggests the system has been fully utilised and has reached its ultimate capacity. However, if the NSM reinforcing ruptures it is likely that the reinforcing has been inappropriately designed as it should not fail prior to concrete crushing and steel yielding. If appropriately designed, the FRP should be close to maximum capacity when steel yields. This allows for ductile failure in the member. (Coelho et al. 2015)
3. De-bonding Failure
 - a. De-bonding failure is typically associated with premature failure and with the proper consideration, the groove detailing, bonded length and adhesive can be designed correctly to ensure sufficient bond. Within the general classification of bond failure there are a number of types of bond failure that can occur.

Concrete crushing and reinforcement rupture are both a function of the member geometry and the strain induced from the applied load. As a result they can be easily designed and detailed to prevent premature failure. However de-bonding failure requires more

complex analysis to ensure de-bonding does not occur prematurely, therefore concrete crushing and reinforcement rupture will not be discussed further in this paper.

System level de-bonding

For a beam in flexure, de-bonding is likely to develop from cracks in the concrete beam under load. Critical Diagonal Shear Cracks, Flexural Cracks and Shear cracks are typical origins for de-bonding, Figure 7 from Coelho et al (2015) identifies these typical origins.

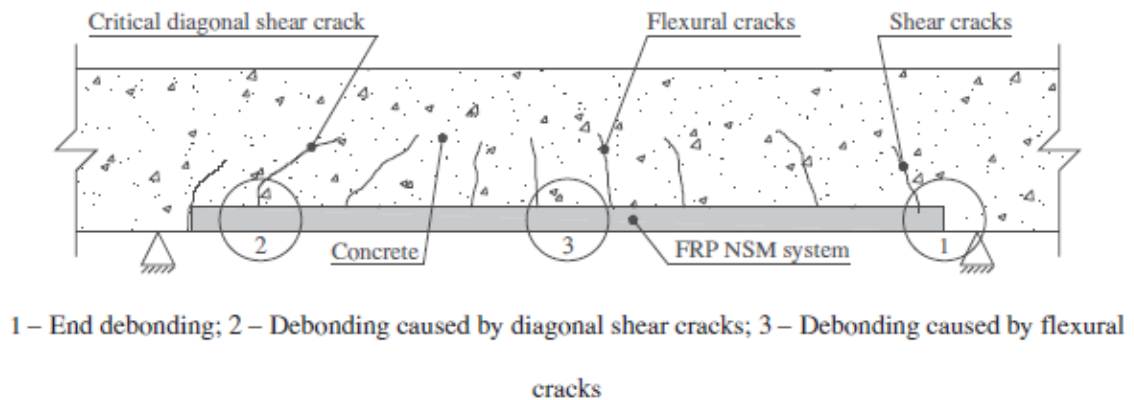


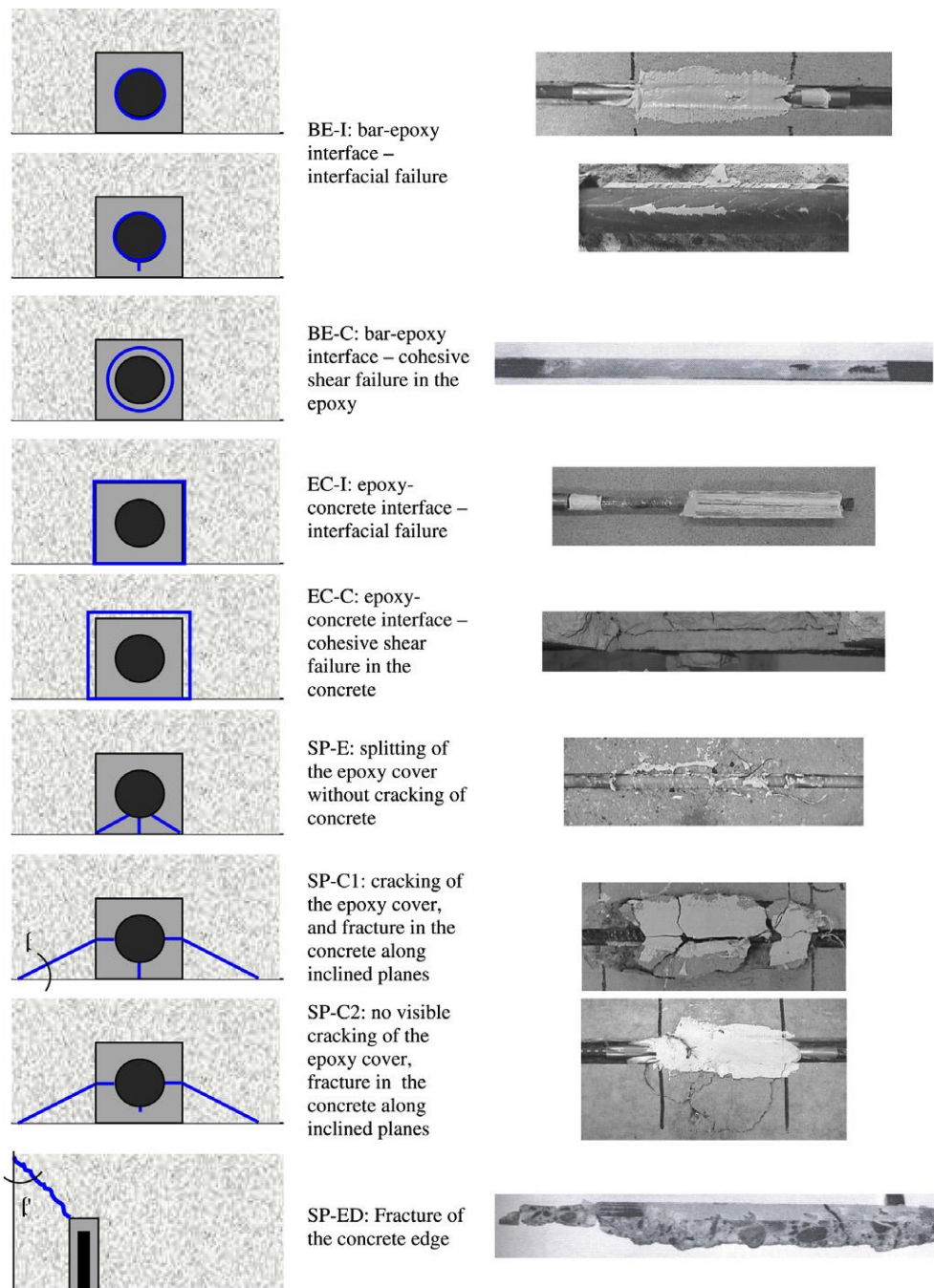
Figure 2-7 De-bonding Origins in NSM Systems (Coelho et al. 2015)

Local level de-bonding

De-bonding at the local level is associated with the material failure. There are two basic types, being:

- Cohesive failure, which is a failure within the material, generally associated with internal shear stress.
- Adhesive/Interfacial failure. This is an adhesive failure between two dissimilar materials and can occur between the reinforcing and the adhesive, or the adhesive and substrate.

In De Lorenzis & Teng (2007) assessment of NSM investigations of these de-bonding failures was further classified into nine sub-types as illustrated in Figure 2-8.



Note: Most figures refer to round bars but modes BE-C and EC-C have also been observed for strips

Figure 2-8 NSM De bonding classifications (De Lorenzis & Teng 2007)

In order to study the bond between the FRP and adhesive in a near surface mounted system, De Lorenzis proposes splitting the analysis into two studies (De Lorenzis 2004). First the longitudinal plane is assessed, this is characterised by the bond stress-slip relationship. Secondly the transverse plane is assessed, in this plane the cohesive/adhesive performance is studied. If there is insufficient interfacial bond the failure will be and interfacial de-bonding, but if there is good bond the forces will be transmitted to the cover material and failure will be as a result of excessive shear stresses

in the cover material. Understanding how these forces transmit from the tensile force on the reinforcement to shear force within the cover material is critical.

Longitudinal Plane Bond Stress - Slip Relationship FRP/Adhesive

The critical component of this study will be to identify the bond slip relationship between the substrate and the reinforcement. This relationship has been studied significantly in regard to concrete and steel reinforcement and is critical in determining the appropriate bond length for reinforcement, typically referred to as development length. There must be sufficient length of bond such that the tensile stress in the reinforcement is equal to or greater than its tensile capacity. If this is not the case, then it is likely that there will be bond failure prior to full utilization of the reinforcement, hence the reinforced concrete member will not perform as expected. This relationship is well understood in traditional reinforced concrete and there are guidelines in the Australian Standards (amongst others) on how to determine development length.

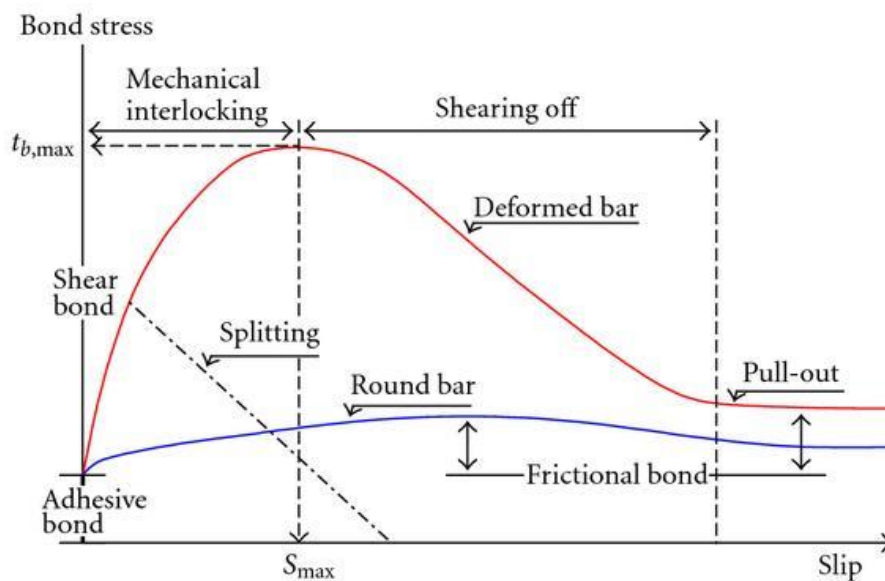


Figure 2-9 Bond Stress - Slip Relationship (Hong & Park 2012)

Bond stress – slip relationship in NSM systems, with its distinct material and interfacial characteristics, requires experimental analysis to develop an understanding. It is essential that the following three components of the bond capacity are fully understood. They are:

- Adhesive Bond – the only adhesive bond will be between the sand coated FRP and the cement matrix. The PVA fibres will not form an adhesive bond to the FRP rod.
- Friction Bond – there will be a friction bond between the sand coated FRP and the ECC adhesive.
- Mechanical Bond – the Mechanical bond is typically found when using deformed bars, the deformations in the reinforcing bars act as shear keys and convert the shear stresses into tensile and compressive stresses. In the ECC FRP relationship the existence of a mechanical bond is unclear as the FRP is only sand coated, non-deformed. However there may be instances where the PVA fibres interlock with the sand particles and provide some level of mechanical bond. This will become clear in the experimental testing.

By completing experimental analysis using a direct shear test it is hoped that the bond stress – slip relationship will be able to be understood and from this an understanding as to whether ECC has sufficient shear capacity to provide effect bond strength to fully engage the FRP rod.

Transverse Plane

To study the transverse plane, the interaction of the confining pressure, the coefficient of friction and the shear stress at the interfacial bond must be understood. Material characteristics such as tensile capacity and ductile performance, play a critical role in transverse analysis as well as reinforcement bar treatment, groove preparation and detailing.

Mathematical Models

The goal of experimental research such as this is to produce and validate mathematical models which can predict the bond strength of an NSM system. This in turn leads to the potential to develop models to predict the positive effect on strength and serviceability of a retrofitted structure.

Due to the various modes of failure numerous models have been produced which have varying degrees of accuracy when applied to the alternate failure modes. It is widely held that the optimum failure mode is cohesive failure in the concrete substrate, refer to failure modes SP-C1 & SP-C2 in Figure 8 (De Lorenzis & Teng 2007). This is based on the fact

that the limiting factor is the original structure and based on this it can be concluded that the introduced reinforcement is fully utilised and strengthening effect maximized. It should be noted however, that this type of failure would be brittle failure, which is contrary to the objectives of this study. As such it is suggested that the goal of the ECC NSM system should be to demonstrate strain hardening prior to cohesive failure of the concrete substrate. This would leverage the safety benefits of the ductility as well as achieving an efficient and effective system.

A bond strength model which is based on a substrate cohesion failure mode was developed by Zhang et al (2014). In this mathematical model the ultimate tensile force in the FRP reinforcement evaluated as a function of bond length, groove detailing, the compressive strength of the concrete substrate and the CFRP characteristics. This model has no input requirements for the groove filler/adhesive as it is only of use when the failure is cohesive failure in the concrete substrate which is induced by the radial pressure from the reinforcement when loaded in tension. Therefore if the failure mode is debonding between the FRP and adhesive or adhesive and concrete substrate the model cannot be used.

2.5 Engineered Cementitious Composites

The investigation into engineered cementitious composites started in the late 1990's. Much of the work completed during this time was produced in some part by Victor C. Li. In 1997 Victor C. Li along with Zhong Lin produced the paper 'Crack Bridging in Fibre reinforced cementitious composites with slip hardening interfaces' (Lin & Li 1997). In this study polyethylene fibres were used and concluded that the strain hardening ('slip hardening' or 'pseudo strain hardening' as noted in the text) is mainly due to the surface abrasion between the fibres and the cement. This is the earliest paper found during the course of this literature review that presents this finding and subsequently leads to many further studies.

The selection of fibres for use in engineered cementitious composites is critical in producing a product with characteristics best suited to a particular application. For example, steel fibres tend to produce a high tensile strength and moderately ductile ECC, Alternatively polyethylene produces an ECC with excellent ductility and moderate tensile strength (Li et al. 1994). PVA fibres have been shown by Horikoshi et al (Horikoshi et al. 2006) to produce engineered cementitious composites with an excellent balance of tensile strength and ductile performance. This is due to its excellent ductile performance and

tensile strength of the PVA fibres. Horikoshi also demonstrated that PVA does not suffer losses in strength from exposure to an alkali environment such as being combined in the cementitious matrix.

Li & Kanda discuss many potential applications for ECC in their 1998 paper 'Engineered Cementitious Composites for Structural Applications'(Li & Kanda 1998). Li also conducted research into the use of ECC with FRP reinforcement and presented his results in 2002. In the paper 'FRP reinforced ECC structural members under reversed cyclic loading conditions', Gregor Fischer and Victor C. Li (2002) concluded that 'Deformation Compatibility between FRP reinforcement and ECC is found to effectively eliminate interfacial bond stress'. In simple terms, the ECC is able to move with the FRP reinforcement when the reinforcing is under strain and prevent de-bonding and spalling of the ECC cover material. These findings are in line with the expected outcomes of the proposed project.

As noted in section 2.4, one de-bonding failure mode is cohesive failure resulting from shear stress in the adhesive. Cohesive failure is a result of excessive shear stress within the material. It is commonly understood that shear strength is directly related to a materials tensile strength. It is for this reason that epoxy adhesives are more commonly used in NSM systems than plain cement paste as they have much greater tensile strength. In another paper by Li et al(1994) Portland concrete, Reinforced(steel) concrete, Fibre reinforced concrete and two distinct types of Engineered Cementitious composites were tested in pure shear. The results showed the ECC materials had a much higher shear capacity than Portland concrete.

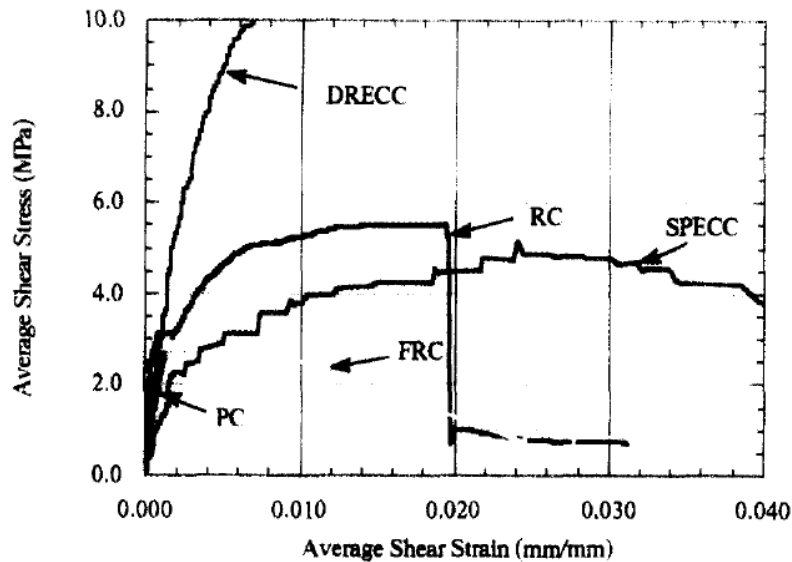


Figure 2-10 Shear Stress/Strain Test results showing Steel fibre ECC(DRECC) with excellent shear strength and PE Fibre ECC with excellent ductility (SPECC). (Li et al. 1994)

As is illustrated by Figure 10, DRECC is a steel fibre ECC, and it showed excellent shear capacity, while SPECC, a polyethylene fibre ECC showed excellent ductility, having the greatest failure strain, an order of magnitude greater than Portland concrete.

In order for the ECC to perform as expected the interfacial bond between the cementitious grout and the PVA fibres has to be reduced. As explained by Li, this can be achieved by coating the PVA fibres in an oiling agent. Obviously this process must be tightly controlled. Too much oiling agent and the bridging strength will be reduced and adversely affect the ductility. Too little oiling agent and the fibres will tend to rupture and adversely impact the bridging strength also. Alternatively (or in combination with an oiling agent) Fly ash may be used to reduce the interfacial bond between the PVA fibres and the cement matrix. Fly ash is also effective in reducing the overall toughness of the matrix which aids ductile performance.

Further Potential Benefits.

Another aspect of engineered cementitious composites which may be of benefit to NSM installation is its potential to “self-heal”. In one recent study, (Qian et al. 2009) ECC was able to demonstrate self-healing properties. A similar study by (Termkhajornkit et al. 2009) was able to demonstrate that concrete with fly ash present were able to demonstrate self-healing capabilities.

This is of importance to the durability of NSM systems using ECC as epoxy adhesives do not have the same properties and may be prone to damage by UV radiation and alkali environments. If ECC can demonstrate suitable durability it will be more likely adopted.

2.6 Finite Element Analysis

At the inception of this project the aim was to attempt to develop a finite element model of a NSM strengthening system using ECC. Unfortunately it was not possible to complete this component of the work within the time frame, however given the amount of work completed in the research phase of this project it has been included in the literature review as it may inform or guide future research into this field.

While there has been no research into producing a finite element model for a NSM system using ECC, the strategy employed during this literature review was to find finite element models which addressed the component parts of the system, namely models for ECC, models for interfacial bonds between adhesive, FRP and concrete.

2.6.1 ECC Models

Kunieda et al (2011) presented a method that accurately simulates a tensile fracture in ECC, this model was compared to experimental results and was found to ‘roughly simulate the mechanical response’.

The Figure 2-11 below is one example if the comparative results from the experiments (Exp.) and the numerical model (Num.).

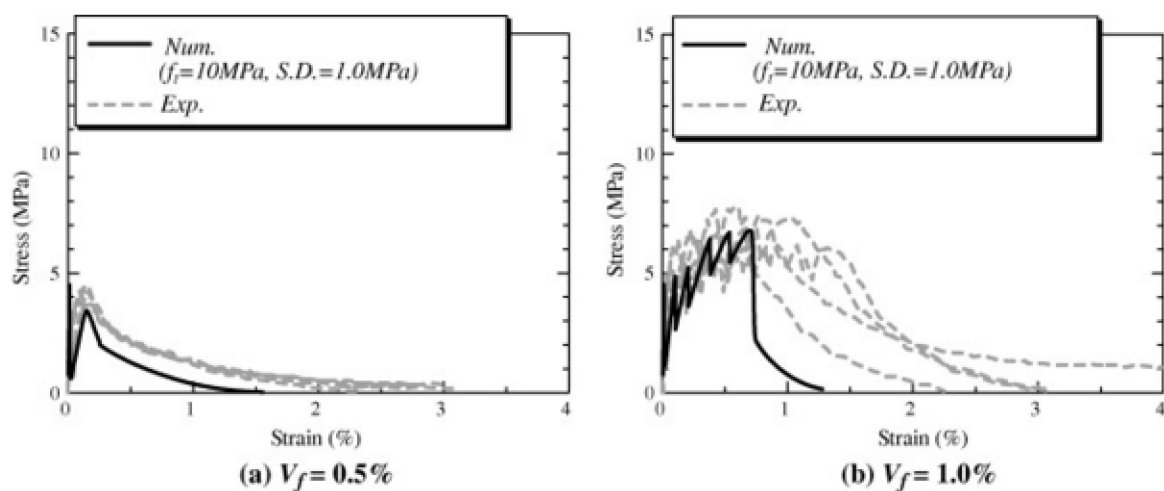


Figure 2-11 Comparison of Numerical Model and Experimental results for Tensile testing of ECC. (Kunieda et al. 2011)

Figure 11 illustrates that Kunieda et al's (2011) model is representative of the behaviour of ECC, however it is quite conservative in comparison to the observed results. The model uses a spring model to simulate the strain hardening behaviour between cells in the matrix.

2.6.2 Interfacial Bonds

Smith and Teng (2001) produced a method to model the interfacial bond between CFRP plates and reinforced concrete structures. This study was focused on surface mounted CFRP reinforcement. Zhang and Teng (2013) were able to present an adaptation of this study that modelled the behaviour of near surface mounted FRP reinforcement. This study presents a comparison between analytical estimates and the finite element model. No experimental comparisons were made.

The finite element analysis literature review to date has highlighted that there seems to be little consideration of friction effect between the concrete and the bonding agent. This boundary tends to be only modelled as a tensile force. Further study into the reasons for this is required as the surface preparation of concrete for structural components such as ground anchors on dams and foundation is considered critical for developing suitable friction factors. It seems strange that the friction effect has been ignored in some models.

Biscaia (2015) however demonstrates a bond slip model that utilises the Mohr–Coulomb rupture criterion that defines the maximum bond stress as a function of cohesion, internal friction angle of the interface material and compressive stress. This model then uses dry friction once the bond has ruptured, suggesting that the cohesion replaces the effect of friction.

This research presents concepts similar to the methods proposed by Strand7 developers, however due to time constraints these were not able to be explored further. It may be an option for future research projects.

2.7 Literature Review Summary

The demand for cost effective systems to strengthen existing structures is only going to increase. In Australia the demand is driven by its vast transport network and evolving engineering standards that are constantly under review to adapt to changes in the environment and community expectations. Repairing and strengthening existing infrastructure is more sustainable than complete replacement, particularly if the remnants of the previous structure are sent to landfill.

Strengthening systems such as surface mounted and NSM have emerged over the past decade not just in academic study but also commercial application due to their performance, cost benefit and ease of installation. The availability and performance of FRP reinforcement has had a significant impact on the level of uptake of these systems as attempting to install steel reinforcing in this manner is very difficult due to the weight of the steel reinforcing. NSM systems also offer advantages over surface mounted FRP, in particular:

- Protection from damage as it is installed in the groove.
- Confinement pressure from the groove aides bond strength
- Finishes flush with existing substrate so surface treatments are not required prior to final surfacing

The use of ECC as an adhesive in a NSM system has some potential benefits over traditional epoxy binders that this research project aims to explore. The cost benefit of ECC over epoxy binders is a marginal saving when compared to the total cost of installing an NSM system on an existing structure. The durability against ultraviolet radiation of the ECC compared to epoxy binders is of significant benefit. It is hoped that the additional tensile strength of ECC will also be a benefit to an NSM system, improving the overall performance. Finally the ductility of ECC is also expected to be of benefit to the NSM system.

On this foundation of research it is hoped that a suitable experimental program will be developed that meets the objectives and potentially inform future research projects.

3 METHODOLOGY

3.1 Experimental Analysis

3.1.1 Method of test

There are a number of ways to test the effectiveness of a near surface mounted system. De Lorenzis and Teng (De Lorenzis & Teng 2007) have discussed the various options and completed a number of studies using the following alternatives:

- Bond pull-out test.
- Beam flexure test.
- Direct shear test.

A Bond pull-out test is the same method as is used to establish required development length for reinforcing bars, typically the bar is cast directly into the base prism rather than being glued in place with an adhesive. While very similar to the elected method of test it is not representative of the system in which the components are used as it is contained on all sides evenly.

A beam flexure test, as detailed by De Lorenzis et al (2002), uses a beam placed under load in 4 point bending. The beam is modified in such a way as to ensure consistent bending around a central hinge at the top of the beam. On one side of the beam the reinforcement is secured with a limited bond length, the other side is fully bonded so as to ensure adequate anchorage such that the side with the limited bond length fails first. While this experimental model more accurately represents the system, De Lorenzis (2002) has demonstrated that results from a simple direct shear test are reliable and consistent with this approach and are much quicker and easier to complete as well as requiring less resources.

The simple direct shear test was selected for this experimental program as it is reliable and relatively cheap and easy to construct samples. It is also much more efficient in terms of resources required to complete the experimental study. There are also significant number of other testing regimes that have used this method which provide data for a comparative assessment of the results.

The logistics of transporting such large samples between Canberra and Toowoomba were impractical, and the results from a direct shear test could be considered just as reliable as beam flexure test, hence the direct shear test was selected.

3.2 Direct Shear Test Design – Sample

The sample used in a direct shear test consists of a concrete prism, the adhesive and the FRP rod.

3.2.1 FRP Rod

The FRP rod for this project was donated by V.ROD Australia. The rod, #3 GFRP, has a nominal diameter, excluding sand coating of ~10mm. This rod was selected based on availability and was an appropriate size for the other testing equipment. For full characteristics please refer to the specification sheet at Appendix 5. This FRP bar is not deformed, it is however coated in a layer of coarse sand to improve the interfacial bond between the bar and the adhesive. This coating gives the bar a typical physical diameter of 13mm.

Deformed FRP reinforcement is available internationally, however, due to low demand it could not be sourced locally. Another locally available option was CFRP rod produced by Sika. This product has a textured finish generated by a layer of peel ply that is removed before installation. Given the expense of this option and the focus of the study the decision was made to use the V.ROD product.

3.2.2 Concrete Prism

The focus of this test is to determine the bond slip behaviour between the ECC, FRP and concrete prism, as such the design of the concrete prism should be completed in a manner which ensures the results are relevant to the study.

Characteristic strength (f'_c)

Two issues govern the selection of concrete strength used in the prism

1. The Tensile strength of the concrete should be sufficient that the bond failure occurs prior to the concrete failure.
2. The characteristic strength should be representative of a typical concrete installation where such a NSM system would be installed.

To satisfy these requirements f'_c of 40MPa was selected. A 40MPa mix with 10mm aggregate was used, this concrete was sourced from a Holcim premix concrete in Canberra. The material was mixed as a larger 13m³ batch and the concrete prisms were cast at the Holcim batch plant. The smaller aggregate size was selected to ensure the aggregate did not introduce planes of weakness and premature failure in the prism.

During the pour of the base prisms a number of samples were taken to confirm the concrete as specified. It was important the strength of the concrete prism was confirmed as the mathematical models used to predict capacity in the NSM system required accurate substrate concrete strength to determine fracture energy. The max concrete strength at 28 days was 41 MPa. The quality assurance test results are available at Appendix 4.

Groove Detail – Width and depth

Le and Cheng (2013) completed a review of previous studies to develop an understanding of the effects of groove detailing on NSM bond strength. Based on this study the optimum groove dimension should be in the range of 1.5 to 2.5d_r, the value selected was 2d_r, given the typical physical diameter was 13mm groove dimensions used was 26mm. Note that the physical diameter of the reinforcing is used in this relationship rather than the nominal diameter of the structural component of the reinforcing rod.

Groove Detail – Edge Distance

The distance from the edge of the concrete to the centre of the FRP reinforcement (a'_e) is a critical dimension in the design of a near surface mounted system. Referred to as edge distance, a'_e should be sized so there is no premature failure of the concrete. Lee & Cheng (2013) references work by Kang et al that suggests an edge distance no less than 40mm to prevent premature failure in the concrete prism. Unfortunately the paper by Kang et al was not able to be sourced prior to the delivery of this report. Based on the summary information provide in Lee and Cheng's report the minimum edge distance should considered a function of the reinforcement size, the reinforcement type, the strength of the base concrete as well as the groove filling material and dimensions. Hassan & Rizkalla (2004) acknowledge this in their studies, suggesting a minimum edge distance of four times the diameter of the reinforcement. This would suggest an edge distance no less than 52mm. An edge distance of 60mm was selected. This simplified the construction of the base prisms and provided further assurance that there would be no premature failure of the base prism.

Groove Detail – Required Bond length

It has been found in numerous studies that average bond stress will increase with bonded length significantly up to a limiting value and then it will begin to decline (Coelho et al. 2015). By determining the maximum shear stress it is possible to better understand the bond stress – slip relationship and then, hopefully, understand the capacity of the adhesive bond between the FRP and ECC.

One particular research project completed by Yan et al (1999) studied effects of bond length on CFRP rod embedded in a concrete prism using an epoxy grout. This study found that the bond stress increased significantly until the bond length reached $9.1d_r$, after which it began to drop off. While this experiment was completed using CFRP and epoxy adhesive, the development of maximum shear stress is linked to the dimensional detail (i.e. nominal diameter of reinforcing rod) and the base prism concrete strength. Based on $9.1d_r$ this would be a 118mm bond length in this system, however the stress values in Yan's experiment for the samples with smaller bond lengths than $9.1d_r$ are higher than the stress values for those with larger bond lengths. This is consistent with other studies (Novidis & Pantazopoulou 2008) that have found a lower bond length ($5d_r$) generates the critical shear stress at the interfacial zones. The different findings could be related back to the type of bars used in each experimental program. In the work by Yan (1999), the bars were either smooth or lightly treated. This resulted in a greater length required before the critical shear stress is generated. Conversely the materials used in Novidis's (2008) experimental program had deformations along their length providing greater mechanical bond, hence the bonded length required to achieve critical stress is less than a non-deformed bar with little to no surface treatment.

The reinforcing used in this experimental program is coated in a coarse sand, with a nominal aggregate size of 1.5mm. This treatment provides the reinforcement with greater mechanical bond than a smooth or sandblasted bar, but less than a deformed bar. A bonded length of 100mm made construction of the samples much easier, this resulted in a bonded length of $7.7 d_r$. This is less than that used for smooth bar and greater than that used for deformed bar. As this is a preliminary study this was deemed sufficiently suitable and one bond length was tested. Variations to bond length may be a suitable progression of this study.

3.2.2.1.1 Anchorage distance

Similar to the required edge distance, anchorage distance refers to the distance between the loaded end of the prism and the start of the bonded length. There are very few research papers that discuss this detail although many suggest the distance should be sufficient to prevent premature failure. This distance is relevant to the loaded end and the unloaded end of the prism.

3.2.3 Final dimensions for prism.

The schematic presented in figure 3-1 details the final dimensions of the concrete prism

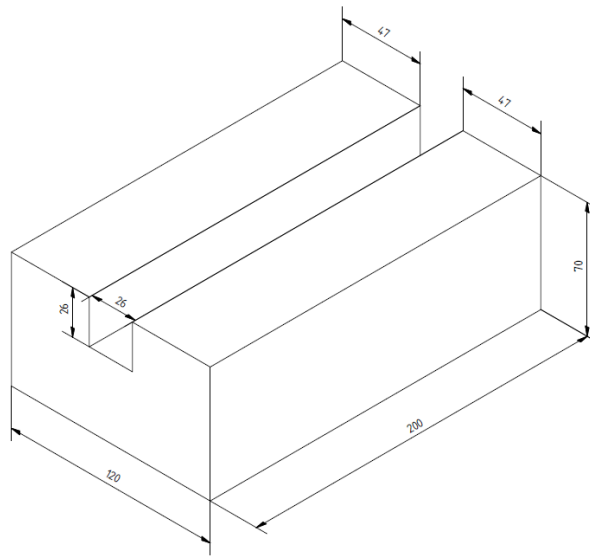


Figure 3-1 Base Prism

3.2.4 Construction of Base Prism

The prism molds were designed to cast the notch into the based using a timber 19mm x 19mm void former. The molds were coated in a lanolin based form release agent (Lanotec) to ease stripping. Once poured they were allowed to cure for 7 days in the mold prior to stripping. This ensured appropriate curing and reduced the risk of damaging the prisms during removal from the form.



Figure 3-2 Prism Molds - Ready for Casting

On the day of casting the prisms, two test cylinders were cast to confirm the concrete would reach the desired 40 MPa. A slump test was also completed, the result was 90mm slump. This was in line with the anticipated results. The results of this test are available at Appendix 4.



Figure 3-3 Concrete Testing On Prisms



Figure 3-4 Base Prisms Cast

Once stripped from the forms, the prisms grooves were cut to final dimensions using a diamond blade. This process was essential to remove any residual form release agent from the groove and also to remove the layer of laitance typically found in the first 1-2mm of a concrete casting. The process also ensured the surface roughness would be the same as a typical a near surface mounted installation. The slight uneven surface generated by the diamond blade provides a slightly better surface to assist bond performance between the ECC and the prism. It was also necessary to ensure the surface was relatively uniform to ensure no unexpected stresses were introduced to the system.



Figure 3-5 Prisms Stripped ready for final notch detailing.

3.2.5 Engineered Cementitious Composite.

There has been significant study completed on ECC mix design. In order to reduce the volume of physical testing required for this project and reduce the demand for the Expensive PVA fibres, an exemplary mix design based on the work by Wang & Li(2005) was used in this project. This mix design has also been further in works by Zhuge (2014) and Hesse (2014) so there is a significant amount of experimental data that can be utilised by this research project .

After considering the goals of the research project, four adhesive types were tested.

- Sample Set C1 – This samples set will be a simple cementitious paste with no fibres or fly ash. The purpose of this set is to get a simple understanding of the typical failure mode that should be expected using cement paste without any fibre reinforcement and low ductility
- Sample Set ECC1 – This sample set is used to compare the capacity and failure mode of exemplary mix design. It is expected that the fibre content will improve tensile capacity but still demonstrate little ductility.
- Sample Set ECC2 – This sample set will be based on Wang & Li’s exemplary mix design(Wang & Li 2007). The mix, identified as M45, has been proven to demonstrate the highest ductility of all the PVA based ECC mix designs. The key characteristics are a 1:1.2 cement/fly ash ratio and 2% super plasticiser.
- Sample Set ECC3 – This sample set will be a variation of the M45 mix design. The difference will be a superplasticiser content of 1%. This variation is being tested to assess the workability of the ECC adhesive rather than the capacity of the NSM system

- Sample Set ECC4 – This sample set will be another variation of the M45 mix design. In this case no superplasticiser will be used. It has been noted in some literature that ECC with little or no fly ash content require the super plasticiser to avoid clumping, however it is hoped the high proportion of fly ash in this mix will aide mixing and avoid clumping of the fibres. This variation is being tested to assess the workability of the ECC adhesive rather than the capacity of the NSM system

Expected variations in performance

The ECC is expected to demonstrate a level of ductility, so once peak load is achieved the bond should reduce in a controlled fashion before reaching residual friction stress between the ECC and reinforcement or prism, dependant on the failure mode. A typical cementitious grout will have very little tensile strength and it is expected to demonstrate a brittle failure once peak stress is reached. Therefore it is expected that the failure will be sudden and catastrophic with little or no residual strength. The zero fly ash mix, ECC1, should demonstrate greater tensile strength but little ductility. Wang & Li (2007) has identified that fly ash plays a critical role in the ductility of ECC. Fly ash reduces the cohesive bond between the PVA fibres and the cement matrix, this allows the PVA fibres to slip a little before taking load. This characteristic is critical in achieving a ductile behaviour.

Table 3-1 Adhesive mix designs

Mix ID	Cement	Water	Sand	Super-plasticiser	PVA Fibre
Cementitious Grout	1	0.25	0.363	2%	0
ECC 1 (No fly ash, reduced ductility)	1	0.25	0.363	2%	2%
ECC 2 (Li M45 Mix fly ash)	1 <i>Ratio of 1:1.2 Cement:fly ash</i>	0.25	0.363	2%	2%
ECC 3 (Reduced S.P. to improve overhead workability)	1 <i>Ratio of 1:1.2 Cement:fly ash</i>	0.25	0.363	0.5	2%
ECC 3 (Zero S.P. to improve overhead workability)	1 <i>Ratio of 1:1.2 Cement:fly ash</i>	0.25	0.363	0	2%

Based on the results of Hesse’s work (Hesse 2014), the ECC2 mix should demonstrate the characteristics as detailed in Table 3-2. The ECC2 mix will be used to compare the experimental results with predicted results based on mathematical models. The other mix designs are to be used to compare failure modes and workability. Further research will be required if these mix designs demonstrate greater performance than the ECC2 mix design. This is beyond the scope of this project.

The amount of superplasticiser should have no effect on the potential strength of the various mix designs, it is simply an admixture utilised to prevent clumping of the fibres. Any variation in strength would be a result of reduced workability and uneven distribution of fibres throughout the ECC adhesive.

Table 3-2 ECC Characteristics – Previous Studies

Engineered Cementitious Composite Characteristics (Hesse 2014)	
Compressive Strength (MPa)	Ultimate Tensile Strength (MPa)
65	5

3.2.6 ECC Materials

ECC consists of the following

- Cement – The cement used in this project was Cement Australia G.P. Cement Powder
- Fly ash – The fly ash was also a Cement Australia bagged product.
- Sand – The sand used in this was River Sands W9 filter sand. In order to comply with Li’s exemplary mix design the sand had to be sieved further to ensure there were no particles greater than 250 µm.
- PVA Fibres – PVA fibres provide the critical tensile capacity and strain hardening characteristics found in ECC materials. The PVA fibres used were Nycon – PVA RECS15

Table 3-3 Samples Summary

Sample Group	Number of Samples	Adhesive
C	6	Cementitious Grout
ECC1	6	ECC1
ECC2	6	ECC2
ECC3	2	ECC3
ECC4	2	ECC4

3.2.7 Building the samples

The C and ECC1 samples were made on the 7th April within 1hr and allowed to cure for 28 days prior to testing. The ECC2-4 samples were made on 18th August within 2 hrs of each other.

To ensure a 100mm bond length the reinforcing rod was held in place with extruded polystyrene foam cubes. The foam cubes had 13mm holes drilled, the loaded end cubes had full penetration and the non-loaded end cubes were only drilled 5mm to hold the reinforcing bar. The cubes were set exactly 100mm apart with a silicon sealant used to hold the cubes in place. The sealant also ensured any cement slurry was not lost during curing.

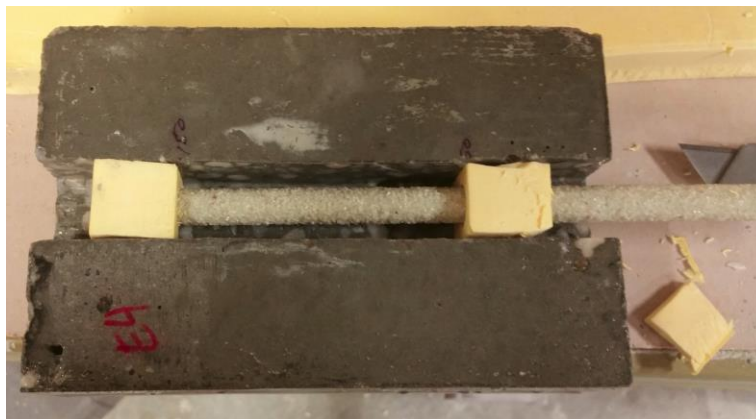


Figure 3-6 Prism and reinforcing rod setup ready for ECC adhesive. The Prisms were washed thoroughly prior to remove any dust that may affect the bond strength.

All adhesives were mixed using the recommended mix procedure from Wang & Li (2007). This consisted of a 5 minute mix of all the dry ingredients, to ensure the cement, fly ash and PVA fibres were well combined. It also gave the PVA fibres a chance to separate as they tended to clump when stored together. The super plasticiser (when used) was then mixed with the water prior to introduction to the dry mix. Once the water was added, the materials were mixed for a further five minutes, with consistent checking to ensure all the material was being introduced to the mix.



Figure 3-7 All materials ready for mixing. Note: syringe was used to measure out super plasticiser.

Once the ECC was thoroughly mixed it was allowed to rest for 5 minutes prior to placement. The ECC was placed from one side carefully to ensure the notch was completely filled and no air pockets introduced underneath the reinforcing rod. A small pointing trowel was used to work the ECC adhesive into the groove and finish off the ECC to a neat finish on top. Discussion on the mixture consistency and workability is included in the results chapter.



Figure 3-8 Completed Specimen shortly after ECC pour.

3.2.8 Tensile Testing

The testing was carried out in the laboratory at the Centre for Excellence in Engineered Fibre Composites (CEEFC), Toowoomba, using the MTS Insight 100 tensile test machine.



Figure 3-9 Tensile Test Machine MTS Insite 100 (MTS 2011)

Using the Tensile test machine the force and displacement were measured until failure and resistance was 0 or residual stress levels had been reached. The tensile test was completed using displacement control method at 1mm/minute. In order to hold the samples in place a testing frame was designed and fabricated to hold the prism down while allowing free movement of the FRP reinforcement.

3.2.9 Design of Testing Base

The testing base was designed with a capacity of 80kN, this was based on the maximum tensile strength of the FRP rod. In the event that something unforeseen occurred within the prism and the ECC & concrete did not break, the maximum tensile capacity of the GFRP would become the highest failure load. This is overly conservative, but given the scale of the base it was not un-economical

The uprights were spaced so the sample could be inserted with the FRP rod protruding through the load plate so there would be no need to bolt down the sample. The gap between the uprights also provided a window that would allow observations during the testing. The uprights were fabricated using 90 x 90 equal angle to provide sufficient weld length and also sufficient depth to ensure no eccentricities were introduced when the FRP rod was loaded. Finally, a web plate was welded between the top plate and uprights to prevent any uneven deflection in the top plate under load.

Design, in particular the determination of the welded connections, of the base was based on the Australian Institute of Steel Construction, Design Capacity Tables for Open Sections (ASI 2009).

The base was fabricated using grade 350 steel and a combination of 16mm plate and 90x90x6 Equal angle welded together using 5mm G.P. fillet welds.

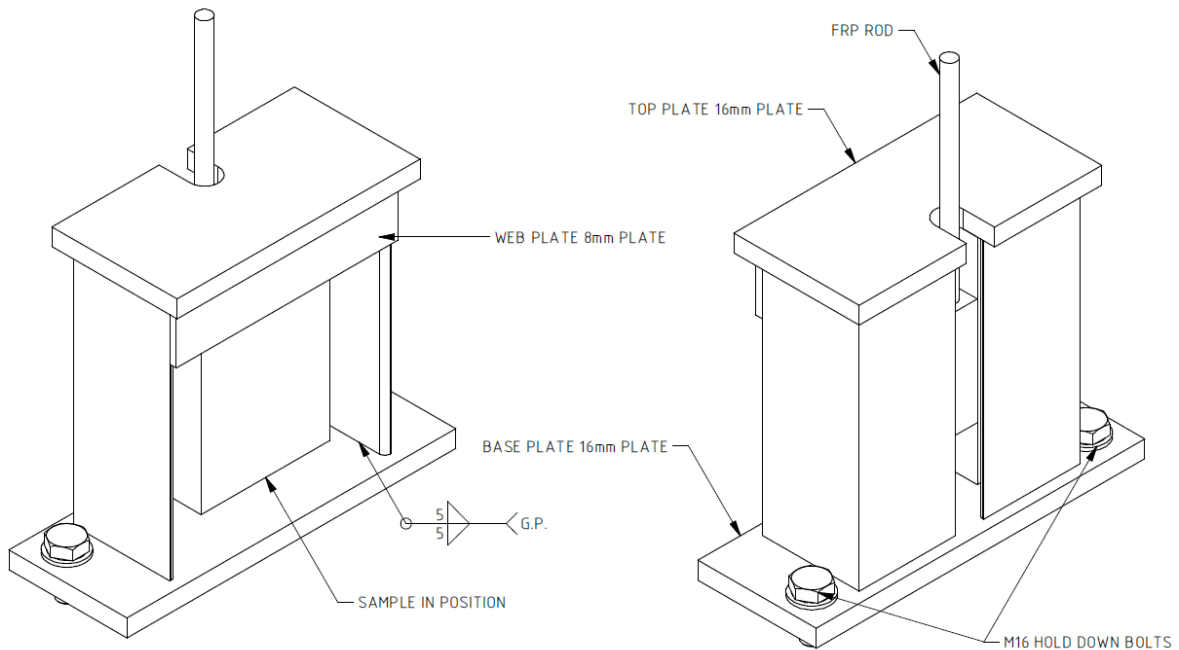


Figure 3-10 Test Base, Isometric View.

The Equal angle sections (90x90x6) were selected to match the geometry of the sample, their axial capacity is 240kN each. The critical element in the design was the weld length connecting the uprights to the base plate and the load plate. A quick check of the length of weld connecting the uprights confirms that there is a significant factor of safety in this connection.

$$\text{Minimum Tensile strength of \#3 GFRP V-Rod} = 1100\text{Mpa}$$

$$\text{Nominal Cross Sectional Area} = 71.3\text{mm}^2$$

$$\text{Failure load of GFRP} = 1100 \times 71.3 = 78430\text{N}$$

$$\text{5mm G.P Fillet weld capacity} = 0.7\text{kN/mm}$$

$$\text{Millimetres of 5mm G.P. Fillet weld required} = 78.4/0.7 = 112\text{mm}$$

$$\text{Millimetres of 5mm G.P. Fillet weld completed} = 540\text{mm}$$

$$\text{F.O.S.} = 4.8$$

The rig is held to the test base using 2 M16 grade 8.8 bolts which have a tensile capacity of 66.5 kN each, this provides a F.O.S. of 1.7.

Given it is unlikely that the test will reach this load and the speed of displacement, a failure in the base rig would not be explosive. After all the tests were completed the test base proved very effective and has been donated to the University for future testing.

Once installed on the Insite 100 machine, a dial gauge, accurate to 1/100th millimetre was setup to test for deflection between the Insite base plate and the top of the base prism. There was no recorded deflection.



Figure 3-11 Testing Base

3.3 Dye penetration

Upon completion of the testing the samples were subjected to a dye penetration test. This is something typically reserved for steel materials however it was employed to help identify the failure planes within the various samples to try and identify particular patterns. It works on the basis that the dye will find its way by the path of least resistant, and provided the dye is sufficiently low viscosity, it will track through the cracks, staining the areas as it passes through, making it easier to identify the cracks.

3.3.1 Method

After the testing was complete the samples were trimmed with a diamond saw to expose the loaded and unloaded ends of the bonded section. The Samples were stood on the loaded end and a liberal amount of red dye was dropped onto the non-loaded end of the FRP. The non-loaded end was used as the loaded end had a collar of ECC material that had pulled out on during the tensile testing. The idea being the dye would follow the cracks generated by the failure planes through the bonded length. The dye was given an hour to dry before 5mm was trimmed off, this removed the surface stained portion and expose, if present, the red stained cracks.

It is important to note that this is not a statistical test method. It is a means to assist observation of the test results by highlighting the cracks and failure planes.

This test was not completed on the C1 sample set as the failure mode was too catastrophic and it would provide no significant input to this research project.

3.4 Post processing of raw data

3.4.1 Correction for initial settlement

With all samples there was a settling in process which included the vice grips getting enough grip as well as the prisms achieving correct bearing onto the load plate of the test base. A two stage process was used to eliminate this false reading and correct all subsequent slip values.

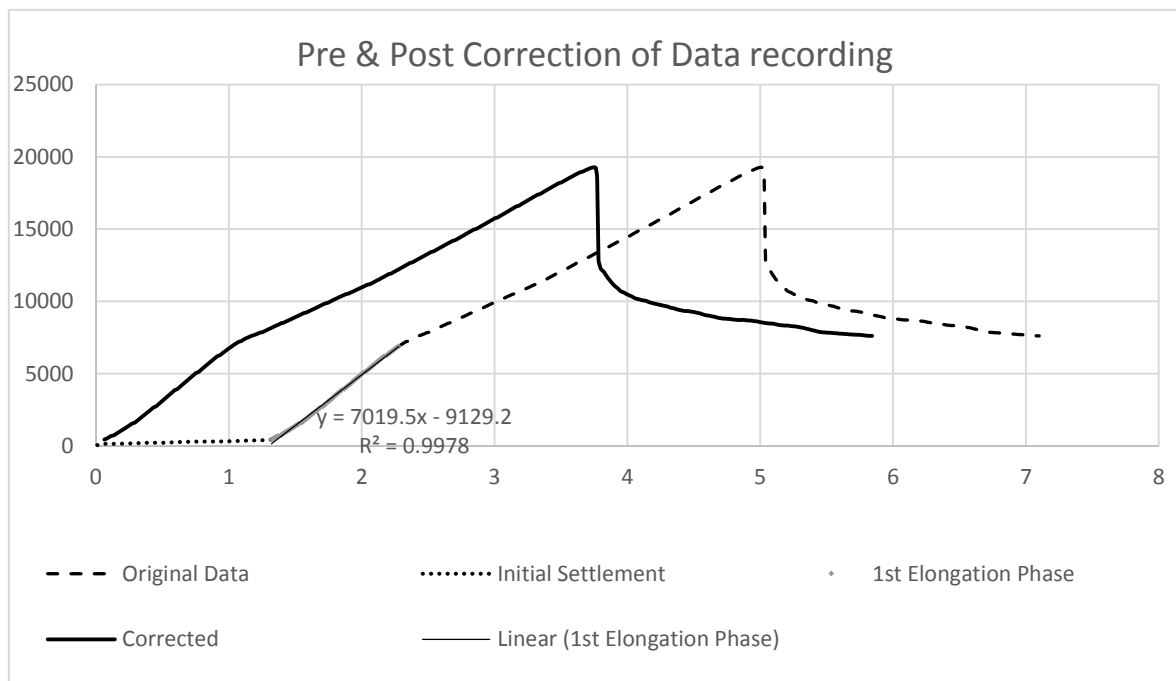


Figure 3-12 Correction of data for initial slip

The process is illustrated in figure 3-12 above. The initial settlement phase was identified visually from the original data plot. It was relatively simple to identify the limits of the initial settlement phase. Once this was removed the first elongation phase was identified and used to determine a line of best fit.

3.4.2 Example of Correction method Using Sample ECC3-1

1. Data points 1 -124 represent the initial settlement

2. Data points 125 – 215 represent the 1st phase of elongation, from this subset linear regression is used to extract a line of best fit using Microsoft Excel. The quality of the fitted curve is checked using the R squared value, in this case it is 99%. The Resultant equation;

$$P = 7019.5s - 9129.2$$

3. The Curve needs to originate at 0 so the -9129.2 is dropped;

$$P = 7019.5s$$

4. Using this equation and the known force value for the initial value in the first phase of elongation the corrected slip can be calculated;

$$P = 7019.5s$$

$$442 = 7019.5s$$

$$s = \frac{442}{7019.5}$$

$$s = 0.063 \text{ mm}$$

3.4.3 Correction for Elongation in the FRP

Given there would be significant length in the FRP bar it was elected to use the published tensile modulus to determine the elongation in the bar at a given load and deduct that value from the slip value.

$$\varepsilon = \frac{\Delta l}{l} = \frac{\sigma}{E} \text{ therefore}$$

$$\Delta l = l \left(\frac{\sigma}{E} \right) \text{ where } l = \text{length of bar between bonded length and machine grips}$$

Given force P is known, the formula becomes

$$\Delta l = l \left[\frac{(P/A)}{E} \right]$$

3.4.4 Calculation of Bond Stress

As the bar being use was non-deformed bar, the system will depend on the cohesion between the ECC and the FRP as well as the friction generated by the sand coated surface on the FRP bar. This will be Therefore the ultimate bond stress was calculated based on the bonded length and the nominal bar diameter.

$$\tau_{ult} = \frac{P}{\pi d_r L_b}$$

4 RESULTS

The following chapter will present the results of the testing, with further discussion to follow in the next chapter.

4.1 Sample Set C1 Summary Results

Table 4-1 Sample Set C1 Quantitative Result Summary

Number of Samples	Average Ultimate load (kN)	Average Ultimate Bond Stress (MPa)	Max Ultimate Load (kN)	Max Average Stress (MPa)	Average Slip at ultimate load (mm)
6	27.5	7.0	30.1	7.7	4.5

Table 4-2 Sample Set C1 Qualitative Observations

Typical Failure Mode	Number of Erroneous Results	Workability
Brittle Failure, Cover cracking in cementitious adhesive.	1 – Prism cracked in half during test. Removed from dataset	Extremely Flowable, self-consolidating paste.

4.1.1 Discussion

Workability

The cementitious paste was what could be described as high flow, completely incapable of supporting itself in any particular shape. This made filling the grooves very easy from above, however it would have been impossible to install the paste in an overhead application. It may have been possible to install this paste in a vertical application with the use of a water tight form, however this would require significant work to ensure the cement paste was injected into the form in a manner that did not trap air resulting in air pockets in the adhesive. The cement paste was easily finished by screeding off with a flexible steel blade. No further work was required.

Curing

Initial hardening occurred within four hours of mixing with nominal bleed water still present five hours after initial set.

Performance

The Average Ultimate load was 27.5kN, with a range of 5.7kN. The standard deviation of the results was 2.8kN, and given all results were within two standard deviations from the average, minimum recorded value was 1.1 standard deviations from average and maximum value was 0.96 standard deviations from sample average. Based on this, the sample set generated reasonably consistent results.

The purpose of this sample set was to witness and understand the typical failure mode of cementitious paste. Every one of the samples failed by adhesive cover splitting. This failure mode was sudden and catastrophic, in one instance the shock of the failure resulted in the entire base prism splitting longitudinally. This failure mode is consistent with other studies and demonstrated that the weakest component of the NSM system was the internal tensile capacity of the cement adhesive.



Figure 4-1 Cover splitting in Sample C1-1

The average failure strain along the bonded length of the rod was 4.5%. Considering the typical failure strain of concrete is 0.3% it is apparent that there is slippage present in the system. There are three regions this slippage could be occurring;

- Interfacial bond between sand coating and FRP – epoxy generally has lower modulus (Epoxy 4 GPa (Malano 2008), Concrete: 30GPa (SAI 2013)) so it will demonstrate higher strain for a given stress.
- Interfacial bond between the FRP rod and the cement paste - as the cement paste matrix interlocks with the sand coating on the FRP rod.

- Interfacial bond between cement paste and concrete substrate.

It is also worth noting that the strain values could be a combination of the above values.

4.2 Sample Set C1 Detailed Results

Table 4-3 Sample Set C1 Detailed Results

Sample ID	Ultimate Load (kN)	Ultimate Bond Stress (MPa)	Measured Slip (mm)	Corrected Slip (mm)	Failure Mode
C1-1	24.6	6.3	5.8	4.8	Brittle
C1-2	28.7	7.3	5.8	4.7	Brittle
C1-3	24.4	6.2	4.6	3.7	Brittle
C1-4	30.1	7.7	5.8	4.7	Brittle
C1-5	29.8	7.6	5.5	4.4	Brittle

4.3 Sample Set C1 Graphical Results.

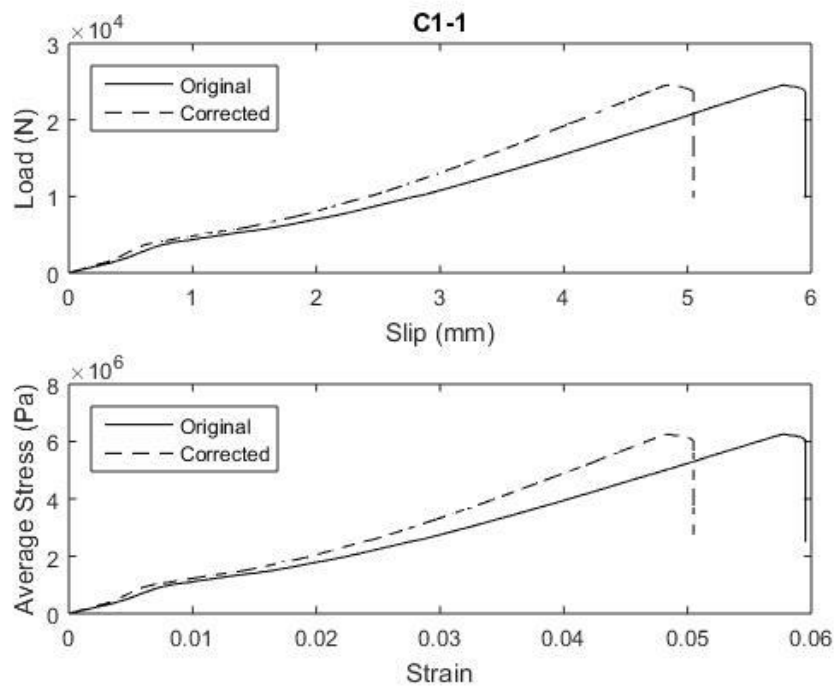


Figure 4-2 Load/Slip & Stress/Strain Relationship, Sample C1-1

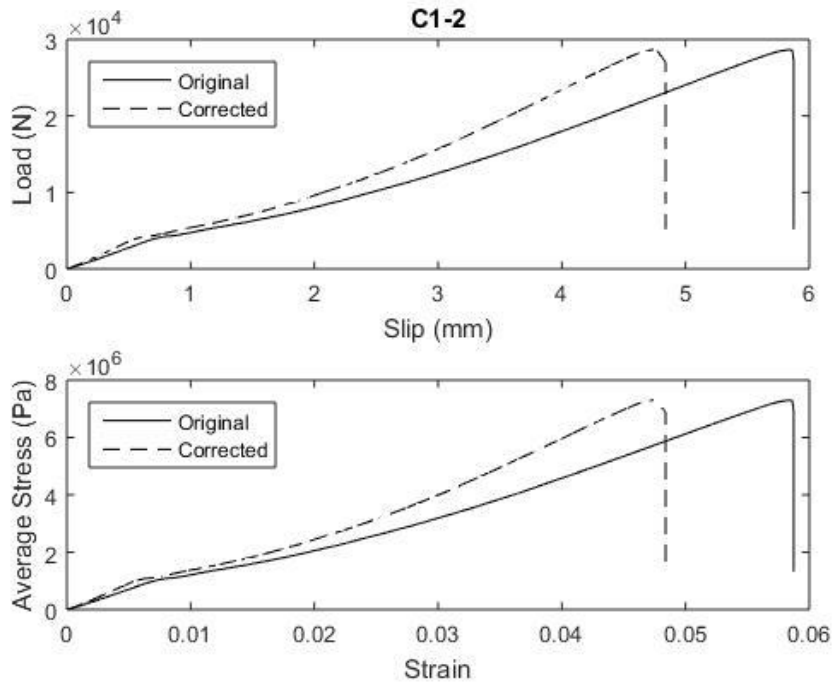


Figure 4-3 Load/Slip & Stress/Strain Relationship, Sample C1-2

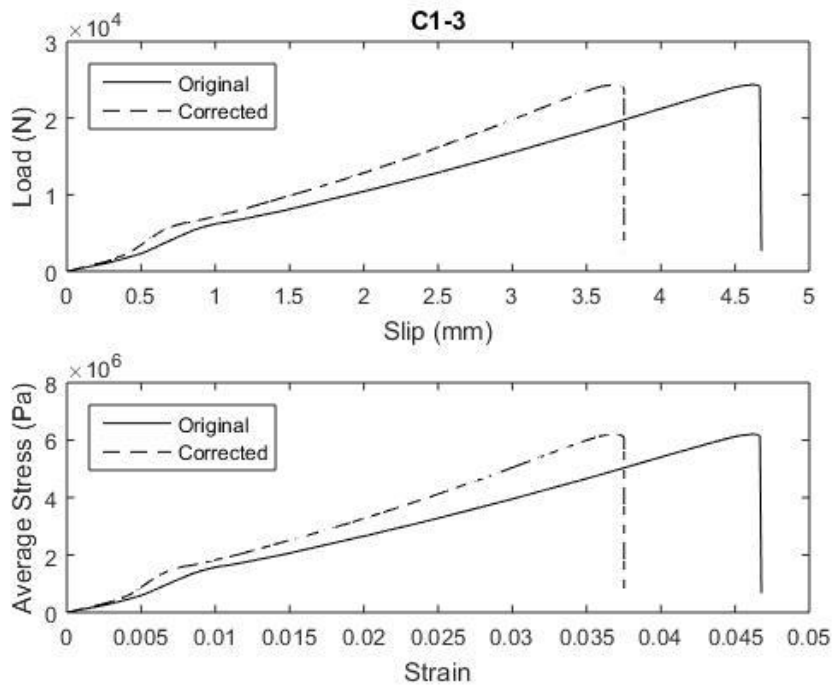


Figure 4-4 Load/Slip & Stress/Strain Relationship, Sample C1-3

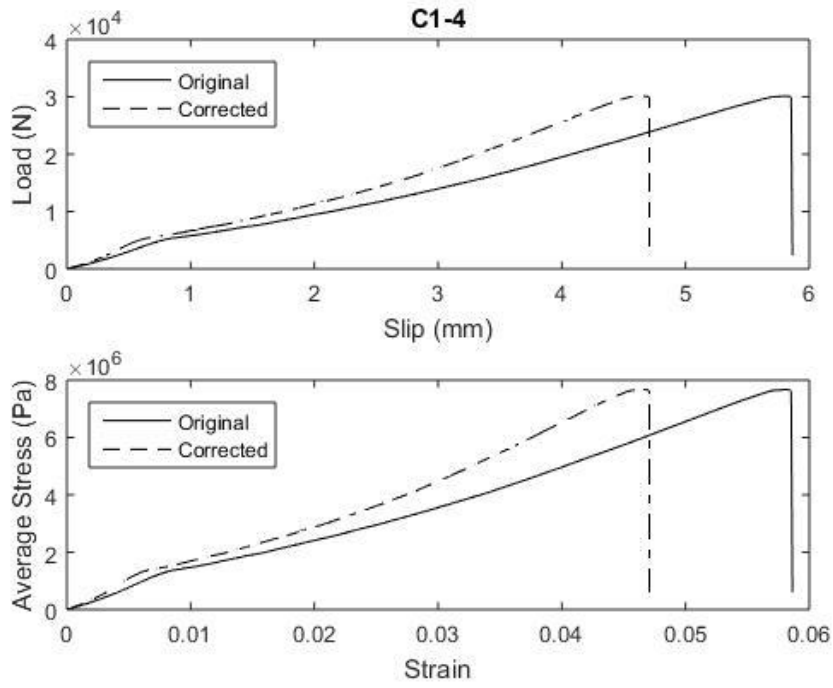


Figure 4-2 Load/Slip & Stress/Strain Relationship, Sample C1-4

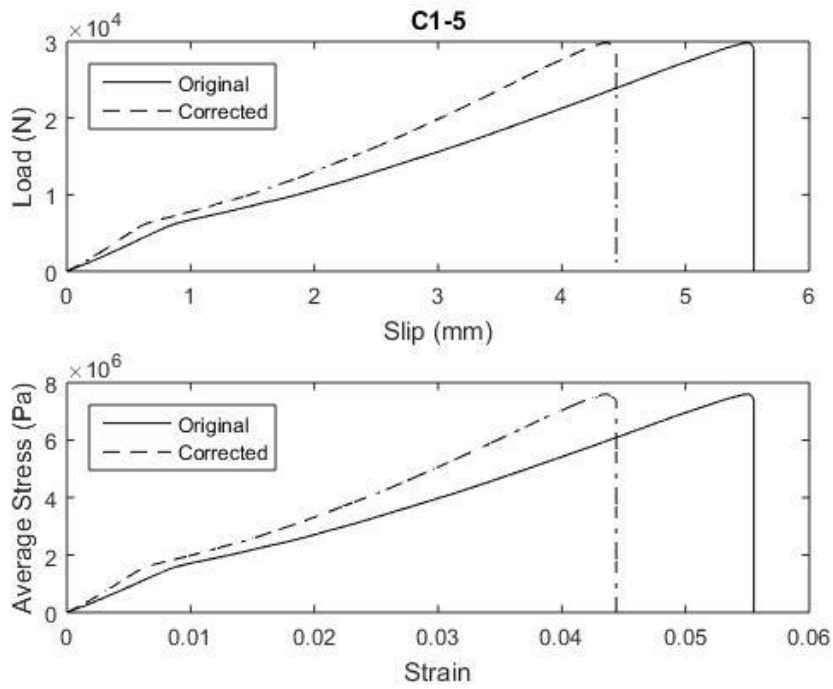


Figure 4-6 Load/Slip & Stress/Strain Relationship, Sample C1-5

4.4 Sample Set ECC1 Summary Results

Table 4-4 Sample Set ECC1 Quantitative Results Summary

Number of Samples	Average Ultimate load (kN)	Average Ultimate Bond Stress (MPa)	Max Ultimate Load (kN)	Max Average Stress (MPa)	Average Slip at ultimate load (mm)
6.0	37.7	9.6	38.9	9.9	7.0

Table 4-5 Sample Set ECC1 Qualitative Observations

Typical Failure Mode	Number of Erroneous Results	Workability
Some Strain Hardening followed by brittle Failure, de-bonding of sand coating on FRP bar	1 – Premature Failure of Prism, bottom corner broke off. Removed from dataset	Flowable, self-consolidating paste. Consistent distribution of fibres

4.4.1 Discussion

Workability

In the wet condition the ECC1 paste was very flowable. This resulted in an even distribution of fibres throughout the adhesive. The fibres did have an effect of holding the matrix together to some extent, but they could not hold it sufficiently for the paste to support a solid form without containment. The groove was easily filled and a little work was required to ensure the fibres surrounded the FRP reinforcement on all sides. This was achieved using a plastic spatula to work the fibre and matrix into the groove. Once filled the ECC1 paste was screeded off with a flexible steel screed to achieve a smooth finish. This process was difficult as the screeding process tended to grab the fibres, pulling them out of the matrix and making it hard to produce a smooth finish.

Before initial hardening it was observed that the matrix was consolidating leaving some fibres exposed, made evident by the white fibres becoming visible as the matrix receded. To remedy this the groove was overfilled and allowed to partially set. Before initial set occurred the stiffening ECC1 paste was screeded off level with the concrete base prism with care being taken not to pull out fibres in the process. This resulted in a reasonable finish with few fibres exposed, but still not as good a finish as the C1 cementitious paste.

Curing

Initial hardening occurred within four hours of mixing with nominal bleed water still present five hours after initial set. The bleed water present seemed less than that of the C1 cementitious paste.

Performance

The Average Ultimate load was 37.7kN, with a range of 3.6kN. The standard deviation of the results was 1.5kN, all results were within two standard deviations from the average, minimum recorded value was 1.7 standard deviations from average and maximum value was 0.8 standard deviations from sample average. With a standard deviation value less than 5% of the average ultimate load, the sample set generated very consistent results. Further to this, the onset of strain hardening behaviour consistently occurred between 30kN and 34 kN.

The average failure strain along the bonded length of the rod was 7%, this value was over 1.5 times that of the C1 cementitious paste. The typical strain value at the onset of strain hardening was between 3.8% and 5%. These values are consistent with the failure strain from the C1 cementitious paste. This indicates that strain hardening occurred when the cementitious matrix tensile strength was overcome by the tensile loads leading to the development of the tensile cracking in the matrix. The PVA fibres were clearly engaged once the crack propagated leading to crack bridging and the onset of strain hardening behaviour.

The strain hardening behaviour observed led to approximately 5kN increase in ultimate load capacity with ECC1-4 demonstrating the greatest increase of 8.2kN. The greatest strain increase was ECC1-3 which saw an increase from 4.7% to 7.7%.

However once the load reached ultimate load the failure was brittle and catastrophic as is evident in figure 2-7 below. This result was not entirely unexpected as the ECC1 paste did not contain any fly ash, which as discussed previously is required for the ECC to demonstrate ductile behaviour.



Figure 4-3 Sample Set ECC1 Typical Failure Mode - Brittle

Upon closer examination of the extracted FRP bar it became evident that there had been some de-bonding between the sand coating on the FRP bar in addition to de-bonding between the ECC1 Paste and the FRP bar. In *figure 4-4* region of de-bonded sand coating is circled. The red hue in the remaining sand coating is from the inspection dye used to check the location of the cracking in ECC1 adhesive. This event was unexpected suggests the NSM system could have greater capacity if the epoxy adhesive used on the sand was greater strength or an alternative mechanical bond device was used.



Figure 4-4 ECC1 FRP bar showing sand coating de-bonding

Once the FRP was removed and the sample cut it was clear that the ECC1 paste was dense and free of visible air voids. *Figure 4-5* below shows the cross-section of the sample.



Figure 4-5 Cross Section of ECC1 sample showing dense adhesive and no apparent air voids.

4.5 Sample Set ECC1 Detailed Results

Table 4-6 Sample Set ECC1 Detailed Results

Sample ID	Ultimate Load (kN)	Ultimate Bond Stress (MPa)	Measured Slip (mm)	Corrected Slip (mm)	Failure Mode
ECC1-1	35.3	9.0	7.0	7.0	Strain Hardening followed by Brittle
ECC1-2	38.0	9.7	9.6	9.2	Strain Hardening followed by Brittle
ECC1-3	38.9	9.9	9.3	9.2	Strain Hardening followed by Brittle
ECC1-4	38.8	9.9	9.5	9.2	Strain Hardening followed by Brittle
ECC1-5	37.7	9.6	8.0	7.8	Strain Hardening followed by Brittle

4.5.1 Sample Set ECC1 Force/Slip and Bond Stress/Strain Relationships

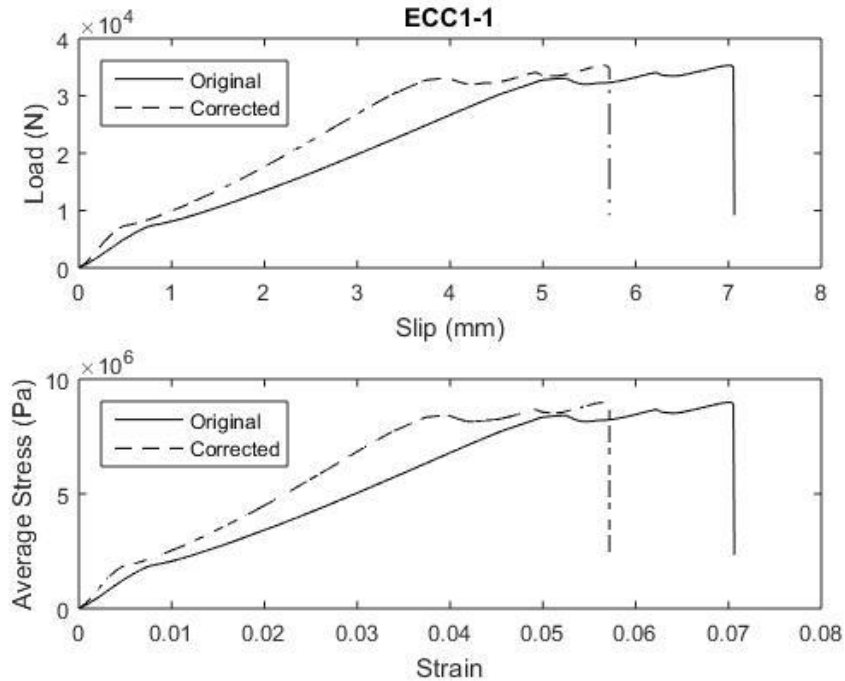


Figure 4-6 Load/Slip & Stress/Strain Relationship, Sample ECC1-1

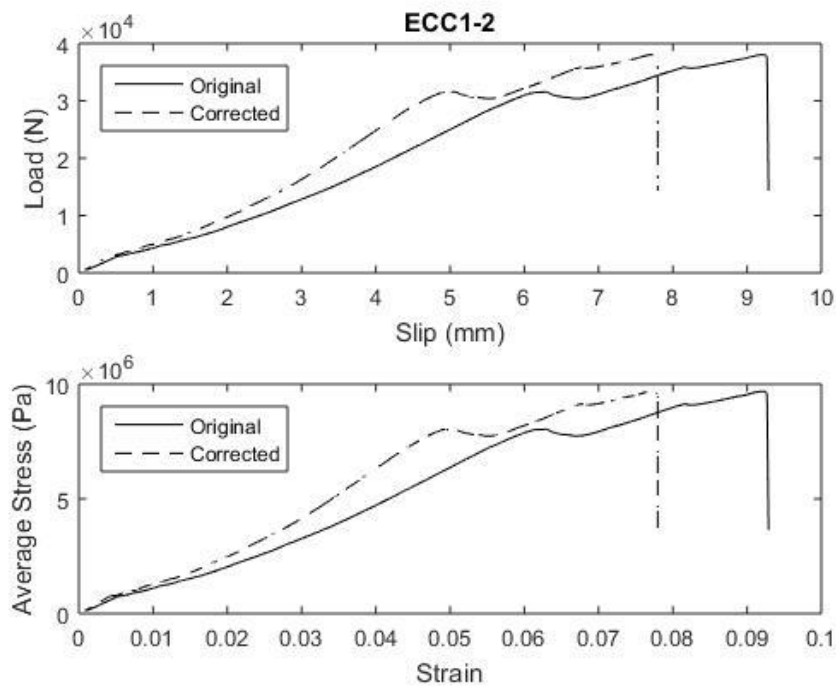


Figure 4-7 Load/Slip & Stress/Strain Relationship, Sample ECC1-2

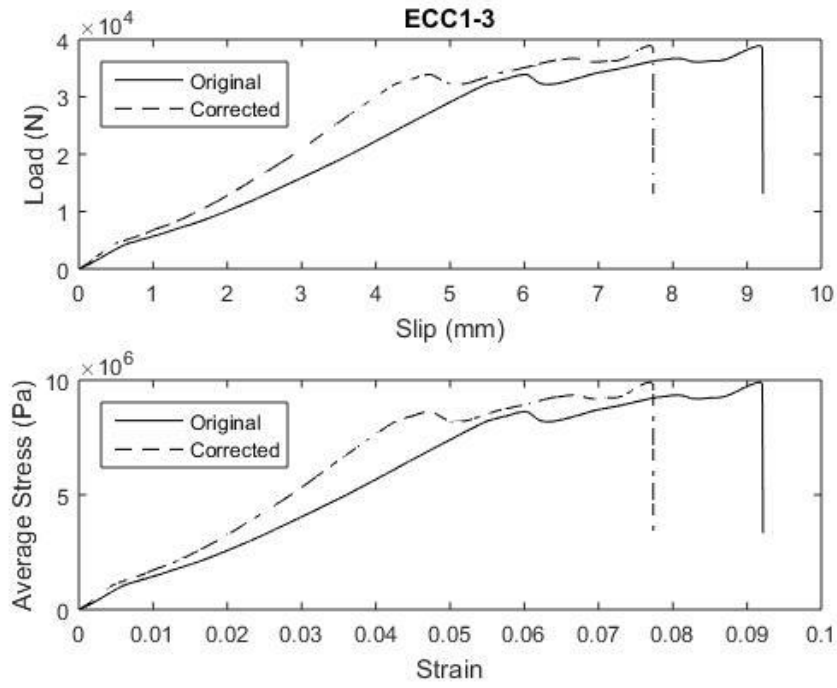


Figure 4-8 Load/Slip & Stress/Strain Relationship, Sample ECC1-3

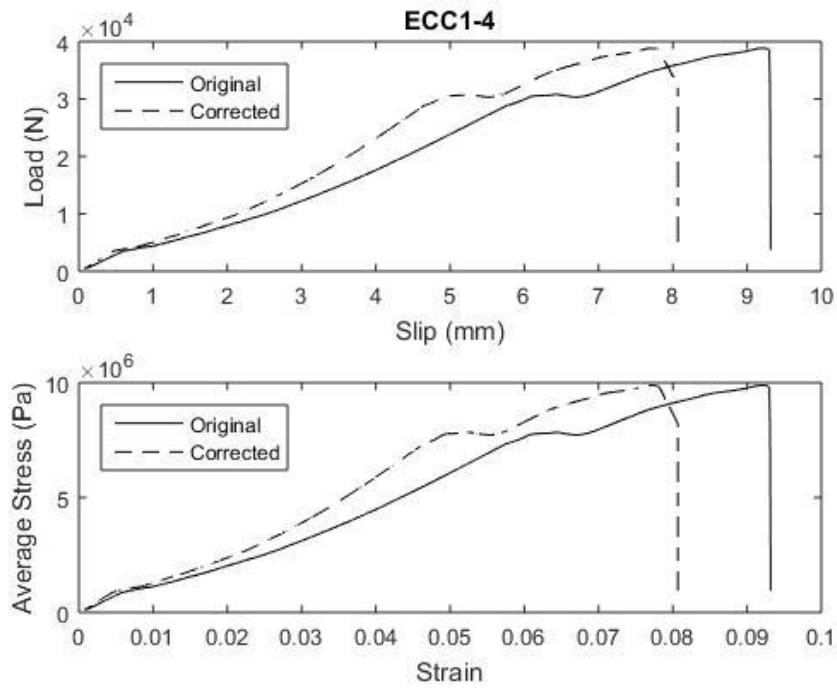


Figure 4-9 Load/Slip & Stress/Strain Relationship, Sample ECC1-4

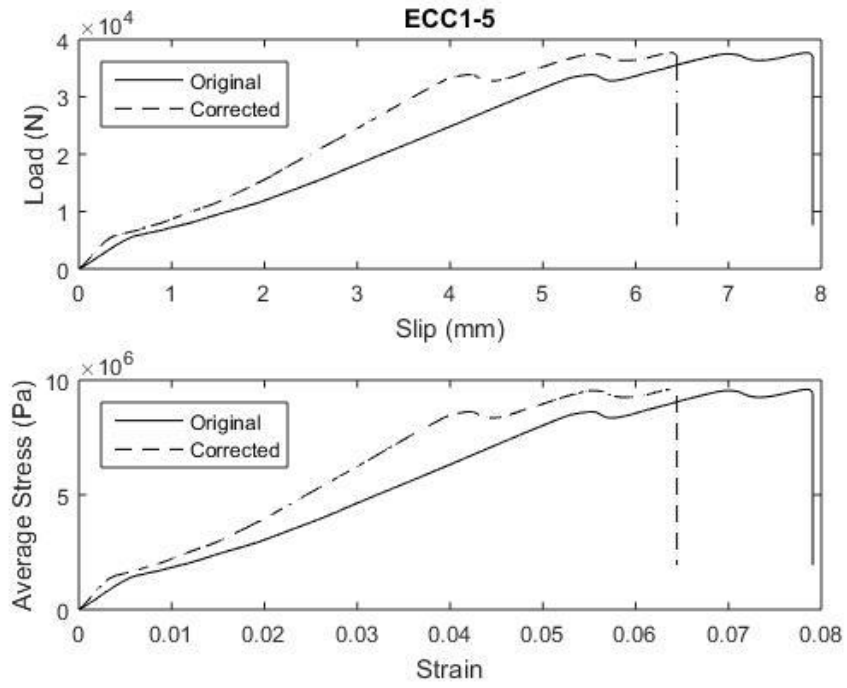


Figure 4-10 Load/Slip & Stress/Strain Relationship, Sample ECC1-5

4.6 Sample Set ECC2 Summary Results

Table 4-7 Sample Set ECC2 Quantitative Results

Number of Samples	Average Ultimate load (kN)	Average Ultimate Bond Stress (MPa)	Max Ultimate Load (kN)	Max Average Stress (MPa)	Average Slip at ultimate load (mm)
6	12.4	3.1	14.2	3.6	2.3

Table 4-8 Sample Set ECC2 Qualitative Observations

Typical Failure Mode	Number of Erroneous Results	Workability
Semi-Ductile Failure after debonding between ECC and FRP reinforcement to residual friction bond between ECC and FRP rod.	0	Extremely flowable, self-consolidating paste with even distribution of PVA fibres, some separation of matrix and fibres if adhesive is uncontained.

4.6.1 Discussion

Workability

In the wet condition the ECC2 paste was extremely flowable. This was the most liquid mix in the test regime. It is believed the addition of the fly ash and the superplasticiser contributed to the workability of the mix design. The extremely flowable nature of the ECC2 batch resulted in an even distribution of fibres throughout the adhesive matrix, however, it was evident that the matrix could flow out of the fibres if not contained.

Due to the flow of the mix it was very easy to pour the ECC2 adhesive into the groove from one side of the FRP bar with little effort needed to ensure the fibres surrounded the FRP. As with the ECC1 adhesive, before initial hardening it was observed that the matrix was consolidating leaving some fibres exposed, in this case it was much more apparent earlier. The same remedy was employed and the groove was overfilled and allowed to partially set, then screeded off before initial hardening.

Curing

Initial hardening occurred within five hours of mixing with moisture from the bleed water still present 16 hours after initial set. The temperature in the workshop had dropped to

around 7°C overnight due to extreme cold (-1.8 according to Australian Bureau of Meteorology).

Performance

The Average Ultimate load was 12.4kN, with a range of 4.2kN. The standard deviation of the results was 1.8kN, all results were within two standard deviations from the average, minimum recorded value was 1.4 standard deviations from average and maximum value was 1 standard deviation from sample average. However with a standard deviation value more than 14% of the average ultimate load, the sample set generated what could be described as varied results. The only consistent result was the post peak load behaviour which showed a rapid drop in capacity followed by a deceleration approaching a residual friction stress value of around 0.7MPa. This would be residual dry friction bond between the sand coating of the FRP bar and the ECC matrix

The results for ECC2 demonstrated ultimate capacity less than half that of the ECC1 matrix, however the failure mode was not as catastrophic.

The Slip and Strain values correlated to the load values, the average values being 2.3mm and 2.3% respectively. As the load values are so low these strain/slip values do not suggest that the ECC2 adhesive is less ductile than the ECC1 matrix. It is likely that the de-bonding failure occurred too early to achieve peak stress in the ECC2 matrix.

The dye penetration test exhibited varied results but presented two distinct cases;

- Case 1 Left image Figure 4-11 Sample ECC2-4 Ultimate Load 14.2kN - The dye was present in the adhesive above the FRP rod and there were what looked like failure planes coming from the edge of the FRP to the corner of the groove.
- Case 2 Right Image Figure 4-11 Sample ECC2-3 Ultimate Load 10.0kN – The dye was not visible other than at the boundary of the FRP rod and the ECC2 adhesive.



Figure 4-11 Dye Penetration - ECC2-4 (Left) ECC2-2 (Right)

Interestingly the samples that showed the most dye penetration were also the samples that exhibited higher strength. It may be a result of the higher forces leading to cover splitting failure instead of simple bond slip at the FRP ECC2 adhesive interface.

Upon extraction of the FRP bar there was clearly good entanglement of fibres from the ECC with the sand on the FRP bar. However, it was evident on all five samples that the ECC matrix and fibres had bonded better to the outward face of the FRP bar compared to the inward face of the bar. This was noticed on extraction of the first bar, so the remaining bars were marked prior to extraction to confirm that this was the case. Figure 4-12 below shows all bars exhibiting the same behaviour. This may be a result of working the ECC adhesive during placement as it is pushed onto the bar once the groove is filled.



Figure 4-12 ECC4 samples showing good of ECC on external facing side and poor bond on internal facing side.

Upon inspection of the sectioned samples a number of issues became apparent. A number of air pockets were visible, the material was placed with the same method and care as all other samples so it is unclear why this occurred in these samples. There were quite a few

of these air pockets it is possible this could be the reason the reduction in ultimate capacity was witnessed. There is also segregation of the matrix and the fibres in the region under the FRP bar. There is a layer 1-2mm thick where there are visibly less fibres suspended in the ECC matrix. This is consistent with the lack of fibres being present on the inward face of the FRP bar. It is unlikely that this will have been caused by settlement as the PVA fibres are the second least dense constituent of the matrix. It can only be assumed that the fibres clumped together as they worked their way around the FRP and came to rest at the bottom of the groove.

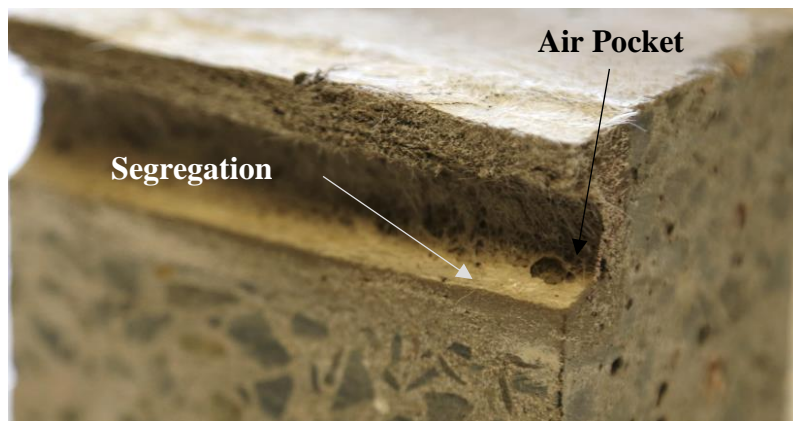


Figure 4-13 ECC2-2 Section View

4.7 Sample Set ECC2 Detailed Results

Table 4-9 Sample Set ECC2 Detailed Results

Sample ID	Ultimate Load (kN)	Ultimate Bond Stress (MPa)	Measured Slip (mm)	Corrected Slip (mm)	Failure Mode
ECC2-1	12.0	3.1	3.3	2.7	Ductile Failure 1 MPa residual bond stress
ECC2-2	13.3	3.4	3.4	3.2	Ductile Failure 0.7 MPa residual bond stress
ECC2-3	10.0	2.5	2.6	2.4	Ductile Failure 0.8 MPa residual bond stress
ECC2-4	14.2	3.6	4.7	3.0	Ductile Failure 0.9 MPa residual bond stress
ECC2-5	10.7	2.7	3.0	2.7	Ductile Failure 0.7 MPa residual bond stress

4.7.1 Sample Set ECC2 Force/Slip and Bond Stress/Strain Relationships

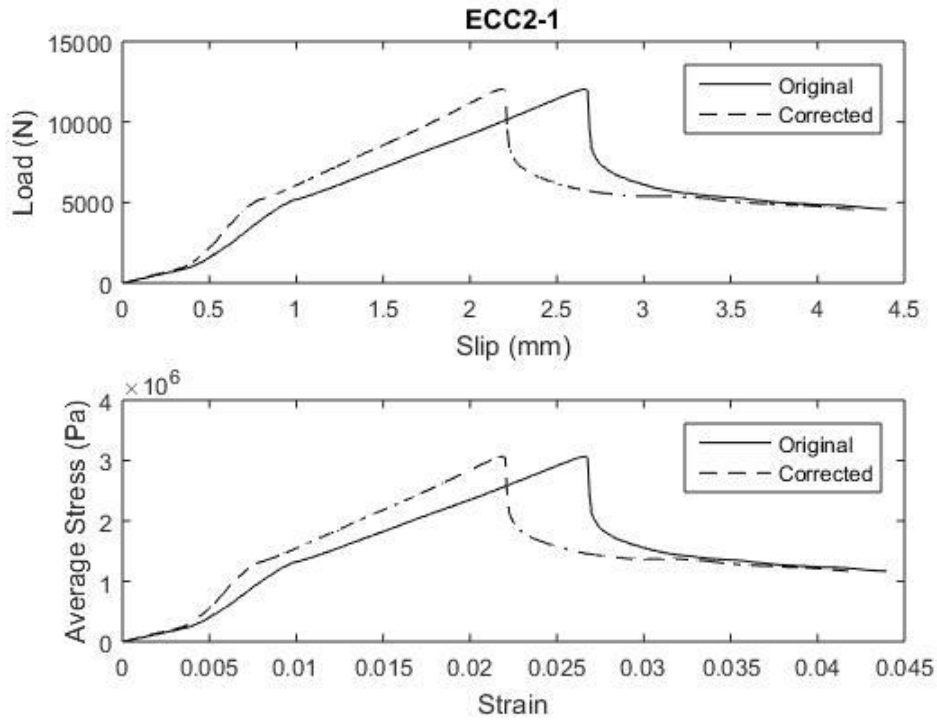


Figure 4-14 Load/Slip & Stress/Strain Relationship, Sample ECC2-1

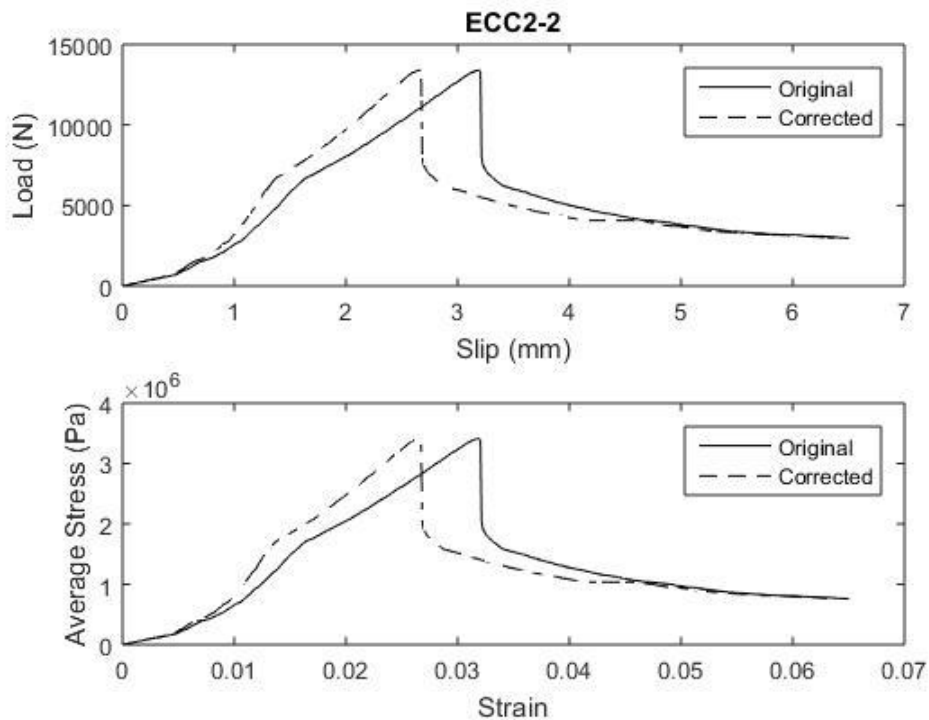


Figure 4-15 Load/Slip & Stress/Strain Relationship, Sample ECC2-2

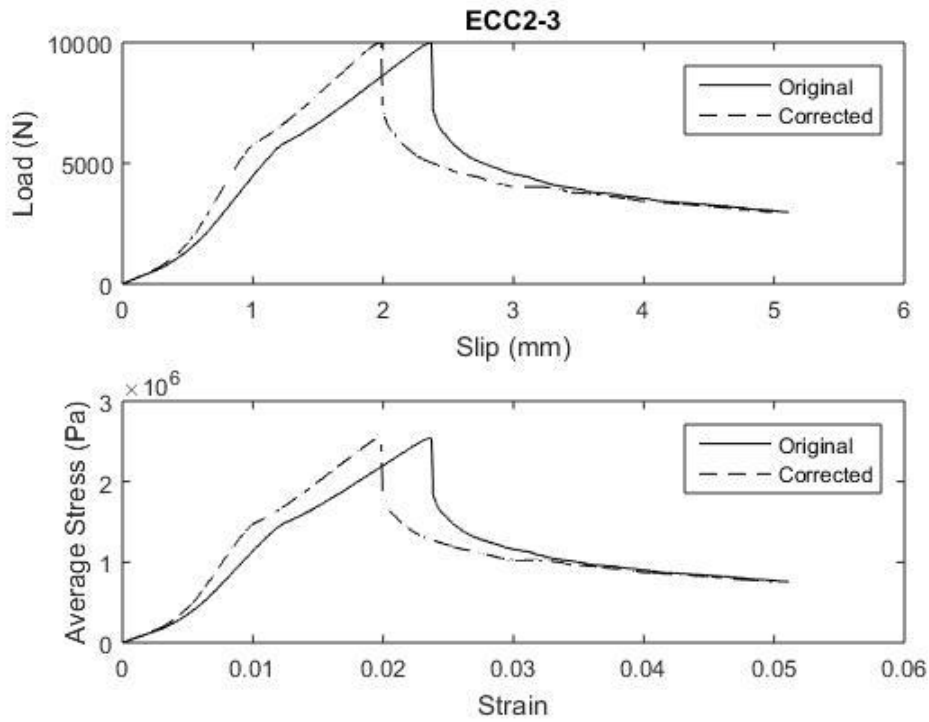


Figure 4-16 Load/Slip & Stress/Strain Relationship, Sample ECC2-3

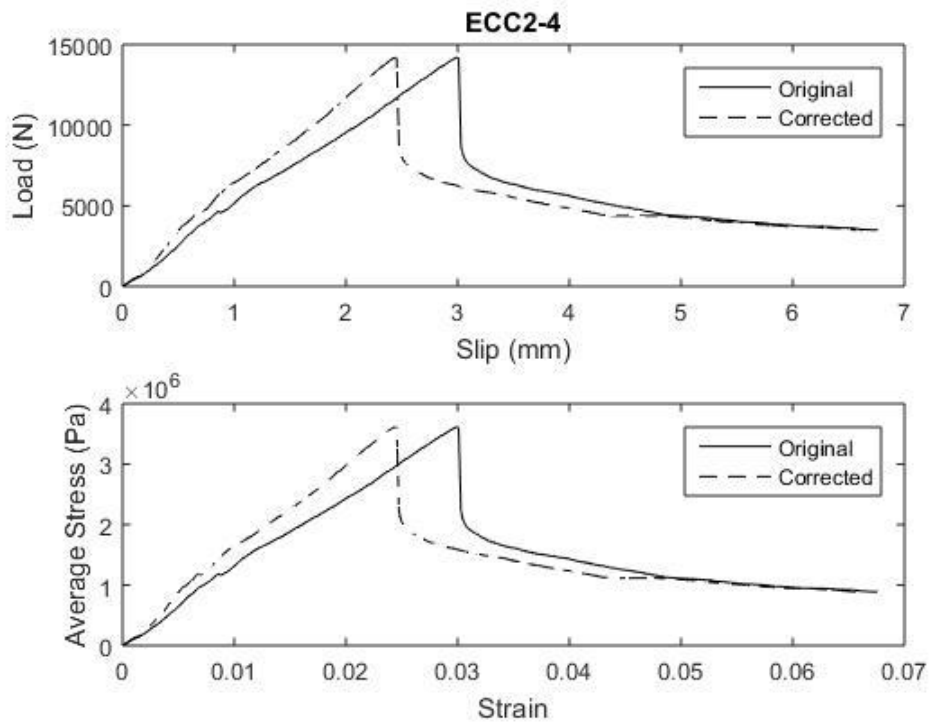


Figure 4-17 Load/Slip & Stress/Strain Relationship, Sample ECC2-4

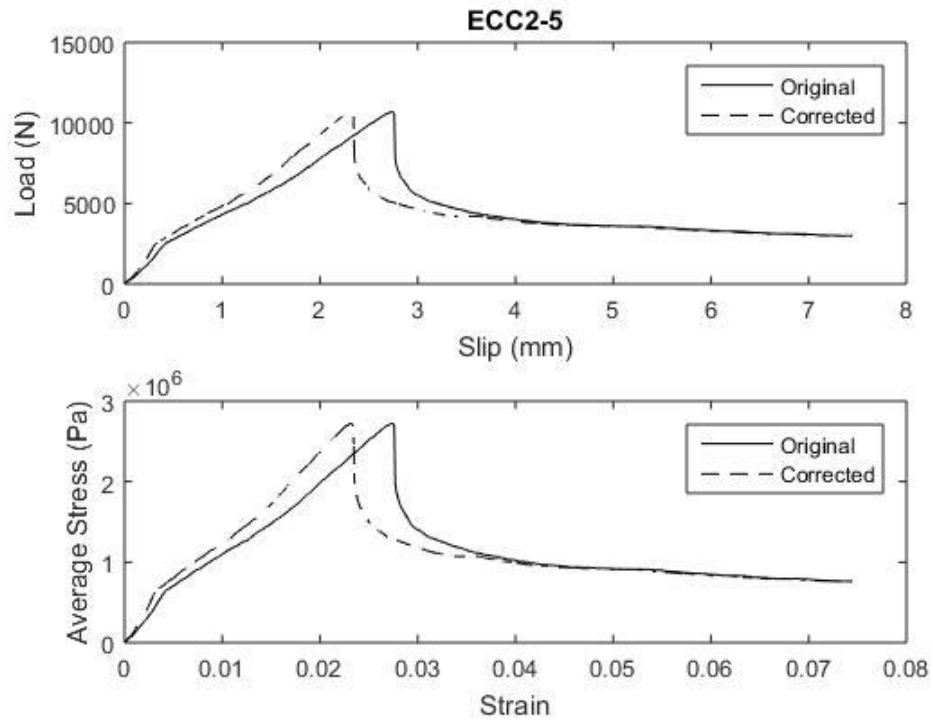


Figure 4-18 Load/Slip & Stress/Strain Relationship, Sample ECC2-5

4.8 Sample Set ECC3 Summary Results

Table 4-10 Sample Set ECC3 Quantitative Results Summary

Number of Samples	Average Ultimate load (kN)	Average Ultimate Bond Stress (MPa)	Max Ultimate Load (kN)	Max Average Stress (MPa)	Average Slip at ultimate load (mm)
2	18.8	4.8	19.3	4.9	3.2

Table 4-11 Sample Set ECC3 Qualitative Observations

Typical Failure Mode	Number of Erroneous Results	Workability
De-bonding between the ECC and FRP reinforcement	0	Very wet slurry with evenly distributed PVA fibres. .

4.8.1 Discussion

Workability

In the wet condition the ECC3 paste was still flowable even with the reduction by half of the super plasticiser. As with the ECC2 mix design the fly ash in ECC3 increased the workability of the matrix. While the adhesive was still relatively flowable it did require a little more effort to place than ECC1 and ECC2 adhesives, but it would still not hold a shape in the wet condition.

Due to the flow of the mix it was very easy to pour the ECC2 adhesive into the groove from one side of the FRP bar with little effort needed to ensure the fibres surrounded the FRP. As with the ECC1 adhesive, before initial hardening it was observed that the matrix was consolidating leaving some fibres exposed, in this case it was much more apparent earlier. The same remedy was employed and the groove was overfilled and allowed to partially set, then screeded off before initial hardening.

Curing

As with the ECC2 curing the initial hardening occurred within five hours of mixing with moisture from the bleed water still present 16 hours after initial set, however it was not as obvious as the ECC2 adhesive samples.

Performance

The Average Ultimate load was 18.8kN, the difference between the two values being 5.6 % of each other. It is acknowledged that this set does not constitute a statistically reliable data set, its primary purpose was to look at workability. The two samples demonstrated

consistent post peak load behaviour which showed a rapid drop in capacity followed by a deceleration approaching a residual friction stress value of around 1.8MPa. This would be residual dry friction bond between the sand coating of the FRP bar and the ECC3 adhesive. It is interesting to note that this is higher than residual friction observed with the ECC2 adhesive.

In the dye penetration test the results were similar to Case 1 with the ECC2 adhesive. The dye had penetrated the top layer of ECC3 adhesive and there seemed to be a failure plane developing, see the right-hand side of the FRP bar in *figure 4-19* below



Figure 4-19 Sample 3-1 Dye Penetration

After extraction of the FRP from the ECC3 adhesive there was significant fibre entanglement. As was the case with ECC2 adhesive the fibres were predominantly entangled on the outward face of the FRP bar.

Upon inspection of the sectioned samples the issues that were present in the ECC2 adhesive samples were not witnessed. While there were a few air pockets, they were small and insignificant. The distribution of fibres seemed to be even and consistent throughout, both above and below the FRP rod.



Figure 4-20 Sample ECC3-1 Section View

4.9 Sample Set ECC3 Detailed Results

Table 4-12 Sample Set ECC3 Detailed Results

Sample ID	Ultimate Load (kN)	Ultimate Bond Stress (MPa)	Measured Slip (mm)	Corrected Slip (mm)	Failure Mode
ECC3-1	19.2	4.9	3.8	3.0	Ductile Failure, residual stress 1.9 MPa
ECC3-2	18.2	4.6	4.1	3.4	Ductile Failure, residual stress 1.7 MPa

4.9.1 Sample Set ECC3 Load/Slip and Bond Stress/Strain Relationships

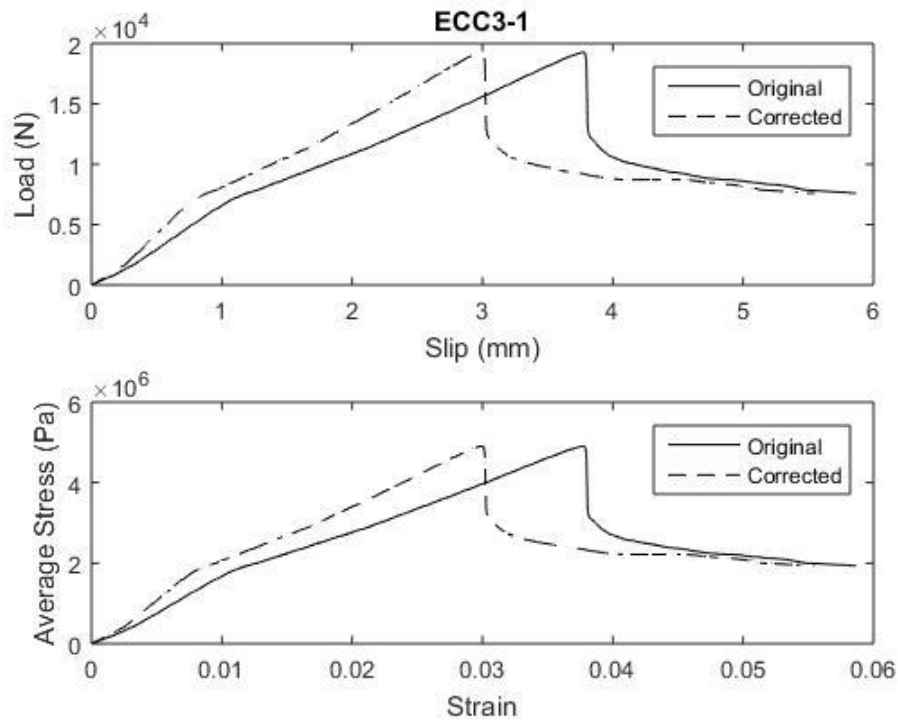


Figure 4-21 Load/Slip & Stress/Strain Relationship, Sample ECC3-1

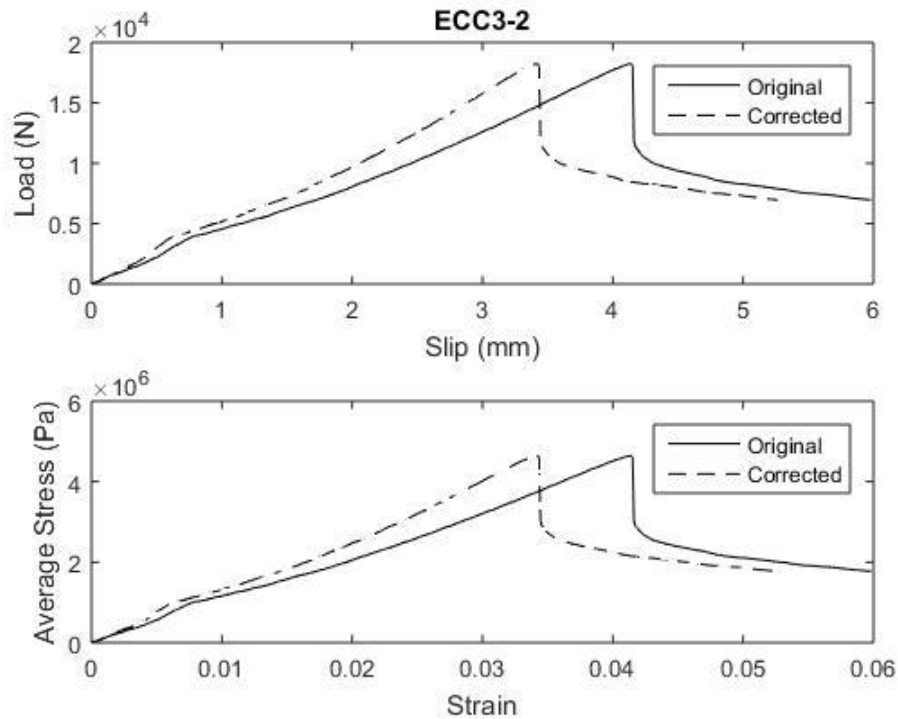


Figure 4-22 Load/Slip & Stress/Strain Relationship, Sample ECC3-1

4.10 Sample Set ECC4 Summary Results

Table 4-13 Sample Set ECC4 Quantitative Results Summary

Number of Samples	Average Ultimate load (kN)	Average Ultimate Bond Stress (MPa)	Max Ultimate Load (kN)	Max Average Stress (MPa)	Average Slip at ultimate load (mm)
2	4.7	0.8	8.1	2.1	2.1

Table 4-14 Sample Set ECC4 Qualitative Observations

Typical Failure Mode	Number of Erroneous Results	Workability
De-bonding between the ECC and concrete substrate	0	Thick paste, consistent and even distribution of PVA fibres. Cohesive capacity capable of holding in ECC and FRP in place while inverted.

4.10.1 Discussion

Workability

The ECC4 adhesive was the only adhesive that formed a thixotropic paste capable of self-support in the wet state. The paste could easily be formed into a ball and displayed zero

slump once released. As a result it is possible that this ECC4 adhesive could be used in an overhead application or a vertical application.



Figure 4-23 ECC4 Thixotropic Consistency

Due to the consistency of the ECC4 adhesive more work was required to install the adhesive compared to the previous ECC adhesives. A spatula was used to push the ECC4 adhesive in from one side and then finished with a steel screed. The paste was easily finished with the steel screed, it was no possible to achieve a perfectly smooth finish due to the fibres, but the finish was the most uniform of all ECC adhesives.

Curing

As with the ECC2 curing the initial hardening occurred within three hours of mixing but there was no obvious signs of bleed water after initial hardening.

Performance

The ECC4 adhesive did not perform well. Unlike the previous samples the mode of failure was de-bonding between the ECC and concrete substrate. This is typically a sign of poor groove preparation or poor groove detailing. Based on the fact that all base prisms were prepared at the same time to the same specifications it is possible that the results are related to the consistency of the wet ECC adhesive. However given the sample size it not possible to draw any solid conclusions, but it may be an area for further study.

The Average Ultimate load was 4.74kN, sample ECC4-1 displayed results less than a quarter of the results for ECC4-2, and therefore the results cannot be considered reliable.

On sample ECC4-2 the dye penetration test did display significant penetration around the FRP rod, as shown in the circled area of *figure 4-24* below. While it is not conclusive, it may be an indication that the paste was not able to be effectively worked into the sand particles on the FRP bars. If the cement matrix is too thick it is possible that the matrix

does not embed into the small surface deformities to assist friction bond leading to premature interfacial failure between the ECC and the concrete substrate.

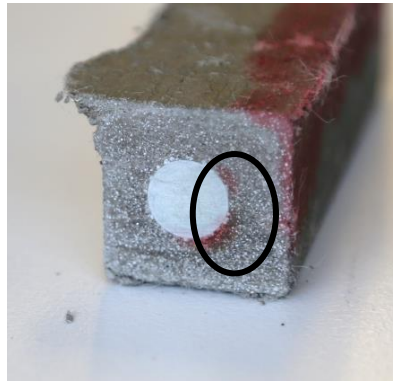


Figure 4-24 Sample ECC4-2 Dye Penetration

Upon extraction of the FRP rod from the ECC4 Adhesive it was evident that there was far less entanglement of PVA fibres in the sand coating of the FRP rod as is clear from figure 4-25 below.

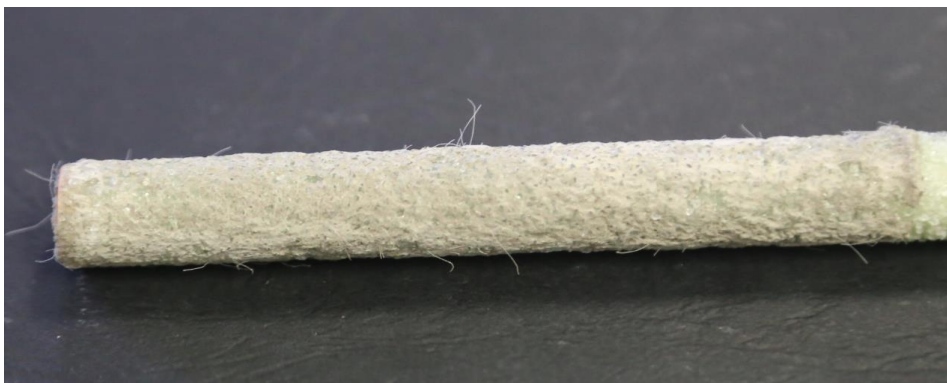


Figure 4-25 Sample ECC4-1 FRP rod after extraction from ECC4 adhesive.

4.11 Sample Set ECC4 Detailed Results

Table 4-15 Sample Set ECC4 Detailed Results

Sample ID	Ultimate Load (kN)	Ultimate Bond Stress (MPa)	Measured Slip (mm)	Corrected Slip (mm)	Failure Mode
ECC4-1A	1.3	0.3	2.9	2.9	Ductile Failure 1 MPa residual bond stress
ECC4-2	8.1	2.1	3.5	3.4	Ductile Failure 0.7 MPa residual bond stress

4.11.1 Sample Set ECC4 Load/Slip and Bond Stress/Strain Relationships

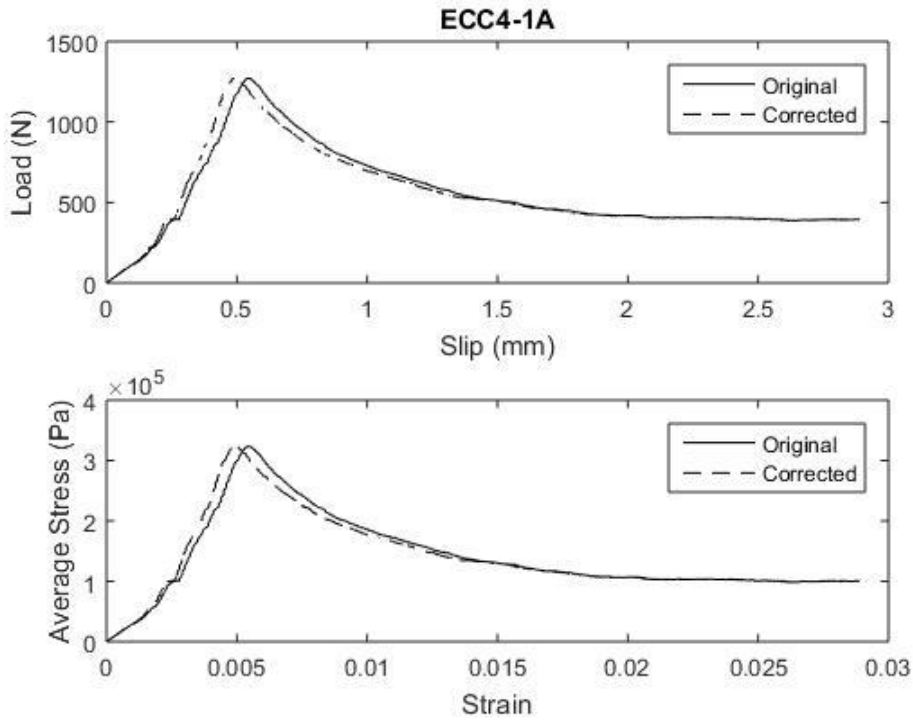


Figure 4-26 Load/Slip & Stress/Strain Relationship, Sample ECC4-1A

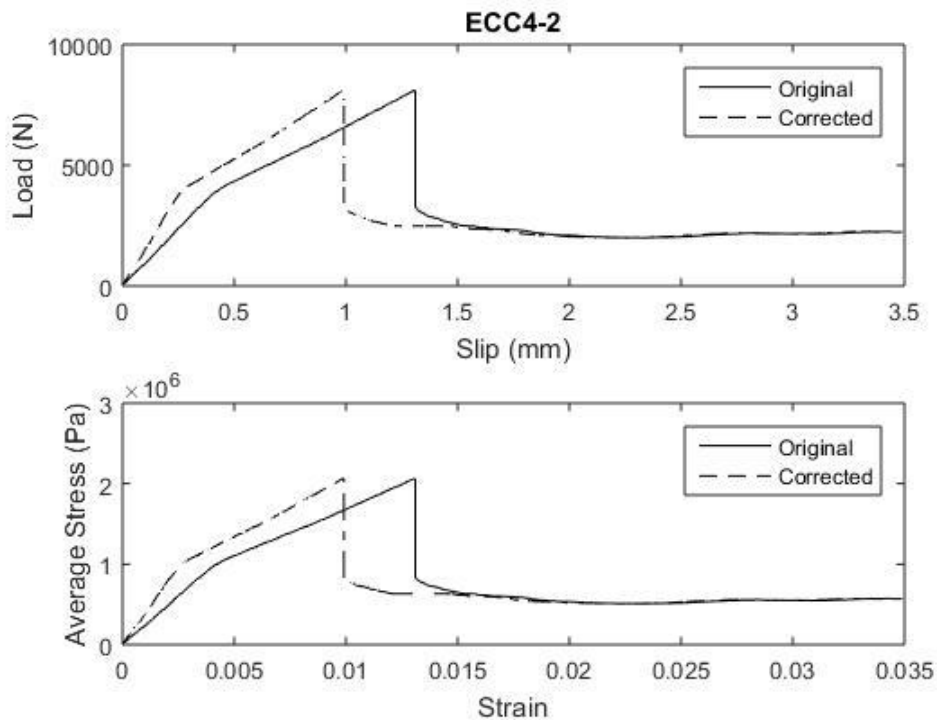


Figure 4-27 Load/Slip & Stress/Strain Relationship, Sample ECC4-2

4.12 Additional Data on ECC4-1

As the ECC and FRP extracted from the concrete prism at such a low force it was clear there was no bond between the ECC and Concrete base. The exact reason for this is unknown. Being opportunistic a simple pull out test was completed on the ECC and FRP that had not been damaged. Steel washers were placed over the ECC to distribute the load and a simplified pull-out test was completed to see what information could be gleaned. While clearly not substantial for accurate analysis it may indicate a direction for further investigation.

Table 4-16 ECC4-1B Detailed Result

Sample ID	Ultimate Load (kN)	Ultimate Bond Stress (MPa)	Measured Slip (mm)	Corrected Slip (mm)	Failure Mode
ECC4-1B	10.3	2.6	7.6	7.4	Ductile Failure 1 MPa residual bond stress

4.12.1 Discussion

The second test on sample ECC4-1 developed a maximum stress higher than either of the original ECC4 samples. Clearly the frictional bond between the ECC and FRP is greater than the bond between the ECC and the concrete substrate thanks to the sand coated surface. The slip values are high, this is a result of the ECC against the bearing washers used to hold the sample in place.

The most interesting aspect of this test was the smoothness of the stress strain curve as it was loaded beyond ultimate capacity and progressed into a strain softening type relationship.

4.12.2 ECC4-1B Load/Slip and Bond Stress/Strain Relationships

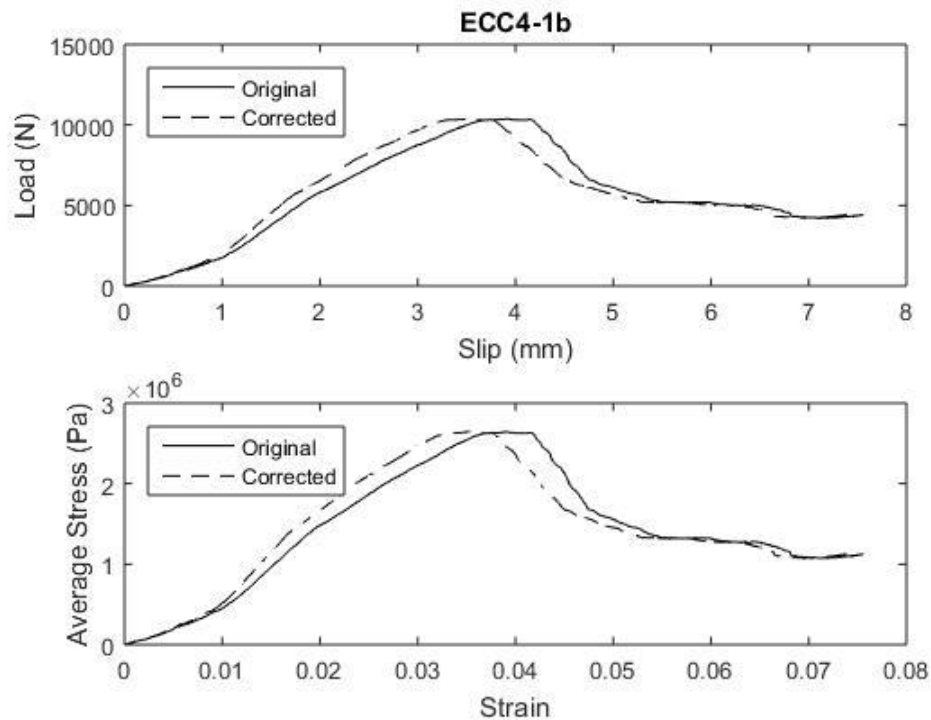


Figure 4-28 Load/Slip & Stress/Strain Relationship, Sample ECC4-1B

4.13 Summary of results

The results were not entirely as expected. The relatively low ultimate capacity of the exemplary mix design ECC2 a surprise. The system failed by interfacial bond slip between the ECC and FRP bar prior to internal tensile stresses developing to a point where it was possible witness strain hardening in the ECC.

The ECC1 test results demonstrated that an NSM system using ECC as the adhesive is capable of developing sufficient internal stress to witness the strain hardening behaviour characteristic of ECC, however the de-bonding between the sand and the FRP rod suggest the failure was premature and the system had more capacity.

The following two figures (Figure 4-29 and Figure 4-30) are regression analysis of the ECC1 & ECC2 sample sets. A sixth order polynomial was required to achieve an acceptable R² value for the ECC1 data set, this is due to the strain hardening behaviour which commences at approx. 4% strain. The R² values offer relatively close fit to the data generated in this study however more data would be required to gain more confidence in the regression analysis. The values for ultimate bond stress calculated from the regression curves offers a close correlation to the average values from the experimental data.

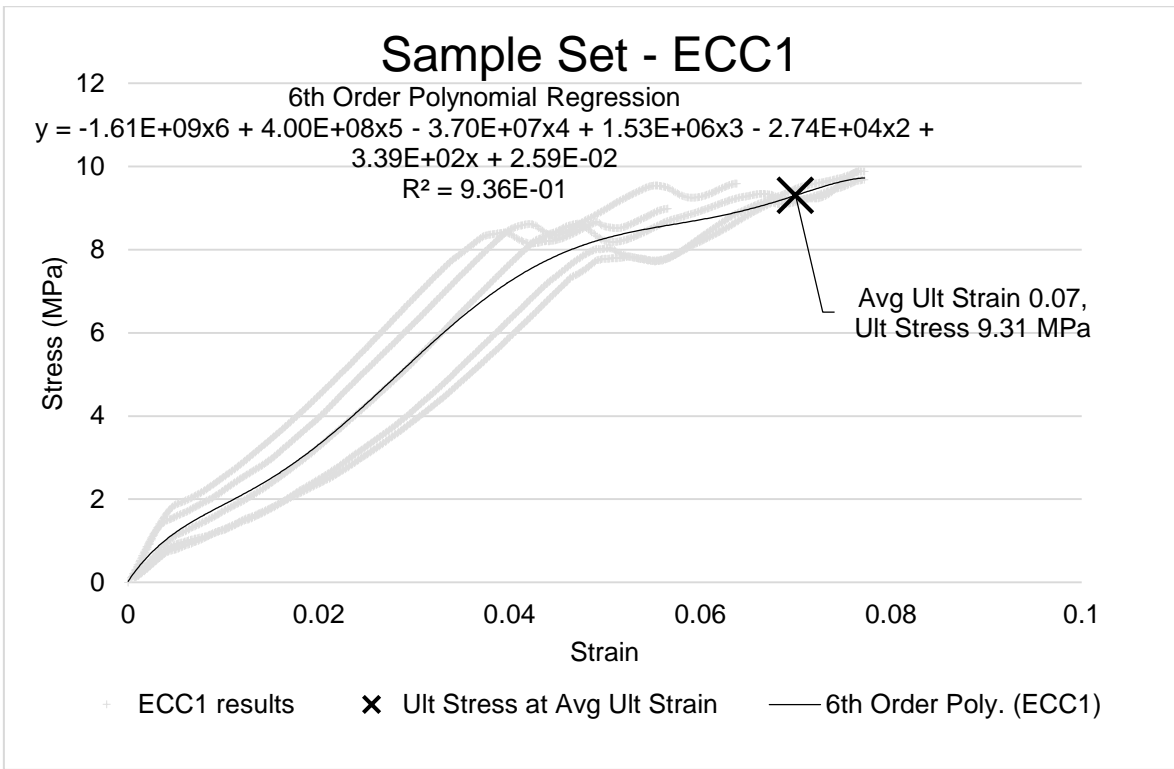


Figure 4-29 ECC1 Regression Analysis

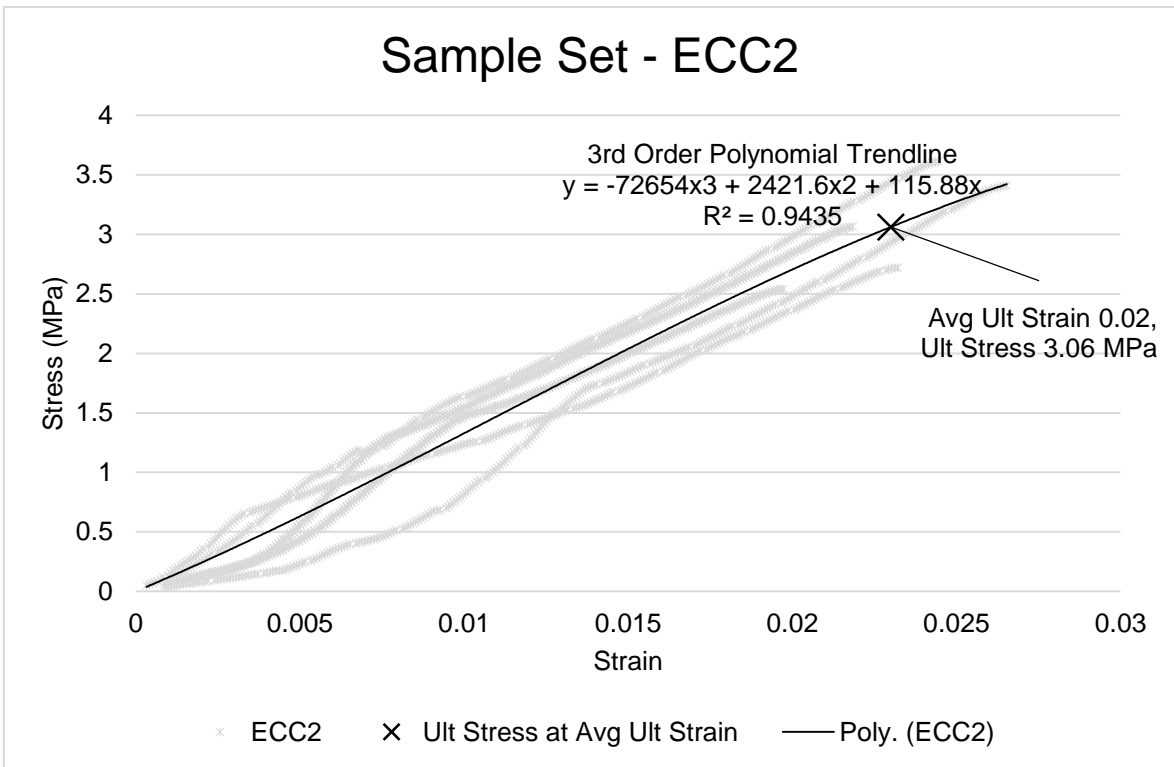


Figure 4-30 ECC2 Regression Analysis

5 DISCUSSION OF RESULTS.

5.1 Bond Strength Results

In terms of strength, the ECC1 adhesive outperformed all other adhesives and was the only sample that demonstrated strain hardening, but was followed by sudden brittle failure with no residual stress capacity. Curiously the C1 adhesive had the second highest ultimate capacity. ECC2, which was based on the M45 exemplary mix design, demonstrated the second lowest capacity, second only to ECC4 adhesive which contained no super plasticizer. These results were unexpected, particularly in regard to the very low ultimate capacity found in the ECC2 adhesive.

5.1.1 Comparison to previous studies

A review of similar studies presents data that show similar results compared to this study. De Lorenzis et al. (2004) completed a study using a cementitious paste as an adhesive. The results from samples with similar groove detailing are presented alongside the results of this study in table 5.1 below. Note that the FRP reinforcement used in the De Lorenzis study was spirally wound CFRP with a superficial sand coating. The cement paste used in De Lorenzis study was a simple cement and water mix at a ratio of 1:0.32. The comparison presented below does not include any samples that used epoxy adhesive. It is worth noting the De Lorenzis study also identified that that sand coated FRP with epoxy adhesive also failed by pull-out where groove dimensions were $2.5 d_r$, although it was generally accompanied by cover splitting.

Table 5-1 Comparison of results with similar studies

Sample Identifier	Stress at interface between bar and groove-filler at failure (MPa)	Failure Mode
SW/k2.00/112-c	4.9	Splitting & Pull-out
SW/k2.00/124-c	6.4	Splitting & Pull-out
ECC1	9.6	Splitting & Pull-out
ECC2	3.1	Pull-out
ECC3	4.8	Pull-out
ECC4	0.8	Pull-out (Concrete/Adhesive)
C1	7.0	Splitting & Pull-out

Notably the ECC adhesive samples tested in this project did not split as the samples in the De Lorenzis study did. This is obviously due to the ECC tensile capacity. The results presented in Table 5.1 highlight the fact that PVA fibre entanglement in the sand coating does not improve the bond capacity between the adhesive and FRP reinforcement. The reduction in bond strength could be due to a number of factors; one being the fly ash content which may have reduced the cohesive bond between the adhesive and the FRP reinforcement.

5.1.2 Impact of fly ash on cohesive bond

Wang & Li completed a study (2007) into the effect of high volume fly ash content on the cementitious matrix used in Engineered Cementitious composites. Prior to this study, ECC mix designs generally had a very high cement content when compared to typical concrete mix designs. This was due to the removal of large volume aggregate which was necessary to ensure the crack bridging of the fibres was not adversely influenced by large aggregate particles. The initial goal of this study was to establish if cement could be replaced in part with fly ash to reduce the environmental impact of ECC concrete. However, by substituting cement with fly ash. Wang & Li observed that with an increase in fly ash ultimate strain capacity increased, one of the key benefits of ECC. Conversely the high fly ash content mix designs suffered losses in ultimate tensile strength and first crack strength.

Of the six mix designs tested, the exemplary mix design (M45) had a 1:1.2 cement to fly ash ratio and an ultimate strain of 2.47%. Mix design M41 had the lowest cement/fly ash proportion of 1:0.1 and an ultimate strain of 0.37%. Conversely the M45 mix design had an ultimate tensile strength of 4.86MPa and M41 ultimate tensile strength was 5.48MPa. While this is not a huge variation in ultimate tensile strength it does demonstrate that the addition of fly ash adversely effects the tensile strength of the ECC matrix.

From the findings of Wang and Li's study it may be deduced that the increased fly ash content adversely affects the cohesive capacity of the cement matrix to the sand coated FRP reinforcement as the cement is reacting with the fly ash instead of the silica sand to create a cohesive bond. The inclusion of fly ash provides ductility to the ECC adhesive at the expense of cohesive bond to the substrate and FRP reinforcement, hence reducing overall capacity of the NSM system. In all the samples tested in this study which used fly ash, the ultimate capacity was low and the failure mode was de-bonding between either the ECC and FRP or ECC and concrete substrate. There was little to no evidence of cover cracking in the ECC adhesives.

The lack of mechanical bond devices may be overcome at the reinforcement/ECC interface through the use of deformed reinforcing bar. The de-bonding between the concrete substrate and ECC is much harder to address. It may be possible to develop a scarifying tool to fit within the groove, but this would be dependent on proving up the capability of ECC as an NSM system adhesive.

It may be possible to increase the bond strength between the ECC and the concrete substrate using a primer binder. Al-Abdwais (2013) demonstrated in their study that the use of MBrace primer added to the cement paste was able to develop average bond stress of 10 MPa, similar to the average bond stress witnessed in ECC1. Al-Abdwais' use of the MBrace primer was innovative in that it was mixed with the cement adhesive to improve tensile strength. If this approach was adopted it is likely that the ECC will lose ductility due to the increase in bond between the matrix and PVA fibres. Alternatively, using the MBrace primer as recommended by the manufacturer (BASF 2016) by painting the interface zones with the MBrace primer may be a more appropriate application. It could aid the interfacial bond strength without negatively affecting ductility of the ECC.

Wang & Li (2007) demonstrated that there is a direct correlation between the addition of fly ash and reduction in the interfacial bond between the matrix and the PVA fibres. In this research project the fibres were not coated in oil as it was presumed the fly ash content

would provide a suitable level of ductility to the ECC adhesives. There may be a case for future study that uses oil coated PVA fibres as opposed to high proportion fly ash mix design. This will improve the cohesive bond between the ECC matrix and the substrate and FRP reinforcement while ensuring a reduction in the interfacial bond between the ECC matrix and the PVA fibres which would ensure ECC adhesive ductility.

5.1.3 Impact of rheology on fibre distribution

As noted in the results chapter of this report, it looked like there was segregation of the cementitious matrix and the fibres occurring under the FRP reinforcement. This may be a result of low viscosity cementitious matrix.

Rheology is the study of the flow of matter, in particular non-Newtonian fluids such as cementitious paste. Li and Li (2012) completed a study in 2012 on the effects of the rheology of cementitious matrix on the fibre dispersion, ductility and strength of ECC, a component of the study looked at the impact on viscosity of the cementitious matrix tensile strength and ultimate strain capacity of the ECC. The experimental data from this study was produced by testing the direct tensile strength of ECC samples with different dosages of Viscosity Modifying Agent (VMA).

In this study Li and Li were able to demonstrate that the ultimate strain and the tensile stress vary significantly depending on the viscosity of the cementitious matrix. In Li and Li's study the low viscosity (free flowing) had a much lower ultimate strain capacity, typically less than 1% and a reduced ultimate tensile capacity ranging from less than 3 MPa to slightly over 4 MPa. The ECC samples with the highest viscosity demonstrated ultimate strain values similar to the exemplary matrix design at approximately 4%. However the ultimate tensile capacity was less than 4 MPa in all samples tested. Figure 5-1 below demonstrates the effect of VMA content on Ultimate tensile strength and ultimate tensile strain.

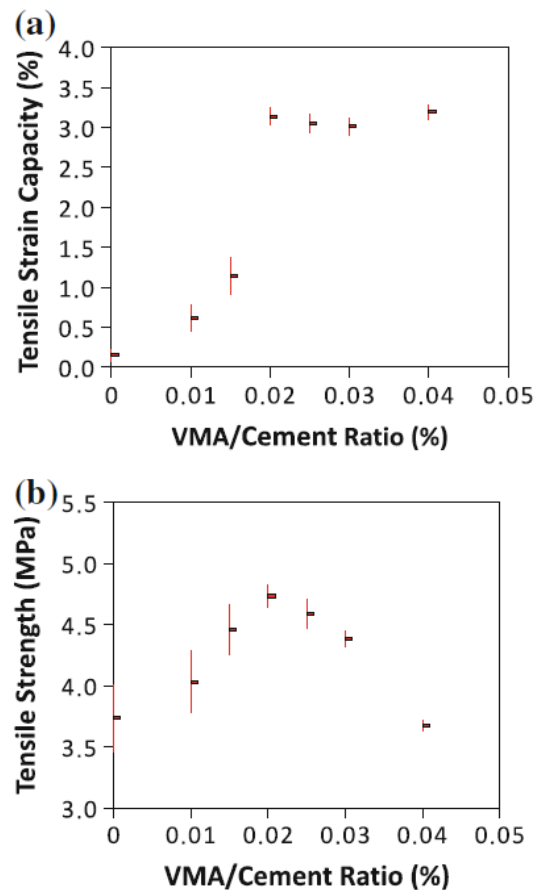


Figure 5-1 a) Tensile Strain/VMA content relationship. b) Tensile strength/VMA content relationship. (Li & Li 2012).

In the samples tested in this project a similar pattern was observed. The ECC3 adhesive samples used $\frac{1}{4}$ the amount of superplasticizer were able to develop ultimate capacity 50% greater than the ECC2 samples and more than 100% greater than the ECC4 samples. It may be the case that the HRWR super plasticiser used in this project may have led to a cementitious matrix with a low viscosity which resulted in an uneven distribution of PVA fibres, hence, an uneven and incomplete entanglement of fibres in the sand coating which in turn resulted in lower ultimate capacities. While the number of samples tested using the ECC3 adhesive is not significant to draw solid conclusion, it is an avenue for future research.

5.2 Workability of wet adhesives

One of the key concerns regarding the ECC adhesives was the workability and its suitability for use in an overhead situation. The ECC adhesives tested in this research project which generated consistent results were not suitable for overhead use. The viscosity of the cementitious matrix was too low, as a result if the paste was applied to

the soffit of a girder for example, it would simply fall off. It may be possible to use a formwork system and inject the ECC as it was very flowable. This would introduce extra complexity and cost to the installation process, limiting its viability in comparison the epoxy adhesive alternatives.

The ECC4 mix design had the right cementitious paste viscosity and cohesion in its wet state. Unfortunately the two samples failed prematurely by de-bonding between the ECC and concrete substrate. The exact cause of this premature failure is unknown and based on the number of samples tested it may just be coincidence. It may be an area for future research.

5.3 Bond Strength Prediction

In the literature review reference was made to a mathematical model developed by Zhang et al (2014) that predicted the bond strength of an NSM system. This model was developed based on the assumption that the system failed due to fracturing in the concrete substrate. Due to the failure mode in the ECC1 and ECC2 adhesive samples sets being cover splitting and interfacial bond failure respectively Zhang's model is not applicable.

The following application of Zhang's mathematical model has been completed in order to determine the potential capacity of an NSM system based on the strength characteristics of the concrete substrate and FRP reinforcement used in the tested system to determine what order of magnitude the improvements to this system have to be.

5.3.1 NSM Potential Bond Strength – Zhang Model

The Zhang Model requires the following input parameters;

- Characteristic Strength of the base concrete

$$f'_c = 40MPa,$$

- Tensile Modulus of the FRP reinforcement

$$E_{frp} = 52.5GPa$$

- Cross Sectional Area of the FRP reinforcement

$$A_{frp} = 126.7mm^2,$$

- Groove width and groove depth

$$Groove_w = Groove_d = 26mm$$

- Groove width to depth ratio

$$\gamma = \frac{Groove_w}{Groove_d} = 1,$$

- Cross-sectional contour of the failure surface, i.e. the perimeter of the groove

$$C_{failure} = 26 \times 3 = 78mm$$

Process for predicting Bond Strength

First τ_{cmax} is calculated. τ_{cmax} in the Zhang model refers to the maximum stress along the failure plane in the base concrete as illustrated by the angled blue lines in figure 5-2 below.

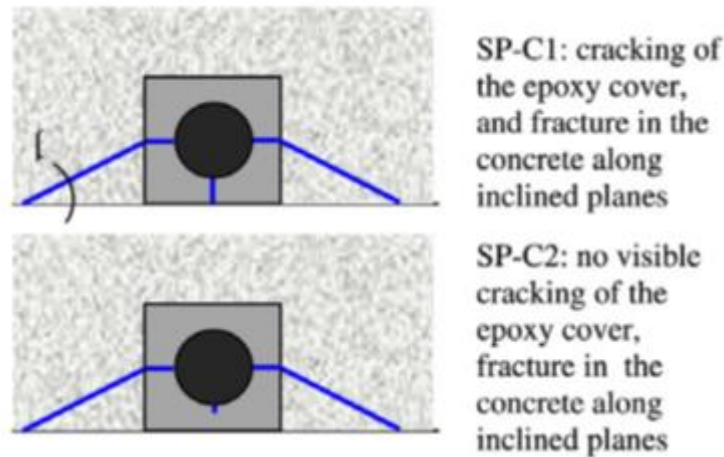


Figure 5-2 Base Concrete Failure Plane (De Lorenzis & Teng 2007)

Equation 1 Max Concrete Bond Stress

$$\tau_{cmax} = 1.15\gamma^{0.138}f_c^{0.613}$$

$$\tau_{cmax} = 11.0 MPa$$

Next the parameter η is calculated, this parameter is essential in determining the effective bonded length for the groove, not to be confused with effective bonded length of the reinforcement.

Equation 2 Fracture Mechanics Parameter

$$\eta^2 = \frac{\tau_{cmax}^2 C_{failure}}{2G_f E_f A_f}$$

$$\eta = \sqrt{\frac{(11^2) \times (78)}{2 \times (3.92) \times (52.5 \times 10^3) \times (126.7)}}$$

$$\eta = 0.0135$$

Using η the effective length of the groove L_{eg} can be determined by equation

Equation 3 Effective Length - Groove

$$L_{eg} = \frac{1.66}{\eta}$$

$$L_{eg} = 123mm$$

If the bonded length is less than the effective groove length the Zhang model also prescribes a reduction factor. The reduction factor is calculated using the equation below.

Equation 4 Bonded Length Reduction Factor

$$\beta_L = \frac{L_b}{L_{ec}} \left(2.08 - 1.08 \frac{L_b}{L_{ec}} \right)$$

$$\beta_L = \frac{100}{123} \left(2.08 - 1.08 \frac{100}{123} \right)$$

$$\beta_L = 0.98$$

It is evident from the reduction factor, the actual bond length selected was very close to effective bond length.

The final parameters calculated to predict bond strength is interfacial fracture energy using equation xxx below.

Equation 5 Interfacial Fracture Energy

$$G_f = 0.4\gamma^{0.422} f'_c{}^{0.619}$$

$$G_f = 3.92 N/mm$$

With all the parameters determined equation xxx below can be used to determine the predicted bond strength.

Equation 6 Zhang Bond Strength Prediction

$$P_u = \beta_L \sqrt{2G_f E_f A_f C_{failure}} \quad \text{eq.1 Zhang et al}$$

$$P_u = \beta_L \sqrt{2 \times (3.92) \times (52.5 \times 10^3) \times (126.7) \times (78)}$$

$$P_u = \beta_L \sqrt{4.1 \times 10^9}$$

$$P_u = 0.98 \times 63.7 kN$$

$$P_u = 62.2 kN$$

It is clear from the results generated using the Zhang model for bond strength that the specimens in this experimental program failed to develop strength that the groove detailing and substrate conditions was capable of achieving. The predicted bond strength is:

- 1.6 times higher than average ECC1 bond strength of 37.7 kN.
- 5 times higher than average ECC2 bond strength of 12.4 kN.

Ultimate bond strength of 62.2 kN would equate to an ECC/FRP bond strength of 15.8 MPa. This is quite high, De Lorenzis et al (2004) was able to achieve this magnitude of local bond stress using an epoxy adhesive which had a direct tensile strength of 27.8 MPa using a similar sized ribbed CFRP reinforcing rod. The highest adhesive to FRP bond stress developed using cementitious paste was 9.8MPa (De Lorenzis et al. 2004), this was achieved using a 9.5mm d_r ribbed carbon fibre bar. Considering the ECC1 adhesive was able of generating similar bond stress on sand coated bar, the use of a ribbed bar may be able to develop higher bond stress. Given the number of variables identified in the previous section it is plausible that this level of bond strength may be achievable.

6 CONCLUSION

The fundamental objective of this research project was to assess the performance of ECC as an adhesive in a near surface mounted reinforcing system. It was anticipated that the increased tensile and ductile capacity of ECC would provide significant benefits in comparison to traditional cementitious paste adhesive. The cost benefit over epoxy adhesives was discussed, and current research into ECC durability have the potential to offer epoxy adhesives as well.

6.1 Key findings

The results of the experiments performed in this research project generated results that did not directly match the expectations. The ductile ECC adhesives (ECC 2-4), the mix designs where high volume fly ash was used to improve ductility, demonstrated lower ultimate strength in comparison to the ECC mix design and in the case of the exemplary mix design ECC2, the ultimate loads and failure strains were lower than cementitious paste.

6.1.1 De-bonding at the ECC/FRP reinforcement interface.

The ECC2 adhesive was based on Li's M45 exemplary mix design, which had the best ductile performance. It was expected that this ECC adhesive would demonstrate good bond strength and significant strain hardening behaviour as it approached ultimate capacity. In all tests de-bonding failure occurred prior to the onset of any strain hardening behaviour in the ECC adhesive.

6.1.2 De-bonding between the sand coating and the ECC1 adhesive.

This failure mode is considered a premature failure as it is failure in FRP reinforcement which is beyond the scope of this study. It does however suggest that there was

potentially more capacity in the system, however it is unlikely to be a significant increase as the ECC had entered strain hardening phase of the stress strain relationship.

6.1.3 Workability

ECC4 was the only adhesive with suitable workability for overhead application. The issue of workability is not a problem for negative moment strengthening and it can be overcome in soffit/vertical applications, but imposes additional cost and complexity.

The positive observation was none of the ductile ECC mix designs split, it demonstrates that failure of the system would not be brittle and catastrophic as was observed with the ECC1 & C1 samples. The reduced bond strength in the ductile ECC adhesives can be overcome with sufficient development length and provide a safe failure mode.

6.2 Future research

The consensus among many of the lead researches in the field is that NSM systems are a highly effective strengthening system, particularly in comparison to surface mounted FRP systems. Due to the depth of research into this type of system it was possible to study the various failure modes and identify potential areas where an NSM system using ECC as the adhesive/groove filler might be refined to achieve better results. Herein is the primary benefit of this study

Use of deformed bar instead of sand coating – In multiple studies by De Lorenzis the use of deformed bar lead to much higher bond strength. The typical failure mode when using deformed bar was splitting failure, either in the adhesive cover or the concrete substrate. Given the ductile ECC adhesives (ECC2-4) failed by bond slip it may be possible to improve interfacial bond such that the ECC adhesive is sufficiently stressed to demonstrate strain hardening which would presumable lead to higher ultimate capacity.

Application of a primer on the bonded surface – The critical failure mode in ductile ECC adhesives was de-bonding between either the FRP reinforcement and ECC or the concrete substrate and ECC. Al-Abdwais (2013.) was able to demonstrate that the use of a primer binder in a cementitious paste improved bond strength of an NSM system. Use of a primer on the faces of the bonded materials may be a suitable method to improve interfacial bond without altering the mix design of the ECC and adversely affecting the ductility of the EC adhesive.

Alternate mix designs – As discussed in the analysis chapter there are changes to the mix design of the ECC that may improve cohesive bond performance. One area of potential research would be the reduction of fly ash in the mix design. In order to counter the adverse effect the reduction in fly ash will have on ductility it may be possible to apply an oil coating to PVA fibres as was customary in ECC designs prior to the introduction of fly ash.

6.3 Closing Remark

It is typical of new systems that the optimum characteristics are not developed on the first study as is evident by this study. The results of testing in this project did not demonstrate the results that were expected, leading to significant research into the various factors that influenced the system performance. With further research and experimental study into areas identified in this study it is possible that engineered cementitious composites may prove to be a preferable alternative to epoxy in a near surface mounted strengthening system.

7 REFERENCES

Afey, HME-D & Mahmoud, MH 2014, 'Structural performance of RC slabs provided by pre-cast ECC strips in tension cover zone', *Construction and Building Materials*, vol. 65, pp. 103-13, <http://www.sciencedirect.com/science/article/pii/S095006181400422X>.

Al-Abdwais, A, Al-Mahaidi, R & Abdouka, K *Modified cement-based adhesive for near-surface mounted CFRP strengthening system*, 2013, <http://hdl.handle.net/1959.3/375553>.

ASI 2009, *Design Capacity Tables for Structural Steel, vol. 1: Open Sections*, 5th edn, vol. 1, Australian Steel Institute, North Sydney.

Asplund, SQ 1949, 'Strengthening Bridge Slabs with Grouted Reinforcement', *ACI Journal*, vol. 52, no. 6, pp. 397-406.

BASF 2016, *MasterBrace® P 3500 Technical Datasheet*, BASF Chemicals & Polymers Pakistan (Pvt) Ltd. ,

Biscaia, HC, Chastre, C & Silva, MAG 2015, 'Bond-slip model for FRP-to-concrete bonded joints under external compression', *Composites Part B: Engineering*, vol. 80, pp. 246-59, <http://www.sciencedirect.com/science/article/pii/S1359836815003674>.

Chen, JF & Teng, JG 2003, 'Shear capacity of FRP-strengthened RC beams: FRP debonding', *Construction and Building Materials*, vol. 17, no. 1, pp. 27-41, <http://www.sciencedirect.com/science/article/pii/S0950061802000910>.

Coelho, MRF, Sena-Cruz, JM & Neves, LAC 2015, 'A review on the bond behavior of FRP NSM systems in concrete', *Construction and Building Materials*, vol. 93, pp. 1157-69.

De Lorenzis, L 2004, 'Anchorage Length of Near-Surface Mounted Fiber-Reinforced Polymer Rods for Concrete Strengthening—Analytical Modeling', *ACI Structural Journal*, no. May/June 2004, pp. 375-86.

De Lorenzis, L & Teng, JG 2007, 'Near-surface mounted FRP reinforcement: An emerging technique for strengthening structures', *Composites Part B:*

Engineering, vol. 38, no. 2, pp. 119-43,
<http://www.sciencedirect.com/science/article/pii/S135983680600120X>>.

- De Lorenzis, L, Rizzo, A & La Tegola, A 2002, 'A modified pull-out test for bond of near-surface mounted FRP rods in concrete', *Composites Part B: Engineering*, vol. 33, no. 8, pp. 589-603,
<http://www.sciencedirect.com/science/article/pii/S1359836802000525>>.
- De Lorenzis, L, Lundgren, K & Rizzo, A 2004, 'Anchorage Length of Near-Surface Mounted Fiber-Reinforced Polymer Bars for Concrete Strengthening— Experimental Investigation and Numerical Modeling', *Structural Journal*, vol. 101, no. 2.
- Development, DoIaR, *Trends: Infrastructre and transport to 2030*, 2014, DoIaR Development, Commonwealth of Australia, Canberra.
- Fischer, G & Li, VC 2002, 'FRP reinforced ECC structural members under reversed cyclic loading conditions', in *Advances in Building Technology*, Elsevier, Oxford, pp. 781-8.
- GHD 2015, *Infrastructre Maintenance: A report for Infrastructure Australia*, GHD, Sydney.
- Haddad, RH & Almasaeid, HH 2016, 'Recovering shear capacity of heat-damaged beams using NSM-CFRP strips', *Construction and Building Materials*, vol. 105, pp. 448-58,
<http://www.sciencedirect.com/science/article/pii/S0950061815308230>>.
- Hassan, TK & Rizkalla, SH 2004, 'Bond Mechanism of Near-Surface-Mounted Fiber-Reinforced Polymer Bars for Flexural Strengthening of Concrete Structures', *Structural Journal*, vol. 101, no. 6.
- Hesse, G 2014, 'Development of Ductile and Ultra-high Performance Engineered Cementitious Composite (ECC) with Lightweight Microsphere Additive', University of Southern Queensland, Toowoomba.
- Hong, S & Park, S-K 2012, 'Uniaxial Bond Stress-Slip Relationship of Reinforcing Bars in Concrete', *Advances in Materials Science and Engineering*, vol. 2012, pp. 1-12.
- Horikoshi, T, Ogawa, A, ASaito, T & Hosiro, H 2006, *Properties of polyvinyl alcohol ber as reinforcing materials for cementitious composites*, Industrial Materials R & D Department and Tokyo Fibers & Industrial Materials Department, Japan.
- Jalali, M, Sharbatdar, MK, Chen, J-F & Jandaghi Alae, F 2012, 'Shear strengthening of RC beams using innovative manually made NSM FRP bars', *Construction and Building Materials*, vol. 36, pp. 990-1000.
- Kunieda, M, Ogura, H, Ueda, N & Nakamura, H 2011, 'Tensile fracture process of Strain Hardening Cementitious Composites by means of three-dimensional meso-scale analysis', *Cement and Concrete Composites*, vol. 33, no. 9, pp. 956-65, <http://www.sciencedirect.com/science/article/pii/S0958946511000990>>.

- Lee, D & Cheng, L 2013, 'Bond of NSM systems in concrete strengthening – Examining design issues of strength, groove detailing and bond-dependent coefficient', *Construction and Building Materials*, vol. 47, pp. 1512-22.
- Li, M & Li, VC 2012, 'Rheology, fiber dispersion, and robust properties of Engineered Cementitious Composites', *Materials and Structures*, vol. 46, no. 3, pp. 405-20.
- Li, VC & Kanda, T 1998, 'Innovations Forum: Engineered cementitious composites for structural applications', *Journal of Materials in Civil Engineering*, vol. 10, no. 2, pp. 66-9.
- Li, VC, Mishra, DK, Naaman, AE, Wight, JK, LaFave, JM, Wu, H-C & Inada, Y 1994, 'On the shear behavior of engineered cementitious composites', *Advanced Cement Based Materials*, vol. 1, no. 3, pp. 142-9,
<http://www.sciencedirect.com/science/article/pii/S1065735594900450>.
- Lin, Z & Li, VC 1997, 'Crack bridging in fiber reinforced cementitious composites with slip-hardening interfaces', *Journal of the Mechanics and Physics of Solids*, vol. 45, no. 5, pp. 763-87,
<http://www.sciencedirect.com/science/article/pii/S0022509696000956>.
- Lu, W, Ling, Z, Geng, Q, Liu, W, Yang, H & Yue, K 2015, 'Study on flexural behaviour of glulam beams reinforced by Near Surface Mounted (NSM) CFRP laminates', *Construction and Building Materials*, vol. 91, pp. 23-31,
<http://www.sciencedirect.com/science/article/pii/S0950061815004936>.
- Malano, A 2008, *ENG8803 Mechanics and Technology of Fibre Composites*, Univeristy of Southern Queensland, Toowoomba.
- MTS 2011, *MTS Insight Universal Test Systems*, MTS Sytems Corporation, Minnesota.
- Novidis, DG & Pantazopoulou, SJ 2008, 'Bond Tests of Short NSM-FRP and Steel Bar Anchorages', *Journal of Composites for Construction*, vol. 12, no. 3, pp. 323-33,
<http://ascelibrary.org/doi/abs/10.1061/%28ASCE%291090-0268%282008%2912%3A3%28323%29>.
- Ombres, L 2012, 'Debonding analysis of reinforced concrete beams strengthened with fibre reinforced cementitious mortar', *Engineering Fracture Mechanics*, vol. 81, pp. 94-109,
<http://www.sciencedirect.com/science/article/pii/S0013794411002360>.
- Qian, S, Zhou, J, de Rooij, MR, Schlangen, E, Ye, G & van Breugel, K 2009, 'Self-healing behavior of strain hardening cementitious composites incorporating local waste materials', *Cement and Concrete Composites*, vol. 31, no. 9, pp. 613-21,
<http://www.sciencedirect.com/science/article/pii/S0958946509000468>.
- SAI 2013, *AS 3600-2009 Concrete Structures*, "Standards Australia Limited", Sydney.
- Seracino, R, Jones, N, Ali, M, Page, M & Oehlers, D 2007, 'Bond Strength of Near-Surface Mounted FRP Strip-to-Concrete Joints', *Journal of Composites for Construction*, vol. 11, no. 4, pp. 401-9, viewed 2016/05/20,
[http://dx.doi.org/10.1061/\(ASCE\)1090-0268\(2007\)11:4\(401\)](http://dx.doi.org/10.1061/(ASCE)1090-0268(2007)11:4(401)).

- Sharaky, IA, Torres, L, Comas, J & Barris, C 2014, 'Flexural response of reinforced concrete (RC) beams strengthened with near surface mounted (NSM) fibre reinforced polymer (FRP) bars', *Composite Structures*, vol. 109, pp. 8-22, <http://www.sciencedirect.com/science/article/pii/S0263822313005722>>.
- Smith, ST & Teng, JG 2001, 'Interfacial stresses in plated beams', *Engineering Structures*, vol. 23, no. 7, pp. 857-71, <http://www.sciencedirect.com/science/article/pii/S0141029600000900>>.
- Termkhajornkit, P, Nawa, T, Yamashiro, Y & Saito, T 2009, 'Self-healing ability of fly ash–cement systems', *Cement and Concrete Composites*, vol. 31, no. 3, pp. 195-203, <http://www.sciencedirect.com/science/article/pii/S0958946508001571>>.
- Wang, S & Li, VC 2005, 'Polyvinyl Alcohol Fiber REinforced Engineered Cementitious Composites: Material Design and Performance', *International RILEM workshop on High Performance Fibre Reinforced Cementitious Composites (HPFRCC) in Structural Applications*.
- Wang, S & Li, VC 2007, 'Engineered cementitious composites with high-volume fly ash', *ACI Materials Journal-American Concrete Institute*, vol. 104, no. 3, pp. 233-41.
- Yan, X, Miller, B & Nanni, DA 1999, 'Characterization of CFRP Rods used as Near-Surface_Mounted Reinforcement', in *International Structural Faults and Repair Conference: Proceedings of the International Structural Faults and Repair Conference*, MC Forde (ed.), Engineering Technics Press, Edinburgh Scotland.
- Zhang, SS & Teng, JG 2013, 'Interaction forces in RC beams strengthened with near-surface mounted rectangular bars and strips', *Composites Part B: Engineering*, vol. 45, no. 1, pp. 697-709, <http://www.sciencedirect.com/science/article/pii/S1359836812005872>>.
- Zhang, SS, Teng, JG & Yu, T 2014, 'Bond Strength Model for CFRP Strips Near-Surface Mounted to Concrete', *Journal of Composites for Construction*, vol. 18, no. 3, p. A4014003, <http://ascelibrary.org/doi/abs/10.1061/%28ASCE%29CC.1943-5614.0000402>>.
- Zhuge, Y, Shen, CJ, Lu, GX, Hesse, G, Chen, S & D.Ruan 2014, 'Material Properties and Impact Resitance of a new Lightweight Engineered Cementitious Composite', *23rd Australiasian Conference on teh Mechanics of Structures and Materials (ACMSM23)*.

APPENDIX 1 – PROJECT SPECIFICATION

For: Jared Hawkins

Title: Using ECC as a filling material for concrete/masonry retrofitting with near-surface mounted FRP bars and strengthening concrete bridges

Major: Bachelor Engineering (Honours) Civil (Honours) Civil

Supervisors: Assoc. Prof Yan Zhuge

Enrolment: ENG 4111 - EXT S1 2016

ENG 4112 – EXT S2 2016

Project Aim: Assess the performance of Engineered Cementitious Composites as an adhesive in a near surface mounted reinforcing system using a bond slip experimental testing program and (if time permits) use the data to develop a virtual model of bond slip behaviour using finite element analysis.

Programme: Issue A, March 16th 2016

- Research the existing methods of retrofitting using near surface mounted FRP bars to strengthen concrete structures.
- Review existing research into near surface mounted systems to develop an understanding of common experimentation techniques and bond slip behaviours of alternative adhesive materials
- Develop an experimental program to test the bond slip behaviour of engineered cementitious composites (ECC) as an FRP reinforcing bar adhesive in a retrofitted system.
- Develop a suitable ECC mix design for use as an adhesive in experimental model.
- Coordinate with USQ staff to perform testing of manufacture samples.
- Analyse test results and identify failure modes and effective bond strength between substrate and ECC, determine bond strength between ECC and FRP reinforcement.

APPENDIX B – PROJECT PLAN

Project Management Plan

There are 3 key components to the this project management plan, they are

- Quality Management
 - Risk Assessment
 - Scheduling
- Health & Safety
- Communication

Quality Management

To ensure the project is completed to an acceptable standard a quality management system has been devised to ensure routine checks are complete and highlight any potential issues in a timely manner so they can be dealt with effectively.

Risk assessment

The first part of the quality management system is to identify the potential issues that may affect the quality of the project and determine measures to mitigate these risks. A preliminary risk assessment has been completed and these risks are recorded in a risk register. Additional risks will be added to the risk register as they become apparent.

Table 4: Project Risk Register

Activity	Risk	Rating	Mitigation
<i>Construction of Test Samples</i>	Unable to source materials	Medium	Ensure early procurement, allowing plenty of time to source materials. Identify alternate suppliers for necessary materials.
	Failure of test samples to meet quality standards	High	Source proven concrete mix design from previous experimental studies. Mix concrete with accurate measurements and ensure curing is undertaken correctly. Suggest Water Bath curing
	Failure of FRP Reinforcement to bond with Engineered Cementitious composites	Low	Ensure FRP Reinforcement is clean prior to casting into ECC. Wipe down with isopropyl prior to casting in to ECC
<i>Transporting Samples to Test Facility</i>	Damage to test samples during transit	Low	Ensure test samples are packed safely and protected from potential damage during transport.
<i>Testing of Samples</i>	Failure to secure laboratory for testing	Low	Coordinate with Laboratory, book in access to testing facilities
	Inconsistent test results	High	Produce a minimum of 3-5 ECC and traditional Concrete samples for testing
	Failure of testing to produce meaningful results	High	Commence testing as soon as possible to allow sufficient time to retry the tests with new samples if necessary
<i>Finite Element Analysis</i>	Failure to produce an accurate simulation	Medium	Produce a 2 dimensional model that accurately represents the results found during experimental testing prior to commencing 3 dimensional model.

Scheduling

The Project schedule aims to commence work on the 13th November 2015. Although this may precede the formal allocation of the project the preliminary work can be completed. The goal of this early start is to mitigate potential risks associated with access to laboratory equipment due to the travel time required.

Administrative Milestones

- Formal Allocation of the Project will be made no Later than 9th March 2016
- Acceptance of Project Specification Submitted 16th March 2016

Project Milestones

- Establish Testing Procedure 22nd December 2015
- Complete testing 8th May 2016
The goal is to complete the testing procedure as soon as possible This will allow enough time to re-run the tests should there be any problems or issues.
- Preliminary Report 25th May 2016
The Finite Element Analysis component will not be completed prior to the Preliminary report, however, the model should be complete and will make up part of the preliminary report.
- Preliminary Draft of Dissertation 7th September 2016
- Seminar Presentation Late September
- Dissertation Submission 13th October 2016.

A Gant chart project program has been produced and is available at Appendix 3.

Health & Safety Management

The Health & Safety plan will address the potential health and safety risks to the student and other individuals involved in the completion of activities required as part of this project. The following health and safety risk assessment is based on a system developed to satisfy AS/NZ 4801.

Central to the management of health and safety issues for this project is the health and safety risk assessment. A preliminary risk assessment has been completed. A review of the risk assessment is required once the experimental testing scheme has been finalised. At this point a potential health and safety risks should be easily identifiable. The preliminary risk assessment follows.

**Table 5. Health & Safety Risk Matrix – Likelihood and Consequence Matrix
Health & Safety Risk Assessment.**

How severely could it hurt someone? Or How ill could it make someone?	How likely is it to be that bad?			
	1 Very likely Could happen at any time	2 Likely Could happen Sometime	3 Unlikely Could happen but very rarely	4 Very Unlikely Could happen but probably never will
A. Kill or cause permanent disability or ill health	H1	H2	H4	M7
B. Long Term illness or serious injury	H3	H5	M8	M11
C. Medical Attention and several days off work	H6	M9	M12	L14
D. First Aid needed	M10	M13	L15	L16
HIGH 1- 6	STOP WORK IMMEDIATELY. Work is not to proceed until controls are implemented to reduce the residual risk to Medium or Low. Ongoing monitoring.			
MEDIUM 7 – 13	ONGOING MONITORING Action needs to be taken in a timely manner but if a quick and easy solution is available, fix it immediately.			
LOW 14 – 16	ROUTINE MONITORING No further action is required where residual risks are Low. However, ongoing monitoring is still required to ensure the risk does not escalate.			

Table 6 – Health & Safety Risk Assessment

Task	Hazard	Risk Rating	Mitigation	Residual Risk Rating
Construction of Test Samples	Irritation of chest, and skin by inhalation or contact with cement dust	M13	Refer to the appropriate Material Safety Data sheets and wear appropriate Respirator, gloves and clothing during activity	M10
	Irritation of lungs by inhalation of polymer fibres during construction of test samples	M13	Refer to the appropriate Material Safety Data sheets and wear suitable respirator during construction of samples	M10
Pull out testing of samples	Eye injury from flying debris in the event of sudden sample failure	M13	Wear appropriate eye protection, stand well clear of test apparatus, ensure speed of testing is within safe limits	M10

APPENDIX C – MIX DESIGN CALCULATIONS

Mix Design Calculation Method

For the mix design calculations the the volume of ECC required for each sample was determined to be the full volume of the notch over the bonded length. This provided sufficient excess to allow for spillage an slight variations in the notch

$$V_{notch} = 100 \times 26 \times 26 = 67.6 \times 10^3 \text{ mm}^3$$

Each sample had a slightly different mix design, as an example of how the weights of the constituent parts were determined, the calculations for ECC1 are presented below. The mix design for ECC1 set was based on Li's Exemplary mix. 6 Samples using ECC1 mix are required

$$V_{ECC2} = 6V_{notch}$$

$$V_{ECC2} = 6 \times 67.6 \times 10^3$$

$$V_{ECC2} = 405.6 \times 10^3 \text{ mm}^3$$

Constituent	Cement/Flyash	Sand	Water	PVA Fibres	Super Plasticiser
Ratio	1	0.363	0.25	2% by volume	2% of combined weight

PVA Fibre Content by Weight- W_{pva} , 2% Fibre by volume. Therefore;

$$V_{pva} = 0.02 \times 405.6 \times 10^3 = 8.1 \times 10^3 \text{ mm}^3$$

Use the PVA Fibre specific gravity to determine the weight required.

$$S.G._{pva} = 1.3$$

$$W_{pva} = V_{pva} \times SG_{pva} \times \rho_{water} \times \frac{1 \text{ m}^3}{1 \times 10^9 \text{ mm}^3} \times \frac{1 \times 10^3 \text{ g}}{1 \text{ kg}}$$

$$W_{pva} = 8.1 \times 10^3 \times 1.3 \times 1000 \times \frac{1 \text{ m}^3}{1 \times 10^9 \text{ mm}^3} \times \frac{1 \times 10^3 \text{ g}}{1 \text{ kg}}$$

$$W_{pva} = 10.5 \text{ g}$$

Cement, Sand and water make up the remaining 98% by volume;

$$V_{c.p.} = 0.98 \times 405.6 \times 10^3 \text{ mm}^3 = 397 \times 10^3 \text{ mm}^3$$

Constituent	Cement	Flyash	Sand	Water	Sum of parts
Mix Ratio	0.455	0.545	0.363	0.25	1.613
Unit Weight (1kg mix; in grams) = Mix Ratio $\times \frac{1}{1.612} \times \frac{1 \times 10^3 \text{ g}}{1 \text{ kg}}$	282g	338g	225g	155g	1000g
S.G.	3.15	2.8	2.65	1	
Unit Volume ($\times 10^3 \text{ mm}^3$) $= \frac{\text{Unit Weight}}{S.G. \times \rho_{water} \times \frac{1 \text{ m}^3}{1 \times 10^9 \text{ mm}^3}}$	89	121	85	155	450
Volume Ratio $= \frac{\text{Required Volume}}{\text{Unit Volume}}$	$V_{ECC1} / \text{Unit Volume} = \frac{405.6 \times 10^3 \text{ mm}^3}{397 \times 10^3 \text{ mm}^3}$ $\text{Required Volume} / \text{Unit Volume} = 0.88$				
Required Volume $\times 10^3 \text{ mm}^3$ $= \text{Volume Ratio} \times \text{Unit Volume}$	79	107	75	137	397
Required Weight = $\text{Required Volume} \times S.G. \times \rho_{water} \times \frac{1 \text{ m}^3}{1 \times 10^9 \text{ mm}^3} \times \frac{1 \times 10^3 \text{ g}}{1 \text{ kg}}$	249g	299g	199g	137g	
Weight of cement paste, W_{cement} $= \sum \text{Required Weight}_i$	$W_{cement} = 254 + 305 + 203 + 140$ $W_{cement} = 883 \text{ g}$				

Note: Readers may note slight variations in arithmetic, this is a result of rounding.

Super plasticiser was added as 2% of Cementitious paste weight

$$W_{SuperP} = 0.02 \times W_{cement}$$

$$W_{SuperP} = 18g$$

Summary Tables of Sample Mix Design Qtys

Mix ID	Cement	Flyash	Water	Sand	Super-plasticiser	PVA Fibre
C1 - Cementitious Grout	1	0	0.25	0.363	2%	0
No of Samples	6					
Volume Required	$405.6 \times 10^3 mm^3$					
Weight	576g	0	144g	209g	19g	0
Total Weight	947g					

Mix ID	Cement	Flyash	Water	Sand	Super-plasticiser	PVA Fibre
ECC1 – Engineered Cementitious Composites No Flyash, reduced ductility	1		0.25	0.363	2%	2%
No of Samples	6					
Volume Required	$405.6 \times 10^3 mm^3$					
Weight	564	0	141g	205g	18g	10.5g
Total Weight	939g					

Mix ID	Cement	Flyash	Water	Sand	Super-plasticiser	PVA Fibre
ECC2 - Engineered Cementitious Composite (Li M45 Mix Design)	0.454	0.545	0.25	0.363	2%	2%
No of Samples	6					
Volume Required	$405.6 \times 10^3 mm^3$					
Weight	249g	299g	137g	199g	18g	10.5g
Total Weight	947g					

Mix ID	Cement	Flyash	Water	Sand	Super-plasticiser	PVA Fibre
ECC3 - Engineered Cementitious Composite (Li M45 Mix Design with reduced S.P.)	0.454	0.545	0.25	0.363	0.5%	2%
No of Samples						2
Volume Required	135 × 10 ³ mm ³					
Weight	83g	100g	66g	46g	2g	10.5g
Total Weight						307.5g

Mix ID	Cement	Flyash	Water	Sand	Super-plasticiser	PVA Fibre
ECC3 - Engineered Cementitious Composite (Li M45 Mix Design with no S.P.)	0.454	0.545	0.25	0.363	0%	2%
No of Samples						2
Volume Required	135 × 10 ³ mm ³					
Weight	83g	100g	66g	46g		10.5g
Total Weight						305.5g

APPENDIX 4 – CONCRETE PRISM TEST RESULTS



Cardno
Shaping the Future

Cardno Construction Sciences
ABN: 74 128 806 735
Address:
26 Lithgow Street,
Fyshwick ACT 2609

Laboratory: Fyshwick Laboratory
Website: www.Cardno.com.au



CONCRETE COMPRESSIVE STRENGTH REPORT

Page 1 of 1

Client: Holcim ACT - Concrete	Concrete Class: S32	Date Sampled / Cast: 24/03/2016	Report Number: 455/R1356-1
Client Address: 26 Lithgow St, Fyshwick	Specified Strength (MPa): 32.0	Norm. Slump / Tol (mm): 80 / +/-15	Project Number: 455/P/9
Supplied To: QC-Fyshwick	Lot Number:	Agg. Corr. Factor (%):	Report Date: 2/05/2016
Project: QC-Fyshwick	Sampled By: Brett Dickson	Air Cont. Comp Method:	Test Request No: 455/T/470
Supplier: Holcim	Sampling Location: Non-Agglator Units	Sampling Method: AS1012.1 (7.2.1)	
Client Reference/s: USQ BASEPRISMS TEST PANELS	Weather: INDOORS	Structure/s: USQ BASEPRISMS TEST SAMPLES	

Test Procedures: AS1012.1, AS1012.1 (Sect 6c), AS1012.8.1 (7.4), AS1012.3.1, AS1012.9, AS1012.12.1		Plant Code / Mix Code: 450 / NS321XC60											
Sample No	Batch No	Time Cast	Concrete Temp (C)	Slump (mm)	Initial Curing (hrs)	Date of Test	Test Age	Specimen Dimensions (mm)		Curing Conditions	Mass per Unit Volume (kg/m ³)	Compressive Strength (MPa)	Test Remarks
								Avg Diameter	Height				
455/C/3319	45005730	06:40	22	90	127	21/04/2016	28 days	99.8	196	23 days - STD	2380	40.5	
455/C/3320	45005730	06:40	22	90	127	21/04/2016	28 days	99.8	196	23 days - STD	2380	41.0	

Note 1: Temperature Zone - Standard Temperature Zone
 Note 2: Curing Conditions: STD = Standard Moist Curing, MST = Moist, DRY = Dry
 Note 3: Ambient On-Site Temperatures - Minimum 12.00C° / Maximum 22.00C°
 Note 4: Sampling from Non-Agglator Units
 Note 5: Ground End used on specimens unless otherwise stated.
 Note 6: All specimens are measured and weighed uncapped.
 Note 7: This report is for concrete sampled and tested by this laboratory.

 Accreditation Number: 1986 Corporate Site Number: 455	The results of the tests, calibrations and/or measurements included in this document are traceable to Australian national standards. Accredited for compliance with ISO/IEC 17025	Approved Signatory: Brett Dickson Form ID: W84Rep Rev 1	Remarks

APPENDIX 5 – MATERIAL DATA SHEET –

V.ROD

PULTRALL

V•ROD STANDARD

Revision: July 2013

V-Rod standard straight bars only, does not apply to bent bars

		#2 GFRP V•ROD	#3 GFRP V•ROD	#4 GFRP V•ROD	#5 GFRP V•ROD	#6 GFRP V•ROD	#7 GFRP V•ROD	#8 GFRP V•ROD
Minimum guaranteed tensile strength *	MPa	990	1100	1140	1130	1110	1100	800
	ksi	143	159	165	164	161	159	116
Nominal tensile modulus	GPa	52,5 ±2,5						
	ksi	7609 ±363						
Tensile strain	%	1,89	2,10	2,17	2,15	2,11	2,10	1,52
Poisson's ratio	(-)	0,25	0,21	0,26	0,25	0,25	0,25	0,28
Nominal Flexural strength	MPa	1200	1161	1005	930	882	811	776
	ksi	174	168	146	135	128	117	112
Nominal Flexural modulus	GPa	48,8	46,1	46,8	46,8	45,1	44,6	45,1
	ksi	7071	6685	6787	6786	6533	6466	6539
Flexural strain	%	2,46	2,52	2,15	1,99	1,96	1,82	1,72
Nominal Bond strength	MPa	14						
	psi	2029						
Bond dependent coefficient	(-)	0,8						
Longitudinal coefficient of thermal expansion	xE-6/°C	6,2						

	xE-6/°F	3,5						
Transverse coefficient of thermal expansion	xE-6/°C	23,8						
	xE-6/°F	13,2						
Moisture absorption	%	0,65	0,47	0,38	0,25	0,21	0,36	0,17
Glass content	% vol	65						
	% weight	83						
Weight	g/m	95	181	298	488	659	887	1132
	lb/ft	0,064	0,122	0,200	0,328	0,443	0,596	0,761
Effective cross-sectional area (including sand coating) **	mm ²	47,0	95,0	149,0	234,0	302,0	396,0	546,0
	inch ²	0,0729	0,1473	0,2310	0,3627	0,4681	0,6138	0,8463
Nominal cross-sectional area	mm ²	31,7	71,3	126,7	197,9	285,0	387,9	506,7
	inch ²	0,0491	0,1104	0,1963	0,3068	0,4418	0,6013	0,7854

* the minimum guaranteed tensile strength must not be used to calculate the strength of the bent portion of a bent bar.

Instead use the minimum guaranteed tensile strength found in the technical data sheet of bent V-Rod bars.

** Please contact the manufacturer for dowelling applications.

Development and splice lengths are available upon request but should be properly calculated by a design engineer.

Please refer to the bent bar data sheet for designs using bent V-Rod bars.

It is the responsibility of the design engineers to contact the bar manufacturer to get the latest updates of this technical data sheet (also available at www.pultrall.com).

APPENDIX 6 – PVA FIBRE DATA SHEET

NYCON-PVA RECS15
PVA (Polyvinyl Alcohol), Small Denier, Superior Bond



ULTRA-HIGH PERFORMANCE FIBERS

PVA fibers are unique in their ability to create a fully-engaged molecular bond with mortar and concrete that is **300% greater** than other fibers.



NYCON-PVA RECS15 Physical Properties

Filament Diameter	8 Denier (38 Microns)
Fiber Length	0.375" (8mm)
Specific Gravity	1.3
Tensile Strength	240 ksi (1600 MPa)
Flexural Strength	5700 ksi (40 GPa)
Melting Point	435° F (225° C)
Color	White
Water Absorption	<1% by Weight
Alkali Resistance	Excellent
Concrete Surface	Not Fuzzy
Corrosion Resistance	Excellent



Description

NYCON-PVA RECS15 fiber products are 8 denier, monofilament PVA fibers for use in fiber reinforced concrete, stucco and precast. NYCON-PVA RECS15 is specifically designed for use in concrete products for the purpose of controlling plastic shrinkage, thermal cracking and improving abrasion resistance. When NYCON-PVA RECS15 is used at high doses it can dramatically improve flexural characteristics of concrete products.

NYCON-PVA RECS15 meets the requirements of ASTM C-1116, Section 4.1.3 and AC-32 at 1.0 lb (0.45 kg) per CY.

Applications

NYCON-PVA utilizes the mixing activity to disperse the fibers into the mix. NYCON-PVA acts with a molecular bond in the concrete with a multi-dimensional fiber network. NYCON-PVA does not affect curing process chemically.

NYCON-PVA can be used in all types of concrete. Synthetic fibers help the concrete at early ages, which is especially beneficial where stripping time and handling is important.

800-456-9266

www.nycon.com

sales@nycon.com

APPENDIX 7 – MATLAB CODES

The following scripts and functions were used to process the data once corrected for initial settlement. Due to the nature of the results no further analysis was completed with Matlab.

```
% The following script requires a data file and then accepts the
% parameters for sample id and FRP frelength. Once the data is corrected
% for bar elongation the stress is calculatated and graphs that present
% the force/slip relationship and then the stress/strain relationship
% are produces. Once complete the data is saved to a new file for further
% analysis

clear;
% Constants
cBLength = 0.1; %m
cBDia = 0.0125; % m
cBPerimeter = pi()*cBDia; % m
cBondedArea = cBLength*cBPerimeter; %m2

% Read the data file
[fileName filePath] = uigetfile('*.csv');
rawIn = readtable(strcat(filePath,fileName));
strSample = input('Enter Sample ID: ','s');
freeLength = input('Enter Free Length(mm): ');

% % Used for testing
% rawIn = readtable(' \Pullout Test-06.csv');
% strSample = 'ECC1-3';
% freeLength = 100;

rawIn.Properties.VariableNames{1} = 'N';
rawIn.Properties.VariableNames{2} = 'oSlip'; %original slip readings
rawIn.Properties.VariableNames{3} = 'cSlip'; %corrected slip readings
after initial settlement

% Correct for elongation in the FRP rod
rawIn.fSlip = fBarExt(rawIn.N,rawIn.cSlip,freeLength);
rawIn.fSlip(length(rawIn.fSlip)) = rawIn.fSlip(length(rawIn.fSlip)-1);

% Generate Stress Column, Stress = Force over area, assuming area is
% perimeter x length
rawIn.avgStress = rawIn.N/cBondedArea;
```

```

% Generate Strain Column, Strain = elongation/bonded length
rawIn.avgCStrain = rawIn.cSlip/(cBLength*1000);
rawIn.avgFStrain = rawIn.fSlip/(cBLength*1000);

% Find Max Stress and slip at max stress
ultLoad = max(rawIn.N);
ultStress = max(rawIn.avgStress);
ultcSlip = rawIn.cSlip(rawIn.avgStress==ultStress);
if length(ultcSlip)>1
    ultcSlip = ultcSlip(1);
end

ultfSlip = rawIn.fSlip(rawIn.avgStress==ultStress);
if length(ultfSlip)>1
    ultfSlip = ultfSlip(1);
end

% Present the Cleaned Data in a chart, highlight Ultimate stress and
slip
% at ultimate stress.
figure
subplot(2,1,1) % add first plot in 2 x 1 grid
plot(rawIn.cSlip,rawIn.N, '-k', rawIn.fSlip,rawIn.N,'--
k');%,rawIn.correctedSlip,rawIn.avgStress,maxSlipStress,maxStress,'d',
'MarkerFaceColor','blue','MarkerSize',10);
xlabel('Slip (mm)');
ylabel('Load (N)');
title(strSample);
strValues = strtrim(cellstr(num2str([ultfSlip ultStress], '%d,%d')));
text(ultfSlip,ultStress,strValues,'VerticalAlignment','bottom','Horizo
ntalAlignment','right');
legend('Original', 'Corrected', 'location', 'northwest');

subplot(2,1,2) % add second plot in 2 x 1 grid
plot(rawIn.avgCStrain,rawIn.avgStress,'-k',
rawIn.avgFStrain,rawIn.avgStress, '--k') % plot using + markers
xlabel('Strain');
ylabel('Average Stress (Pa)');
legend('Original', 'Corrected', 'location', 'northwest');

disp(num2str(ultLoad))
disp(num2str(ultStress))
disp(num2str(ultcSlip))
disp(num2str(ultfSlip))

% Save file
writetable(rawIn, strcat(strSample, '_corrected.xls'));

```

```

function [ bCSlip ] = fBarExt( fN, fSlip, freeLength )
% FBAREXT
% This function takes the free length (arg freeLength vartype table
% column) of the bar, the known force (arg fN table column) and calculates
% the elongation in the free length of reinforcement. Then, on the
% condition that the previous load was less than the current load,
% deducts the extension from the current slip value (arg fSlip table
% column). The function cycles through all values of the supplied tables
% and returns a table column with corrected slip values

nomArea = 72.1; %mm2
tensModulus = 52.5; %GPa

rTable = fSlip;
i=2;
for i=2:length(fSlip)
    if fN(i)-fN(i-1)>0
        bExt = freeLength*(((fN(i)/1000)/nomArea)/tensModulus);
        rTable(i)=fSlip(i)-bExt;
    else
        rTable(i)=fSlip(i)-bExt;
    end
    i=i+1;
end

bCSlip = rTable;
end

% End Function

```